Numerical Modeling of an Embankment Slope Stabilized with Ceramic Dust

Session 2019-2023

Project Supervisor

ENGR. MUHAMMAD UMAIR ASHFAQ

Submitted By

ZAIN UL HASSAN	**2019-UET-NFC-FD-CIVIL-48**
MUHAMMAD ZEESHAN	**2019-UET-NFC-FD-CIVIL-50**
RAIF RAFIQUE	**2019-UET-NFC-FD-CIVIL-51**
HAIDER JALAL	**2019-UET-NFC-FD-CIVIL-43**

Department of Civil Engineering

NFC INSTITUTE OF ENGINEERING AND FERTILIZER RESEARCH FAISALABAD

Numerical Modeling of an Embankment Slope Stabilized using Ceramic Dust

This project has been proposed by the students of Civil Engineering of session 2019-2023 who have been designated the given project by civil engineering department in order to fulfil requirements of

Bachelor's Degree

In

Civil Engineering

ZAIN UL HASSAN	**2019-UET-NFC-FD-CIVIL-48**
MUHAMMAD ZEESHAN	**2019-UET-NFC-FD-CIVIL-50**
RAIF RAFIQUE	**2019-UET-NFC-FD-CIVIL-51**
HAIDER JALAL	**2019-UET-NFC-FD-CIVIL-43**

Approved By

Head of Department

Dr. Shehroze Ali

Assistant Professor

Civil Engineering Department

Internal Examiner

Muhammad Umair Ashfaq

Lecturer

Civil Engineering Department

External Examiner

Prof. Dr. Khalid Farooq

Professor

Civil Engineering Department

University of Engineering & Technology, Lahore

Department of Civil Engineering

NFC INSTITUTE OF ENGINEERING AND FERTILIZER RESEARCH FAISALABAD

RESEARCH DECLARATION

We certify that this report is completely our own work and that any usage of other people's work has been properly recognized through in-text citations and reference lists. Wherever content from other sources was used, it was appropriately recognized and referenced. We also certify that the study endeavor was carried out in accordance with the university's research policy.

We agree that the project report can be made available to other students in the department of Civil Engineering and library as a reference document.

Signature

ZAIN UL HASSAN

2019-UET-NFC-FD-CIVIL-48

Signature

MUHAMMAD ZEESHAN

2019-UET-NFC-FD-CIVIL-50

Signature

RAIF RAFIQUE

2019-UET-NFC-FD-CIVIL-51

Signature

HAIDER JALAL

2019-UET-NFC-FD-CIVIL-43

DEDICATION

Every challenging problem necessitates personal effort and the direction of the elderly, particularly those who hold a special place in our hearts. We offer our meager efforts in gratitude to our devoted parents' Love. Together with all the dedicated and well respected teachers, it is only through constant encouragement and day and night prayers that we were able to achieve such achievement and glory.

CONTENTS

ACKNOWLEDGEMENT

We extend our heartfelt gratitude and appreciation to **Engineer Muhammad Umair Ashfaq**, our esteemed supervisor, for his invaluable guidance, unwavering support, and mentorship throughout the journey of this thesis. His profound knowledge, expertise, and dedication have been instrumental in shaping this research and elevating its quality to new heights.

We are deeply thankful to him for providing constructive feedback, valuable insights, and encouragement at every step, which have been crucial in overcoming challenges and achieving significant milestones during the course of this study.

LIST OF TABLES

LIST OF FIGURES

LIST OF ABBRIVATIONS

CD	Ceramic Dust
FEM	Finite Element Modeling
DST	Direct Shear Test
CBR	California Bearing Ratio
SSRM	Shear Strength Reduction Method
FOS	Factor of Safety
FDM	Finite Difference Method
DDM	Discontinuous Deformation Analysis
DEM	Discrete Element Method
MDD	Maximum Dry Density
OMC	Optimum Moisture Content
PLAXIS	Plane Strain And Axial Symmetry
LEM	Limit Equilibrium Method
ASTM	American Society for Testing and Materials
AASHTO	American Association of Highway and Transportation Officials

ABSTRACT

Ensuring stable and effective operation of road infrastructure is crucial for fostering economic growth and connectivity. However, Poor soil quality leading to road embankment failures is now a significant concern due to traffic disruptions and safety risks. Because conventional techniques of soil stabilization can be both expensive and harmful to the surrounding ecosystem, it is necessary to investigate possible sustainable substitutes. This study presents comprehensive findings obtained through laboratory testing and finite element modeling (FEM) to investigate the impact of waste ceramic dust on the compaction and shear strength characteristics of soil, as well as its influence on slope stability. The research explores the behavior of soil with varying percentages of waste ceramic dust and examines its potential as a stabilizing agent for enhancing soil properties and promoting slope stability. The optimum percentage of ceramic dust was found to be 30% based on the results of modified proctor test and direct shear test. It was found that with 30% addition of ceramic dust cohesion (c) and internal angle (Φ) of soil increased up to 200% and 20% respectively. The MDD of soil increased with increase in % of CD, and it increased up to 3.2% at optimum % of CD. OMC decreased with increase in % of CD from 12 to 8.5% at 30% CD addition. CBR value increased up to 293% at optimum addition of CD. The FOS of slope calculated using SSRM, increased with increase in % of CD, such at 30% addition of CD its value is increased by 78%. The combination of laboratory experiments and numerical analysis provides valuable insights into the performance of soil under different conditions, offering valuable implications for sustainable soil stabilization practices and resilient road infrastructure design. According to the findings, the factor of safety (FOS) of the slope improves as the percentage of ceramic dust in the mix rises, which ultimately results in the slope becoming more stable. This study emphasizes waste ceramic dust as an eco-friendly, cost-effective soil stabilization option for road embankments.

Keywords: Ceramic dust (CD), FEM (Finite Element Modeling), SSRM (Shear Strength Reduction Method), OMC (Optimum moisture Content), MDD (Maximum Dry Density), FOS (Factor of Safety), Cohesion (c) and Internal Angle (Φ).

INTRODUCTION

1.1 BACKGROUND

Roads are an integral component of the infrastructure vital to economic growth and transportation. They allow individuals to travel in a manner that is both secure and productive, as well as providing access to a wider range of goods, services, and work possibilities. Yet, enormous investments of time, money, and other resources are required for the building and upkeep of roads. The stability of the road subgrade is one of the essential aspects that affects the performance of the road infrastructure and the service life of the road infrastructure. Natural soils, which are typically used for the construction of road subgrades, exhibit a broad range of varying characteristics and behaviors. The soil's strength and stability depend on its composition, structure, moisture content, and other factors. It is possible for the subgrade to be unstable in regions that have poor soil characteristics, such as soft clay, organic soil, or expansive soils. This may result in differential settling, rutting, and cracking in the subgrade. These issues may lead to distress and failure of the pavement, a reduction in safety, and an increase in the expenses of maintenance. Slope stability is the main factor contributing to the workability of road embankment (Mamat et al., 2020).

Several different approaches of soil stabilization have been devised and practiced over the decades in order to make road subgrades more stable. The adding of gravel or stone to a subgrade in order to increase its bearing capacity was the first method of soil stabilizing ever developed. Later on, methods of soil stabilization were developed. These methods include the addition of chemicals to the soil, such as lime, cement, or fly ash, in order to change the characteristics of the soil and increase its strength and stability. The efficiency of soil stabilization approaches is reliant upon a variety of factors including the type and dosage of stabilizing chemical, the soil's characteristics, the climate and ambient conditions, and the traffic loads. Stabilization and its effect on soil indicate the reaction mechanism with additives, effect on its strength, improve and maintain soil moisture content and suggestion for construction systems (Afrin, 2017).Thus, selecting the most suitable soil stabilization technique demands thorough consideration of the aforementioned variables. There is a wide range of techniques that may be taken to enhance the engineering features of soil in order to make it appropriate for use in construction. Stabilization using dust/powder like waste materials with and without a binder like lime, cement etc. is one of them.

Quarry Dust (A. Sabat, 2012), marble dust (A. K. Sabat et al., 2011), cement, sodium chloride and brick dust (Obianigwe & Ngene, 2018), pyroclastic dust (Ene & Okagbue, 2009),waste ceramic dust (WCD) (A. K. Sabat, 2012) are some of the prominent dust/powder like waste materials which have been successfully utilized for stabilization of soil.

It is recommended to employ numerical techniques (in our scenario, the FEM) for a greater accuracy on the assessment of slope stability when doing a good analysis of the stability. This will allow for a more accurate determination of the stability of the slope (Abderrazak, 2018). There are several different approaches that may be used in order to evaluate and analyses the stability of slopes (Abderrazak, 2018). The finite difference method (FDM), the finite element method (FEM), the discontinuous deformation analysis (DDA), and the discrete element method (DEM) are the four primary types of numerical approaches that are used in the investigation of slopes.

Despite the fact that the industry is using advanced numerical analyses more and more, FEM slope stability method is preferred in engineering practice for their simplicity, particularly in the preliminary design stages. One of the advantages of finite element over limiting equilibrium is that no assumption is needed about the shape or location of the critical failure surface. In addition, the method can be easily used with others to calculate stresses, movements, pore pressures in embankments and seepage induced failure as well as for monitoring progressive failure (Hammouri et al., 2008). In the process of evaluating slopes, the factor of safety values continues to serve as the primary indicator for determining whether the slopes are dangerously near to failing or not. The assessment may be carried out by the use of numerical techniques such as the finite element approach. The approach known as shear strength reduction (SSR) may be used within the framework of the finite element method, which underpins the latter analysis. Under the context of this method, the angle of dilatancy, soil modulus, and solution domain size are not considered to be crucial characteristics. If a Mohr-Coulomb failure criteria is assumed, the safety factor may be derived by beginning with un-factored values and lowering the strength parameters in an incremental fashion. This will allow one to calculate the safety factor (Abderrazak, 2018).

1.2 AIMS AND OBJECTIVES

The following are the goals and objectives we have set for the project's completion.

- To calculate the soil's maximum dry density as well as its optimum moisture content for a range of CD (Ceramic dust) percentages.
- To determine Optimum percentage of CD on soil for which there are maximum shear strength parameters (c and Φ).
- To compare the results for CBR value of the untreated soil to that with treated soil (at optimum percentage of CD).
- To analyze the road embankment slope stabilized with CD using FEM and to calculate FOS at varying percentages of CD.

1.3 PROBLEM STATEMENT

In recent years, there has been a rise in public concern over the issue of waste management in general, and specifically on the challenge of managing trash from the industrial sector and the building industry. This problem is becoming increasingly acute due to the growing quantity of industrial, construction and demolition waste generated (Chen et al., 2015). Stabilizing soils for construction may be expensive when standard additions like cement, lime, geo-synthetic fibers, etc. are employed, thus it's important to investigate alternative, less expensive materials or waste products. It has been estimated that about 30% of daily production in the ceramic industry goes to waste. Ceramic dust, which is long-lasting, tough, and very resistant to the biological, chemical, and physical forces that might cause deterioration, is not being recycled in any way at this time (Binici, 2007). In order to solve these issues, we must find practical ways to consume less natural resources and recycle more trash. As a result, a research has been started to look for other ways to reuse the CD in a secure manner, and it is possible that this investigation may uncover a novel approach to recycling the ceramic waste in stabilization of soil. This will contribute to the reduction of expenses associated with the disposal of CD, the preservation of land capacity, the conservation of the diminishing supply of natural raw materials, and the mitigation of any environmental hazards. The road embankment situated in Renala Khurd (Canal Home Society near Lower Bari Doab canal - Right Road), Okara, Pakistan, coordinates 30°48’17.51”N and 73°35’59.99”E, has encountered a critical issue in the form of slope failure. This failure has resulted in substantial disruptions to transportation infrastructure and has the potential to jeopardize public safety.

1.4 UTILIZATION OF RESEARCH

There are a number of possible advantages to using ceramic dust from ceramics as a stabilizing agent. Firstly, it's a viable option for waste management since it may cut down on the quantity of trash produced by the ceramics sector. Furthermore, it may make soil more conducive to building by enhancing its mechanical qualities. This has the potential to be especially helpful in places where the soil condition makes it impractical to utilize more conventional building materials. The findings that were acquired from this study are beneficial for the efficient exploitation of waste material, Ceramic Dust, for the purpose of improving the quality of soils that are accessible locally. The fact that it is waste material means that it is available for free on the market, which makes it a cost efficient solution for the stabilization of soil, and this study will promote future exploration in this sector.

1.5 RESEARCH OVERVIEW

This project named "Numerical and Analytical Evaluation of an Embankment Slope stabilized using Ceramic Dust" is divided into the following sequence of chapters.

- ***Chapter 1***

The first chapter is about the introduction of the project title its objective and scope of research work to be done. The reasons for doing the study are included in the objectives, and the scope of the research effort is the means by which these objectives may be brought into the real world.

- ***Chapter 2***

In the second chapter a precise literature review is provided that is related from different related research articles, technical journals, etc. An explicit review has been provided in the thesis that covers each aspects of research topic.

- ***Chapter 3***

Third chapter is about the methodology followed during the performance of numerical modeling by using software (PLAXIS).

- ***Chapter 4***

Forth chapter is related to calculations and results of numerical analysis have been presented in the form of tables and graphs.

- ***Chapter 5***

Fifth chapter includes the conclusions based on numerical modeling and some recommendations are also derived at the end of this chapter.

LITERATURE REVIEW

This chapter aims to critically examine and synthesize the existing body of work related to geotechnical engineering, embankment construction, soil stabilization techniques, waste material utilization, laboratory testing, numerical modeling using PLAXIS 2D software and factor of safety (FOS) analysis. By reviewing the available literature, we can identify the gaps, limitations and opportunities for further investigations, setting the stages for research conducted in this thesis. With an emphasis on the use of ceramic dust as a stabilizing agent, this chapter seeks to give a thorough review of pertinent studies, research, and advances in the field of soil stabilization techniques. Road embankments are essential components of the transportation infrastructure because they support and stabilize roads built on a variety of terrains. However, embankment slopes are frequently exposed to a variety of outside forces, including gravity, water infiltration, and natural geological conditions, which can cause instability and collapse of the slope.

Researchers and engineers have investigated several soil stabilization techniques to increase the strength and stability of embankments in an effort to reduce these dangers. One promising approach in soil stabilization is the incorporation of ceramic dust, a byproduct of ceramic industries, into the soil matrix. Ceramic dust possesses certain characteristics, such as its fine particle size distribution and pozzolanic properties, which make it a potentially effective stabilizing agent for enhancing the geotechnical properties of soils. By adding ceramic dust to the embankment soil, it is hypothesized that the resulting composite material will exhibit improved shear strength, increase maximum dry density, and decreased optimum moisture content (OMC). The results of this literature study will be taken into consideration in the thesis's next chapters, which will concentrate on experimental research, numerical modeling, and analysis of the embankment soil slope stabilized using ceramic dust.

Overall, the literature review paves the way for further investigation of the issue and establishes the framework for the next chapters, eventually advancing our knowledge and comprehension of soil stabilization techniques for road embankment.

2.1 SOIL

Soil is a mixture of minerals, organic matter, gases, liquids, and countless organisms that together support life on Earth. Numerous physical, chemical, and biological processes including weathering and its related effects on erosion, contribute to the ongoing formation of soil (Afrin, 2017).

2.1.1 Soil Composition

Soil mainly consist of minerals, a certain proportion of decayed organic matter, soil water, soil air, and living organisms which exist in a complex relationship with each other. The precise proportions of the various components that make up soil are determined by a number of factors, including geographic location, the history of the soil's interaction with humans, climate, and the passage of time.

In general, the following elements are the primary components that make up soils:

2.1.1.1 Mineral matter

They consists of all of the minerals that were inherited from the rocks that served as their parents as well as any minerals that were generated by the combination of chemicals found in the soil solution.

2.1.1.2 Organic matter

Organic matter derives in major part from the decomposition of plant matter, which is then broken down and destroyed by the actions of animals and bacteria that are indigenous to the soil. This organic component is what differentiates soil from the geological material that can be found below the surface of the earth, which may otherwise share many of the features of soil. Soil is distinguished from this geological material by its presence of an organic component.

2.1.1.3 Air & Water

The majority of the voids in soil are typically filled with air and, to a lesser extent, water. Both air and water in the soil are vying for the same pore spaces, therefore there is a reciprocal link between the two as a result of this competition. As a direct consequence of this, the dynamic interaction that subsists between air and water in soils is one that is consistently subject to change. The ratio of the components by volume is generically indicated as:

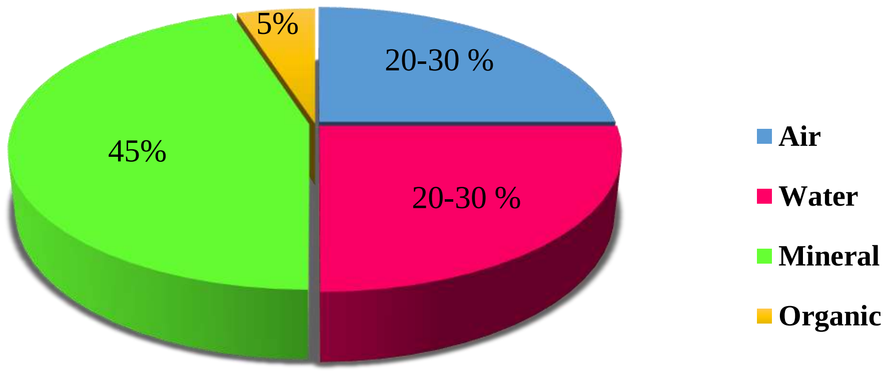

Figure 2.1: Soil Composition by Volume (Soil - Composition and Factors Affecting Soil Formation - Study Wrap, n.d.)

2.1.2 Soil Formation

Soil formation, also known as pedogenesis, is a multifaceted and drawn-out procedure that is affected by a variety of factors, including the parent material, climate, organisms, geography, and time. Soil formation is a process taking many thousands of years.

The process of soil formation begins from the volcanic, sedimentary or metamorphic rock materials and can be seen in operation at an early stage on the recently formed volcanic islands in Pacific regions. Colonization by Airborne microorganisms, plant seeds, insects, visits by migratory birds, etc. occurs after cooling and leads to primary colonization by plants (Lichens and Mosses) suited to bare rocks. Physical factors such as Wind, Rain, Snow and freezing/thawing cycles cause erosion and rock starts to show fractures. These fractures leads to more colonization and physical breakdown of rock materials. The old and dead plant parts starts decaying and thin organic layer is developed over the rocks. From this Parent Rock Material, by the interaction of climate, soil, vegetation and soil fauna, soil starts forming. After thousands of years the upper layer of the rocks gets converted into soils of different types.

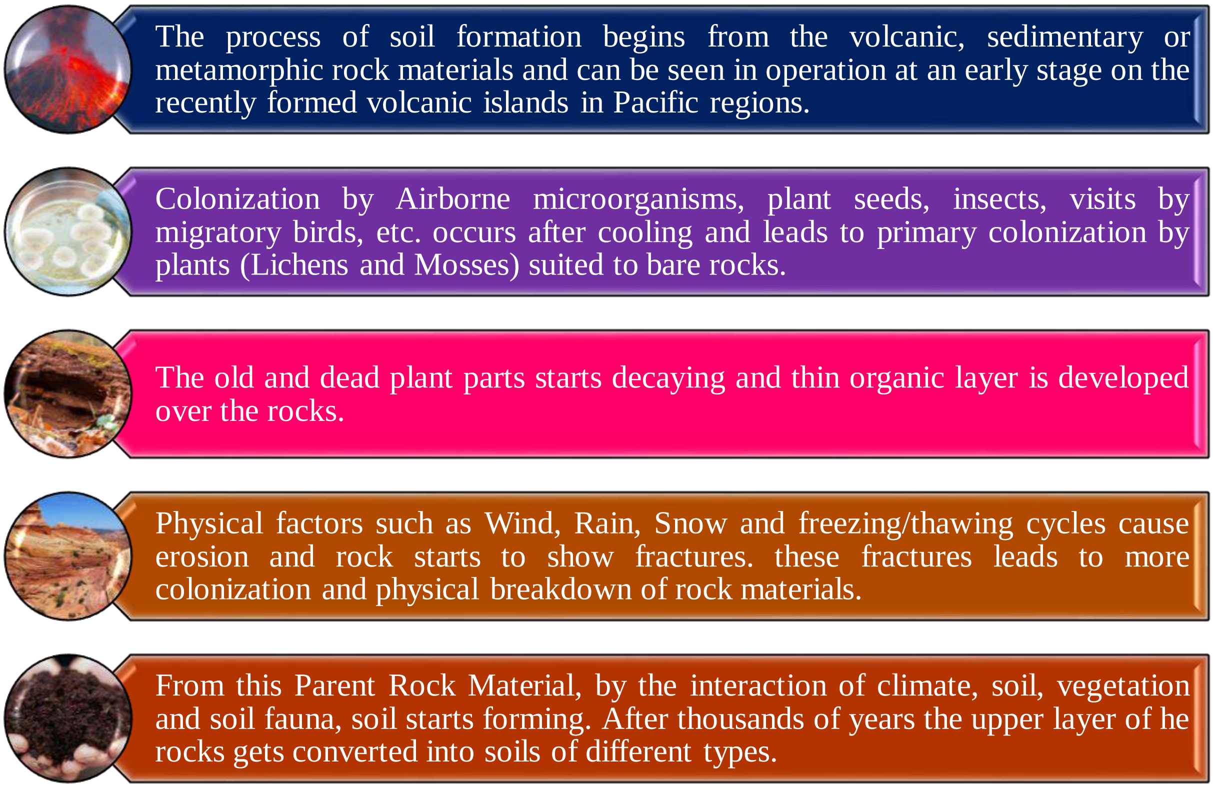

Figure 2.2: The pedogenic Processes (Conversions of rocks to Soils)

2.1.2.1 Phases of Soil Formation

There are typically five primary stages involved in the creation of soil:

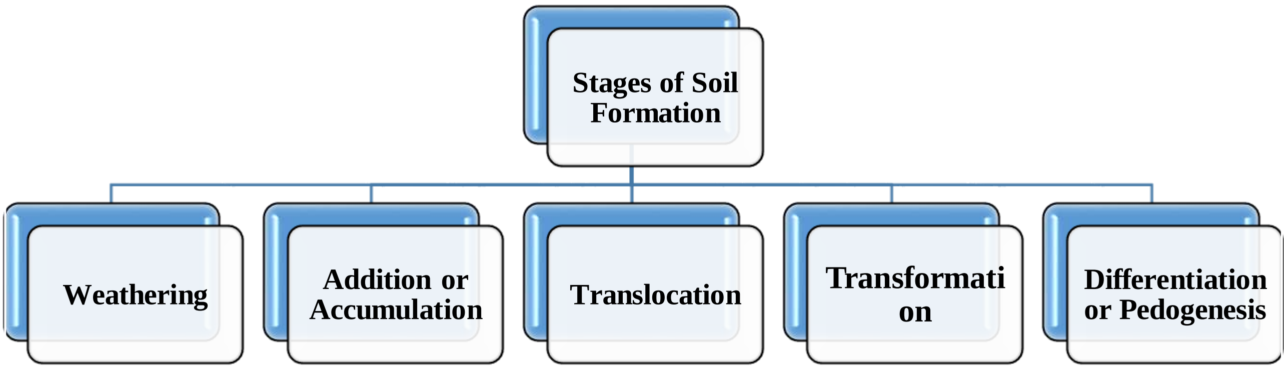

Figure 2.3: Different Stages of Soil Formation

2.2 TYPES OF SOIL

The processes of weathering, which ultimately lead to the creation of soil, can be either physical or chemical in nature. On the macroscopic size, a single particle can have the appearance of a large boulder, but on the microscopic scale, it can exist in a condition known as colloidal. Because of this, we can reach the conclusion that the term "soils" can be used to refer to all of the products that come about as a result of the weathering of rocks.

You may use the following picture as a guide while drawing the line diagram to classify different kinds of soil.

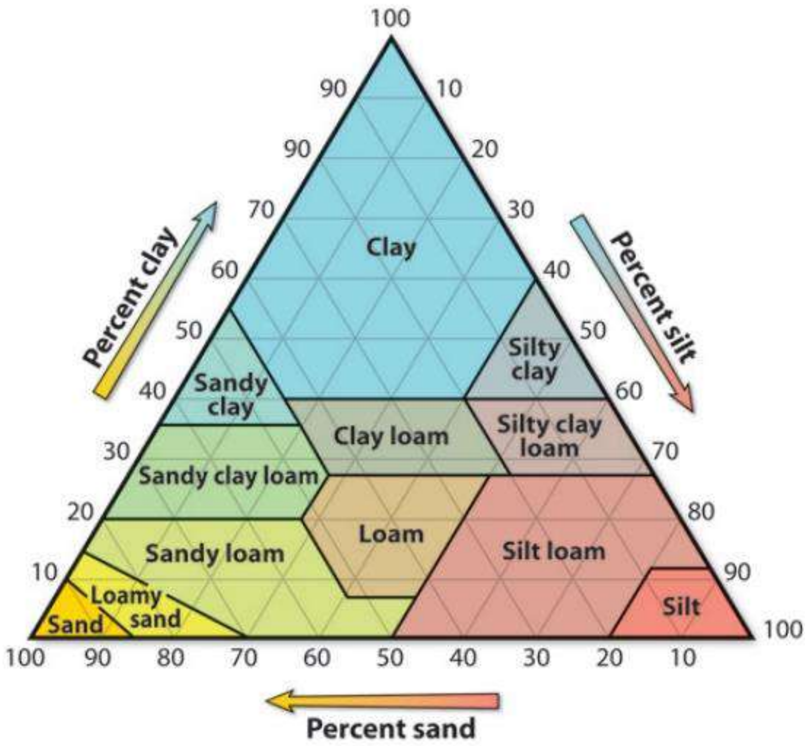

Figure 2.4: The Textural classification system (Park & Santamarina, 2017)

The soil is basically classified into four types:

1. Sandy soil.
2. Silt Soil.
3. Clay Soil.
4. Loamy Soil

2.2.1 Sandy Soil

Sandy soil is warm, dry, acidic, and nutrient-poor. Because clay weighs more than sand, sandy soils are light. These easy-to-work soils drain quickly. They warm faster than clay soils in spring but dry out in summer and lose nutrients to rain. Organic matter boosts plant nutrition and water retention. Sandy soil has worn rock. Sandy soils lack nutrients and water retention, making plant roots struggle to absorb water. This soil drains. Granite, limestone, and quartz become sand.

2.2.2 Silt Soil

Silt soil is light, moist, and fertile. Medium-sized particles make silt soils well-drained and moisture-retaining. Fine particles compress quickly and wash away with rain. Organic substances can stabilize silt particles. Silt is formed of rock and other mineral particles that are smaller than sand but larger than clay. The smooth, fine soil holds water better than sand. Moving currents carry silt near rivers, lakes, and other water bodies. Silt soil is fruitful. It improves soil fertility in agriculture.

2.2.3 Clay Soil

High-nutrient clay soil is heavy. Clay soils are moist and cold in winter and dry in summer. Clay soils, which include above 25% clay, hold a lot of water due to the gaps between clay particles. These soils drain slowly, take longer to warm up in summer, and dry up and crack in summer, which might challenge gardeners. Clay particles are the tiniest. This soil has little airspaces between particles. This soil stores water well and resists moisture and air. Wet, it's sticky, but dry, it's silky. Clay, the densest and heaviest clay, does not drain effectively or allow plant roots to grow.

2.2.4 Loamy Soil

Loam soil is a mixture of sand, silt and clay that are combined to avoid the negative effects of each type. These fertile, easy-to-work soils drain well. Sand or clay loam is their main makeup. The ideal balance of soil particles makes them a gardener's best buddy, but they still need organic matter.

2.2.5 Types of Soils based on Grain Size

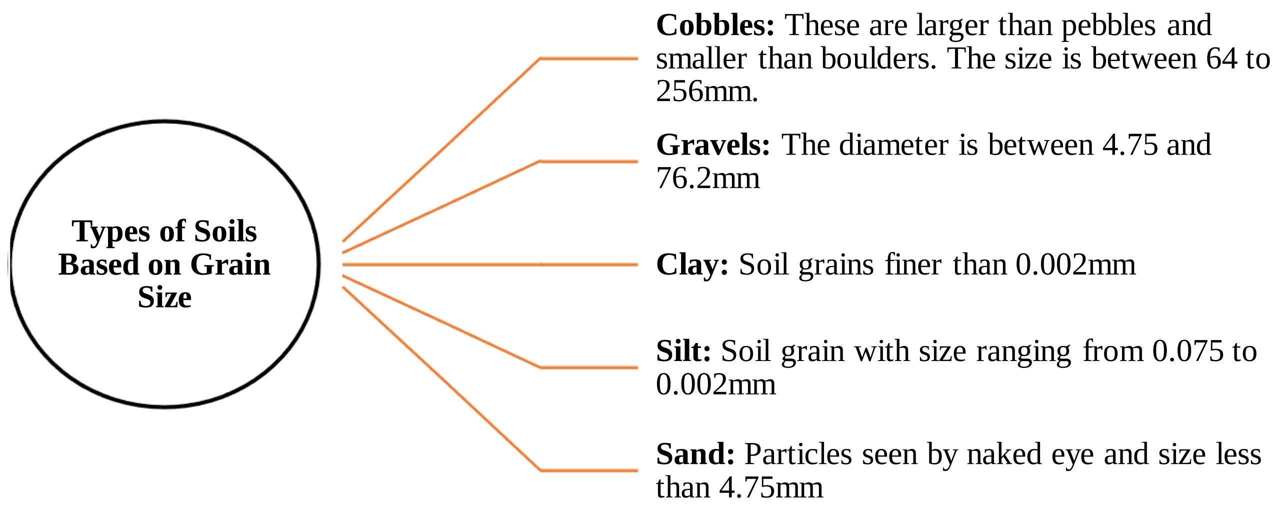

Figure 2.5: Types of Soils Based On Grain Size

2.3 STRENGTH OF SOIL

The capacity of a mass of soil to resist deformation or failure as a result of loads or stresses that are applied is referred to as the soil's strength..

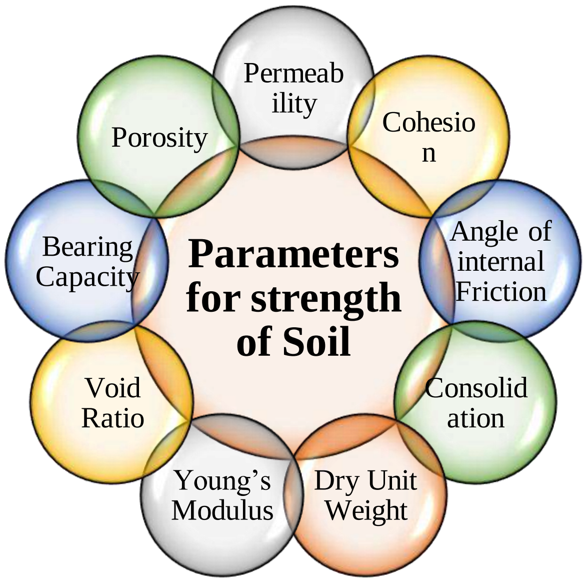

Figure 2.6: Parameters for strength of soil

Langfelder & Nivargikar studied that to a large extent, the shear strength of cohesion less materials is determined by five factors:

1. The mineralogical composition of the material
2. The size and gradation of the individual particles
3. The shape of the individual particles
4. The void ratio or dry density
5. The confining pressure.

2.4 SOIL STABILIZATION

A good strength of soil embankment is necessary in civil engineering projects such as railroad lines, highway networks, airport runways, etc. In general, soil stabilization is a technique for enhancing the qualities of soil by the blending and combining of various elements. In order to reinforce road surfaces and other geotechnical applications, improvements include raising the dry unit weight, bearing capacities, volume changes, and the performance of in situ subsoils, sands, and other waste materials (Firoozi et al., 2017).

2.4.1 Purpose of soil Stabilization

The construction of highways, dams, foundations for various structures, and other engineering structures in places that have poor or low grade soils is a serious challenge for engineers today (Archibong et al., 2020). When a soil lacks the qualities needed for the proposed structure, it needs to be stabilized. Compaction, pre-consolidation, drainage, and many additional processes are all included in the stabilization process. However, the composition of a soil mass is the most important factor in determining whether or not it is stable (Santosh, 1987).This is due to the fact that in the field, pure sands and pure clays react in different ways. Thus, it is essential to enhance the engineering features of such soil by choosing appropriate materials and techniques. The type of building, soil characteristics, cost, and environmental factors all play a role in the choosing of a specific material and method. It is important to consider the various industrial wastes that are created in large amounts.

Although the primary goal of soil stabilization is to improve the natural soil for the construction of highways and air fields (Arora, 2011) it is also used to change the permeability and compressibility of the soil mass in earth structures for controlling the grading of soils and aggregates in the construction of bases and sub-bases of the highways and air fields, parking areas, site development projects, and many other scenarios in which the sub-soils are not suitable for the construction of the desired structure. A wide variety of sub-grade materials, ranging from expansive clays to granular materials, can be treated by stabilization in a variety of different ways.

2.4.2 Classification of soil Stabilization

With respect to the addition of certain additives, soil stabilization process may be roughly grouped into two:

1. Stabilization of existing soil without any additives
2. Stabilization of existing soil with the use of additives

The two primary types of soil stabilization methods are categorized based on their respective approaches. The first type encompasses techniques like compaction and drainage, which aim to enhance the soil's physical properties and overall structural integrity. These methods primarily focus on optimizing the soil's compaction levels and managing its water content for improved stability.

The second type involves the use of various agents such as cement, lime, bitumen, and mechanical means. These methods work by bolstering the inherent shear strength of the existing soil, thereby fortifying its load-bearing capacity and resistance to deformation. For instance, cement stabilization involves blending cementitious materials with the soil to create a more robust composite, while lime stabilization employs lime to alter the soil's chemical composition for enhanced stability. Bitumen stabilization utilizes bituminous materials to reinforce the soil's structural integrity, and mechanical stabilization employs physical interventions to achieve similar results.

The process of using either naturally occurring or artificially produced additives in order to enhance the qualities of soil is referred to as "soil reinforcement" (Ramaji, 2012). When it comes to stabilizing unstable soils, there are several different reinforcing methods available. As a consequence of this, the approaches to soil reinforcement can be arranged into a variety of groups according to a number of distinct vantage points.

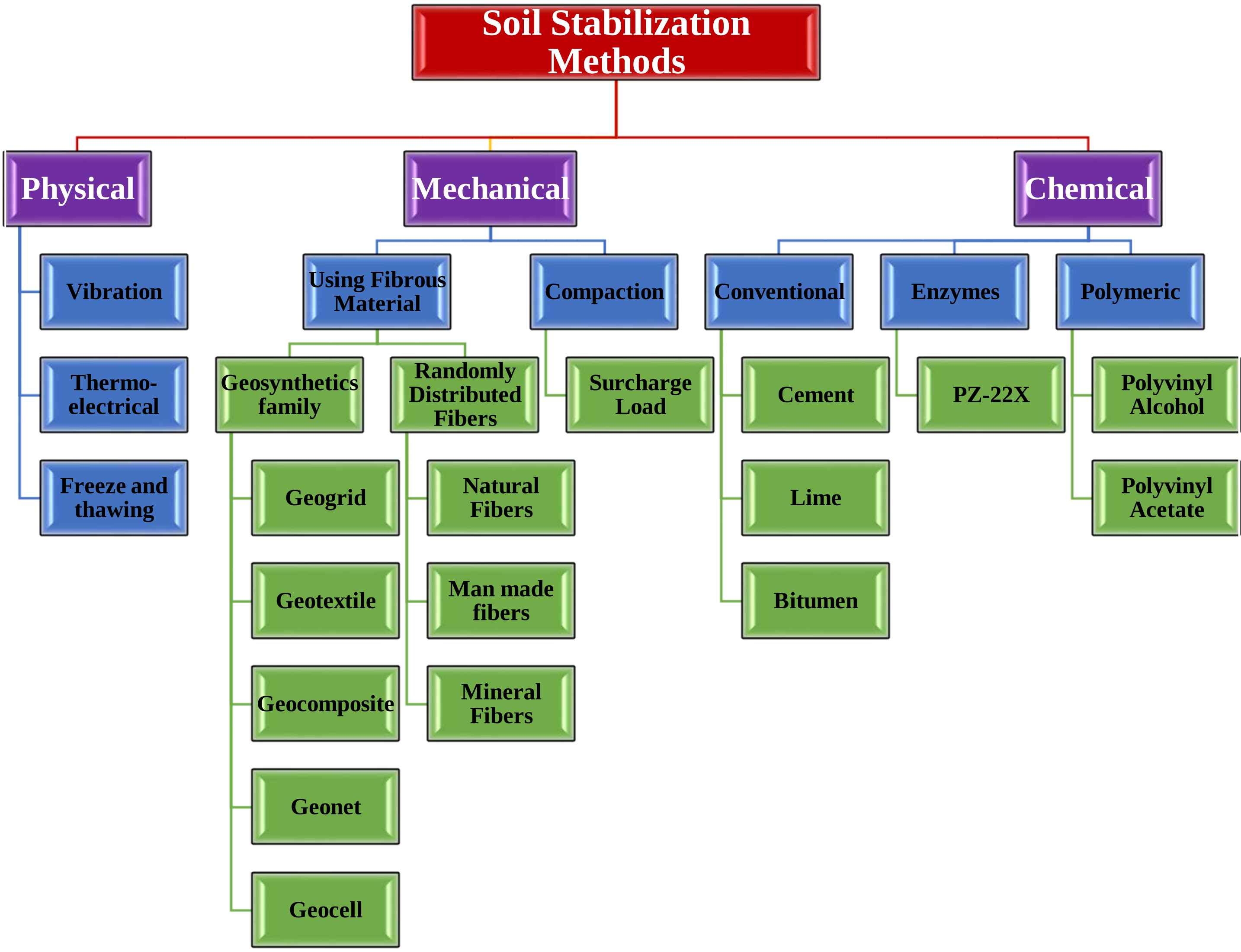

Figure 2.7: Different Procedures of Soil Reinforcement (Hejazi et al., 2012)

2.5 RESEARCH REVIEW AND ANALYSIS ON SOIL STABILIZATION USING CERAMIC DUST

Utilization of ceramic waste has emerged as a pressing issue in the construction industry and the production of raw materials in recent years. The research on recyclable construction material and demolition gives a benefit to waste management. This is one of the features of the research. Ceramic waste may have strong degrading power and durability, according to the findings of some researchers; however, there is still a need for additional work due to challenges in analyzing and modeling ceramic activity. They are also resistant to abrasion and have a low density, all of which are useful characteristics that help boost efficiency and efficacy (Zimbili et al., 2014). The vast majority of ceramic waste is generated throughout the process of manufacturing ceramic tiles, as well as during transportation and installation (Rani et al., 2014). Ceramic powder contain high amount of silica and alumina, usually more than 80% (El-Dieb, A. S., Taha, M. R., & Abu-Eishah, 2019). Ceramic dust is an inorganic, nonmetallic material that is formed by thermal action and cooling from natural materials that have a significant quantity of clay. Its pollution contains 1.6% CaO and 59.1% silica. Ceramic dust can be found in a variety of colors. It is possible to gather waste tiles from construction sites and break them up into smaller pieces. These smaller portions can then be put through an abrasion machine in Los Angeles to further reduce the size of the waste tiles (Ma et al., 2019).

To get better results, the ceramic dust can be combined with other garbage (Upadhyay & Kaur, 2016). As a result, there are several studies on soil stabilization using ceramic dust as an admixture.

Upadhyay & Kaur, 2016 have studied that stabilization using ceramic dust is one such waste material which can be used for improving the properties of poor soils. Ceramic trash is conveniently accessible at many production facilities and building sites. Waste management is a critical issue in developing nations like Pakistan since waste is produced at an accelerated rate. Ceramic waste may be easily used to stabilize soil, and the disposal issue can be solved in a way that is safer for the environment. Thus, using ceramic waste not only enhances the soil's qualities but also offers a solution to the issue of disposal. The qualities of clayey soils have been improved using ceramic waste materials in the study, and the impact of ceramic dust on various soil parameters has been assessed. They concluded that Maximum dry density is attained at a specific optimum content of ceramic waste and declines beyond this optimum content of ceramic waste. The optimal moisture content of the clayey soil decreases as the percentage of ceramic waste increases.

Chen et al., 2015 and colleagues investigated the effects of varying the amount of waste ceramic dust from 0 to 30% when added to shrink-swell soil that was locally sourced from the Baure district of Gombe state in northeastern Nigeria. Based on an examination of the test findings, it was discovered that a rise in ceramic dust led to a drop in the liquid limit, plastic limit, plasticity index, optimal moisture content, free swell, and swelling pressure. Additionally, it was discovered that as the waste ceramic dust content rose, so did the maximum dry density, unconfined compressive strength, and California bearing ratio. According to an X-ray diffraction examination of the shrink-swell soil, montmorillonite makes up the majority of the soil. According to the economic research, ceramic dust can reduce construction costs by up to 30% by reinforcing the subgrade of flexible pavements.

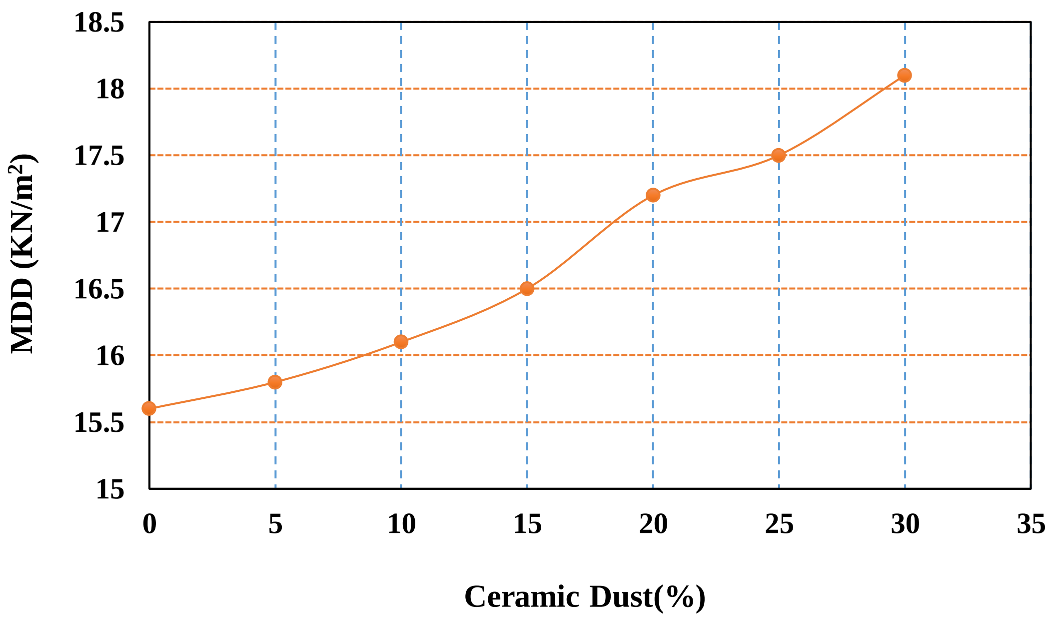

Figure 2.8: Variation of MDD with percentage of CD (Chen et al., 2015)

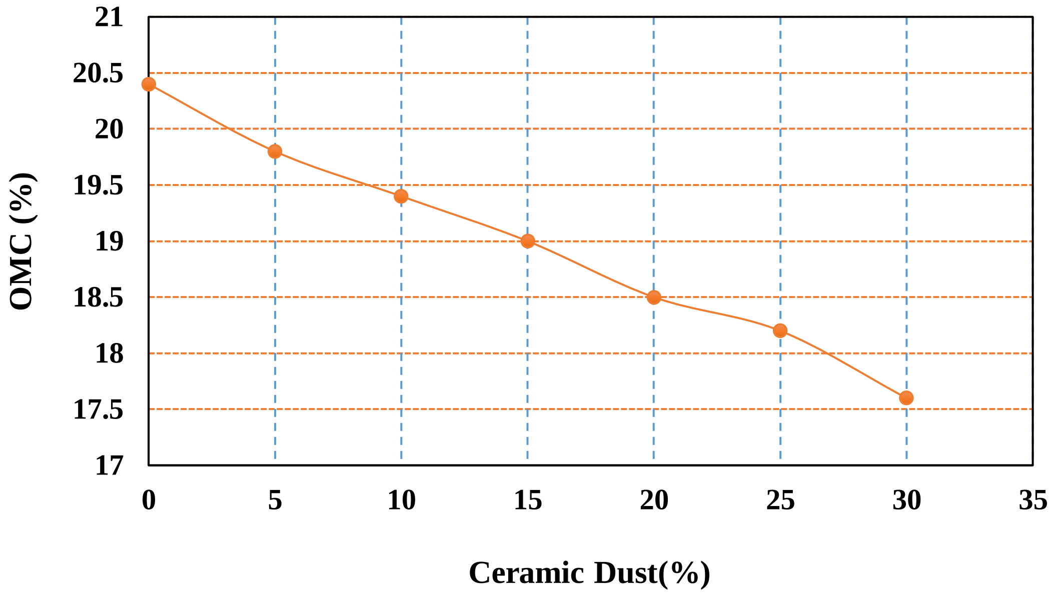

Figure 2.9: Variation of OMC with percentage of CD (Chen et al., 2015)

A. K. Sabat, 2012 investigated the impacts of waste ceramic dust on the liquid limit, the plastic limit, the plasticity index, the compaction characteristics, and the unconfined compressive strength, the California bearing ratio, the shear strength parameters, and the swelling pressure of soil. The soil found in the area was combined with ceramic dust in proportions ranging from 0 to 30%, with each increase of 5%. In the course of analyzing the results of the tests, it was discovered that the liquid limit, the plastic limit, the plasticity index, the optimum moisture content, the cohesion and swelling pressure all decreased, whereas the maximum dry density, the unconfined compressive strength, the California bearing ratio, and the angle of internal friction all increased. These compelling findings lay the foundation for an intriguing economic study that was undertaken alongside the geotechnical investigations. The economic analysis shed light on the potential cost savings that could be achieved by utilizing ceramic dust as a reinforcing agent in the subgrade of flexible pavements. The study revealed that concentrations of ceramic dust up to 30% could be effectively employed, providing a cost-effective means to enhance the strength and stability of the subgrade during construction projects. The results obtained from his experimental investigation are shown in figure 2.3-3 (Effect of variation of ceramic dust on MDD) and figure 2.3-4 (Effect of variation of ceramic dust on OMC).

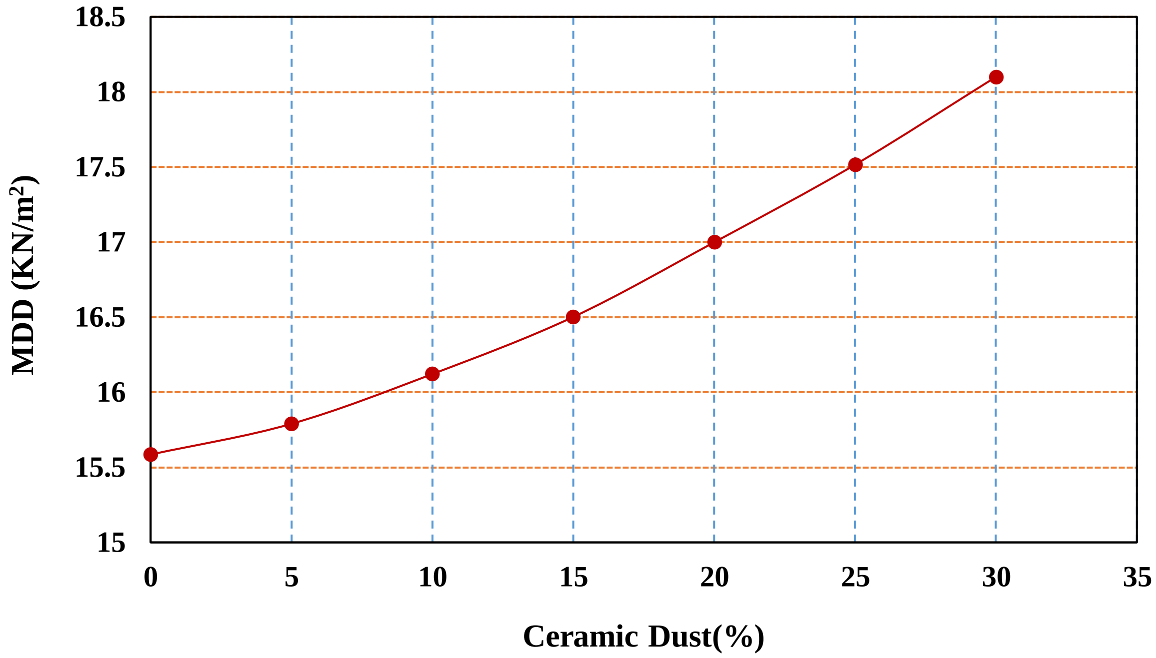

Figure 2. 10: Effect of variation of ceramic dust on MDD (A. K. Sabat, 2012)

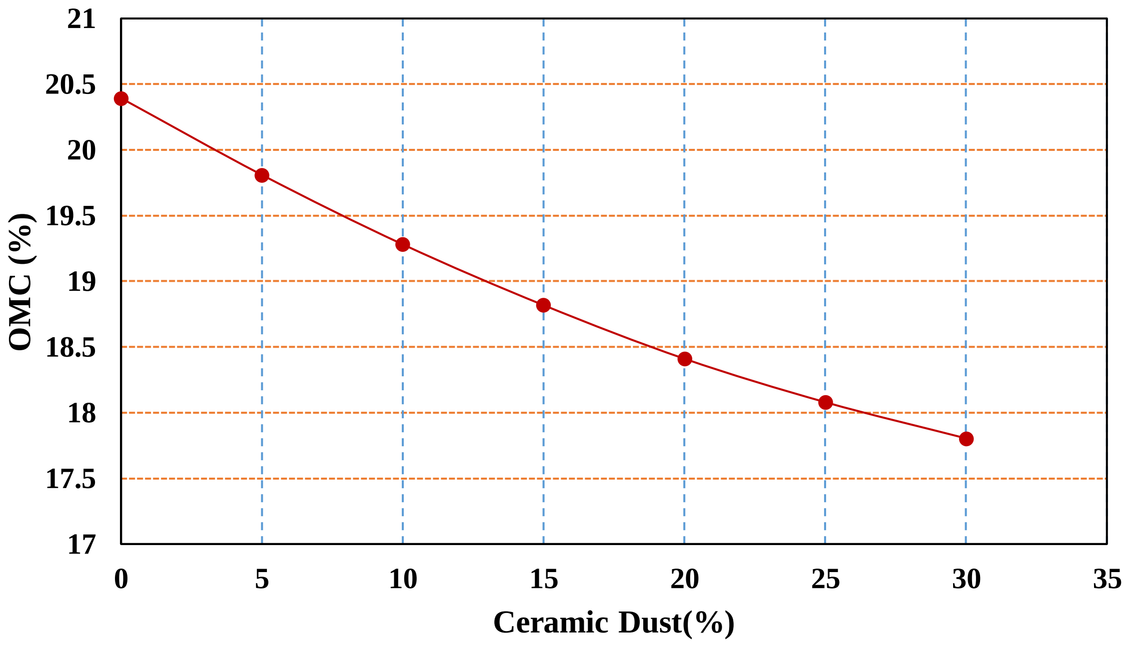

Figure 2. 11: Effect of variation of ceramic dust on OMC (A. K. Sabat, 2012)

Cabalar et al., 2017 conducted research into the possibility of using ceramic dust as a raw material in the construction of road pavement subgrades. Experiments were carried out to explore the behavior of soil that had been mixed with discarded ceramic tile grains in a variety of different proportions. According to the findings of the research, the incorporation of waste ceramic tile into the road pavement subgrade can make a contribution to the qualities of the subgrade that is beneficial. According to the findings of the study, the behavior of subgrades that had been mixed with waste ceramic dust should be investigated further. He discovered that the use of waste ceramic dust as a raw material in soil led to an increase in the soil's CBR value while simultaneously leading to a drop in the soil's UCS value. In addition, the study discovered that a rise in the amount of waste ceramic dust resulted in compaction tests revealing both an increase in the dry unit weight and a matching decrease in the water content of the sample being tested. The findings of the tests revealed that there was a correlation between a rise in the amount of waste ceramic dust and a drop in the void ratio.

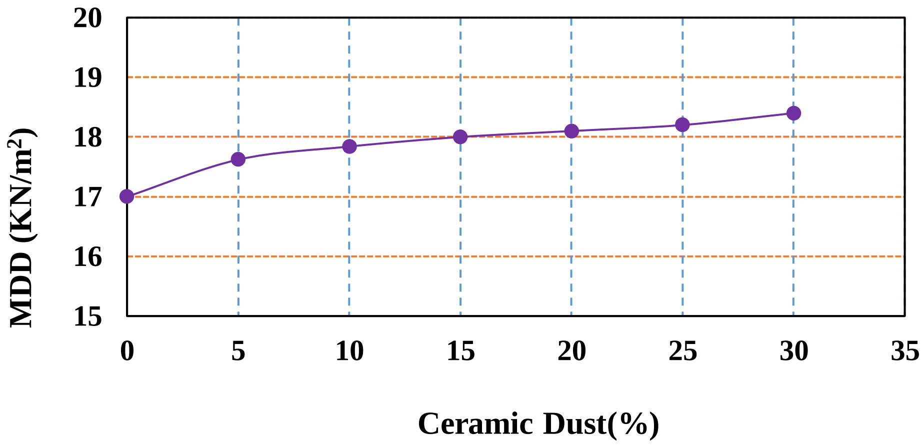

Figure 2.12: Variation of MDD with percentage of CD (Cabalar et al., 2017)

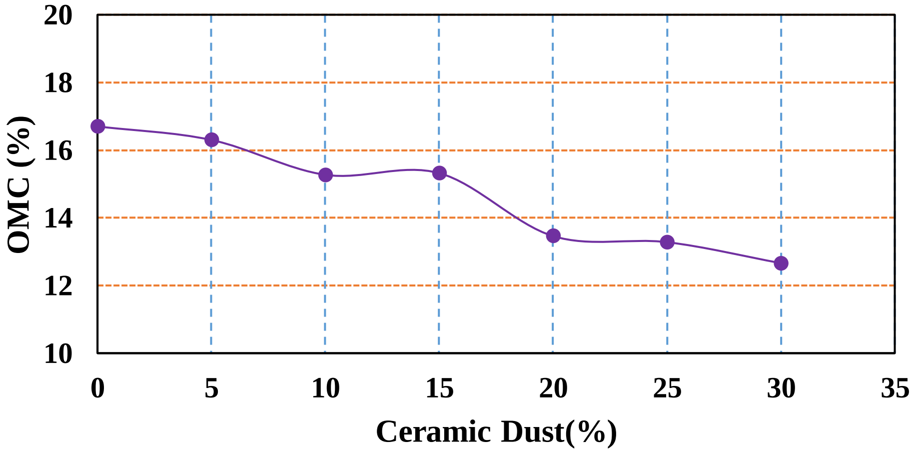

Figure 2.13: Variation of OMC with percentage of CD (Cabalar et al., 2017)

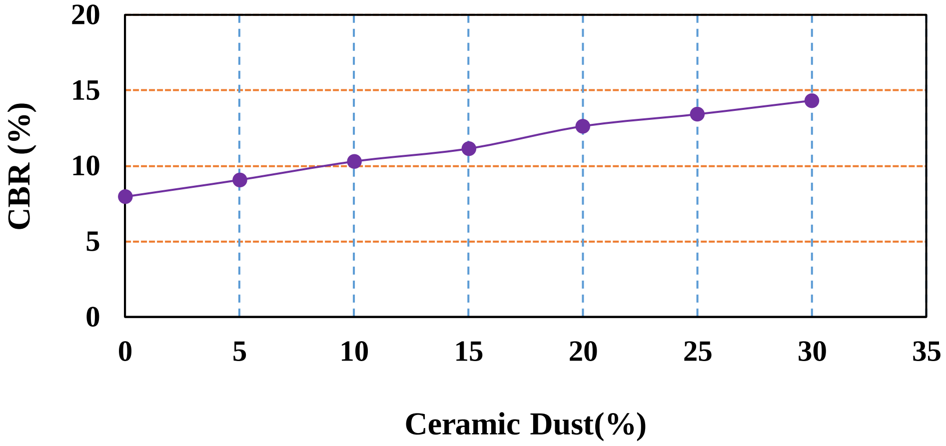

Figure 2.14: Variation of CBR with percentage of CD (Cabalar et al., 2017)

James & Pandian, 2018 investigated what happens when micro ceramic dust (CD) is combined with lime for the purpose of soil stabilization. According to the findings of the researchers, the incorporation of CD resulted in a marginally negative affect on the early strength of the stabilized soil after three days of curing, but it boosted the delayed strength of the soil to acquire between 12 and 14% strength after 28 days of curing. In addition to this, it was discovered that CD had an impact on the plasticity and swell-shrink characteristics of lime stabilized soil. According to the findings of the study, the incorporation of CD as an additive to lime for the purpose of soil stabilization may have significant applications in the building sector in the future.

Agrawal, 2017 explored the use of ceramic waste as a replacement for aggregates in concrete blocks, researching its economic and environmental benefits as well as its effects on the strength and weight of the concrete. He found that the use of ceramic waste significantly reduced the amount of aggregates required in the concrete blocks. According to the findings of the study, ceramic waste can be utilized as a viable replacement for coarse aggregate, resulting in a reduction in both the cost and environmental impact of the manufacturing of concrete. It was discovered that the concrete combination that yields the optimal compressive and flexural strengths is superior to the concrete that serves as a reference. In addition, the use of ceramics helped to slow down the destruction of the environment by recycling previously discarded materials and cutting down on the consumption of naturally occurring resources that were readily available.

Beyene et al., 2022 studied the individual and combined effects of natural lime and waste ceramic dust on the moisture content, compaction characteristics, Atterberg limits, California bearing ratio, specific gravity, swelling index, and soil particle distribution that are crucial for stable road construction. Different mix ratios' degrees of improvement were compared to Ethiopian roads authority's road construction standards. Both natural lime and waste ceramic dust were shown to significantly alter the geotechnical parameters of expanding subgrade. The dose of the stabilizers will determine the extent of the improvement. Natural lime was discovered to be more consistently effective than waste ceramic dust. It was determined that 6% of natural lime and 20% of waste ceramic dust provided the safest subgrades for roads. Both the California bearing ratio swell and the free swell of the clay soil were found to be lowered by adding and increasing the amount of stabilizers. The study concludes that natural limestone and industrial ceramic dust can be employed as stabilizing agents in clay subgrades to enhance their geotechnical qualities. Both the additive and synergistic effects of the two stabilizers were studied to provide a thorough basis for comparison. How much of an improvement is made in the soil's qualities depends heavily on how much of the stabilizers are employed. This research has implications for the design and construction of durable and safe road pavements, especially in regions with a high supply of natural lime and waste ceramic dust.

The research conducted by *Onakunle et al., 2019* aimed to examine the geotechnical properties of lateritic soil stabilized with ceramic waste dust additive. The study concluded that improved ceramic dust-lateritic soil is recommended for economic, durability, and environmental advantages. To achieve the objectives of this study, lateritic soil from Agbara, South-West, Nigeria, and pulverized ceramic materials gathered from construction site rubbles were collected. The lateritic soil samples were mixed with ceramic waste dust from 0 to 30% at an interval of 5%. In total, seven mixes were prepared. The study tested different samples to examine the grain-size distribution, Atterberg Limits, Proctor Compaction tests, and California Bearing Ratio tests. The CBR was done for both soaked and un-soaked samples. The un-soaked California bearing ratio (UCBR) test was performed immediately while the soaked California bearing ratio (SCBR) was performed after ninety-six (96) hours of soaking in water. The study revealed that the maximum dry density (MDD) increases while the optimum moisture content (OMC) decreases with the addition of ceramic dust up to 40%. CBR of the stabilized soil was observed to increase as the ceramic dust powder increased.

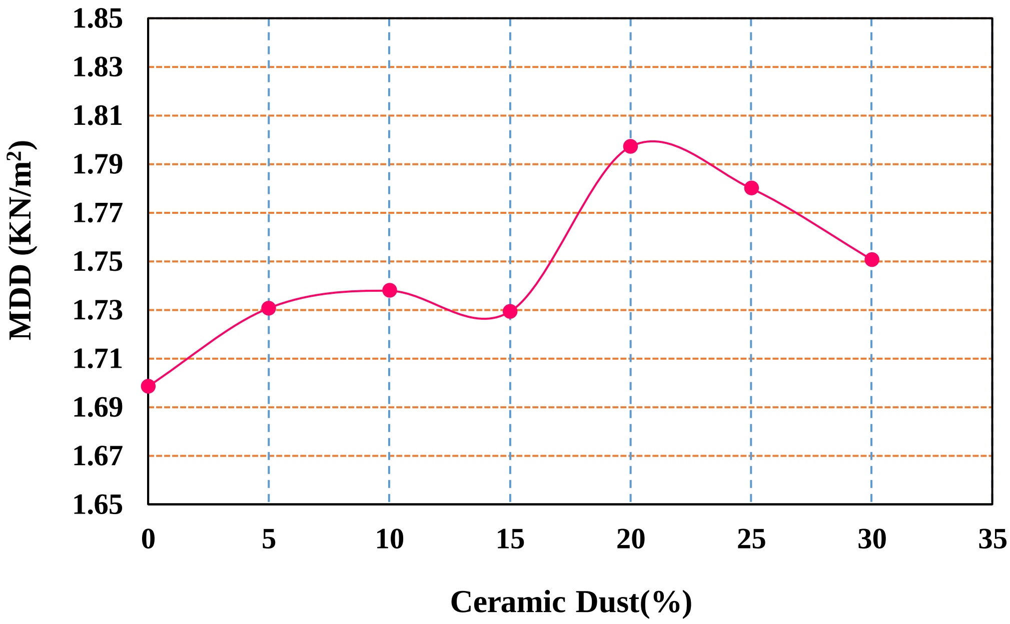

Figure 2.15: Plot of MDD with CD addition (Onakunle et al., 2019)

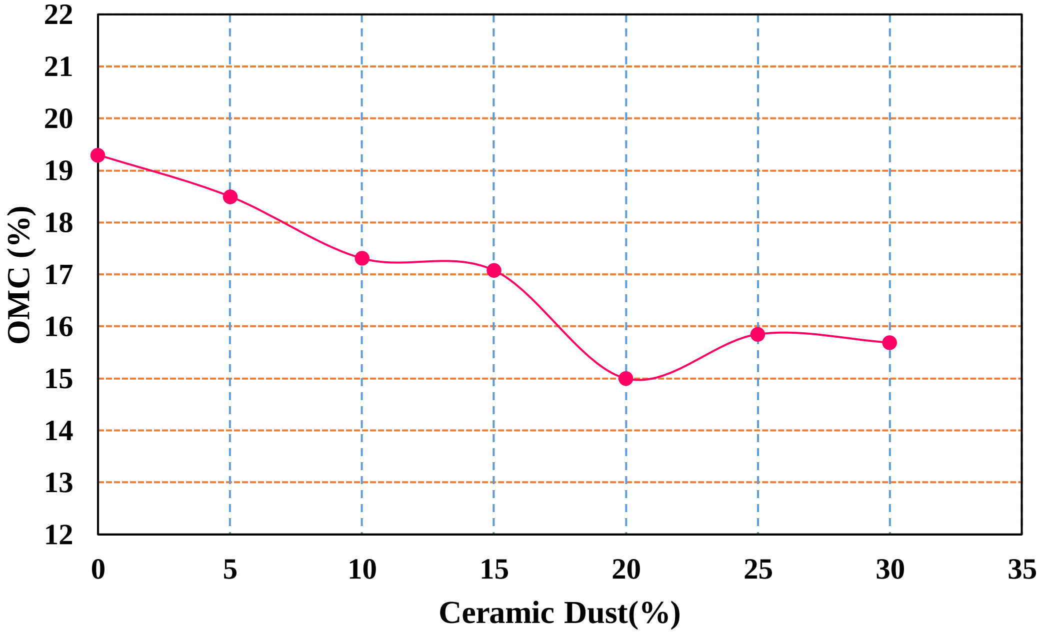

Figure 2.16: Plot of OMC with ceramic dust addition (Onakunle et al., 2019)

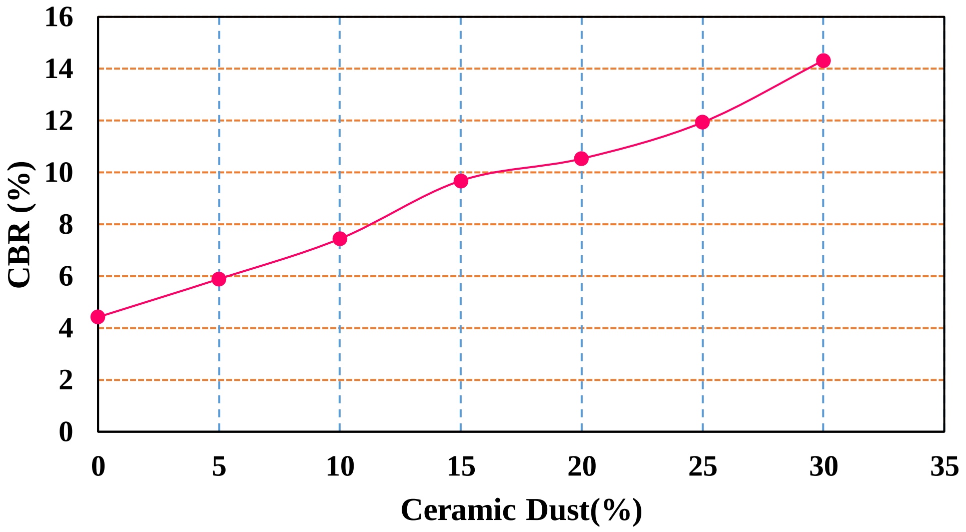

Figure 2.17: Plot of Soaked CBR with CD addition (Onakunle et al., 2019)

Tiza et al., 2016 did some research into the effectiveness of employing industrial waste products in soil stabilization. He investigated the fact that the majority of industrial solid wastes have been demonstrated to be quite helpful in improving the soil engineering features. The research methods and results are discussed regarding a variety of waste materials, including cement kiln dust, red mud, copper slag, brick dust, ceramic dust, polyvinyl waste, and fly ash. Laboratory tests such as the California Bearing Ratio (CBR), the Unconfined Compression Strength test (UCS), the Free Swell Index, the Liquid Limit, the Plastic limit, X-ray diffraction, and compaction are carried out. It has been shown that practically all of the different types of industrial waste that were investigated for this investigation have the potential to make expansive soils better. The vast majority of studies, on the other hand, has not supplied appropriate and exact economic data, longevity, and reliability of stabilized soils, together with the best building equipment and techniques to employ. In his research, he found that adding ceramic dust to soil in proportions of up to thirty percent, with increments of five percent, was both cost-effective and worthwhile in terms of increasing soil strength metrics.

Saxena, 2017 carried out experimental work with the intention of stabilizing dune sand by adding ceramic tiles as an admixture. Because dune sand has little cohesiveness and, as a result, very little compressive strength, its stabilization is very crucial. The analysis included carrying out tests known as the California Bearing Ratio (CBR) and

Direct Shear at the highest possible dry density and the most ideal level of moisture content. According to the findings of the study, dune sand can be made more stable by mixing in waste from ceramic tile production. With an increase in the particle size of the admixture, the maximum dry density of the mix composition of dune sand and ceramic tiles wasted as admixture will also see an increase. In addition, when keeping the particle size of the admixture constant, the maximum dry density will rise as the fraction of the admixture rises. When there is a greater amount of waste ceramic tiles in the mix, the angle of internal friction shifts in a different direction. On the other hand, for a given amount of wasted ceramic tiles of a given size, the angle of internal friction increases as either the percentage of wasted ceramic tiles or the quantity of wasted pottery tiles grows. The research came to the conclusion that the stabilization of dune sand may be achieved by increasing the proportion of admixture as well as the particle size.

Saber & Iravanian, 2021 investigated the viability of repurposing ceramic dust for soil stabilization as an environmentally responsible and economically advantageous means of disposing of this trash. The researchers traveled to Northern Iraq and collected three distinct samples of clay soil. They then carried out a series of experiments in order to investigate the effect that adding waste ceramic dust in two different grading sizes had on the engineering qualities of the samples. According to the findings of the study, the incorporation of waste ceramic dust led to significant enhancements in the material's main mechanical parameters. These included an increase in maximum dry density, unconfined compressive strength, and California bearing ratio. In addition, the clay's liquid limit, plastic limit, and plasticity index all dropped as the quantity of ceramic dust in the clay increased. According to the findings of the research, waste ceramic dust can be put to use to address problems with trash disposal and lessen the impact that ceramic waste has on the environment. However, the researchers came to the conclusion that the effectiveness of soil stabilization is largely reliant on the type of ceramic dust that is used and the quantity that is employed. The findings of this research report reveal, on the whole, that waste ceramic dust may be an environmentally friendly and cost-effective material for soil stabilization, particularly for the construction of highways. The purpose of this study is to provide a detailed review of the possible benefits of employing waste ceramic dust in soil stabilization, with the objective of reducing the negative impact that waste disposal has on the environment and contributing to sustainable development.

A. K. Sabat et al., 2011 studied the influence of marble dusts on the strength and durability of an expansive soil that had been stabilized with the optimal amount of rice husk ash (RHA). According to the results of the Unconfined Compressive Strength (UCS) testing, 10% is the ideal percentage of RHA to include in the material. Marble dust was added to RHA stabilized expansive soil in increments of 5%, all the way up to a maximum of 30% based on the dry weight of the soil. After 7 days of curing, these samples were put through compaction tests, UCS tests, Soaked California Bearing Ratio (CBR) tests, swelling pressure tests, and durability tests. The Unconfined Compressive Strength and Soaked CBR of RHA-stabilized expansive soil both rose by up to 20% when marble dust was added. The continued addition of marble dust brought to undesirable changes in these qualities. No matter what percentage of marble dust is added to RHA-stabilized expansive soil, the Maximum Dry Density (MDD) and Swelling Pressure of expansive soil continue to decrease, while the Optimum Moisture Content (OMC) continues to increase.

Prakash, 2017 conducted an experimental study that was aimed to assess the effects of incorporating crushed ceramic tiles as a potential replacement for natural coarse aggregate in concrete production. The research, published in the reputable journal Construction and Building Materials, investigated various mix proportions by adjusting the percentage of ceramic dust, ranging from 10% to 50%, with increments of 10%. The findings revealed that the inclusion of ceramic dust contributed to enhanced compressibility of the concrete-ceramic dust mixture. Notably, after thorough analysis, Prakash concluded that the optimal proportion of ceramic tile in the mixture was determined to be thirty percent, as this proportion showcased the most favorable and advantageous outcomes in terms of concrete performance and strength. This study's results present valuable insights into the utilization of recycled ceramic materials for sustainable construction practices, further contributing to the growing body of knowledge in the field of construction engineering and materials science.

Table 2. 1: Summary of the research conducted by different researchers on soil stabilization using ceramic dust

Test No.	Conducted By	Material Used	Purpose	Amount of Ceramic Dust used	MDD (kN/m^3)	OMC (%)	UCS (kN/m^2)	CBR (%)	Compressibility	Swell (kPa)	L.L, P.L, P.I	Results
1	(Upadhyay & Kaur, 2016)	Clayey Soil Available Locally was blended with the tile waste	Analyze the effect of the waste on the clayey soil	0 to 30% with an increment of 10%		-		+ 105		- 48	-	Up to 20% ceramic dust can be used to strengthen clayey soil
2	(Chen et al., 2015)	Ceramic powder and shrink swell soil	Effect of ceramic dust on engineering properties of shrink swell soils	0 to 30% with an increment of 5%	+ 15.6 ~ 18.1	- 20.4 ~ 17.6	+ 55 ~ 98	+ 150		- 130 ~ 38	- 71~35 32~18 39~17	Up to 30% can be used in strengthening subgrade of flexible pavement
3	(A. Sabat, 2012)	Ceramic powder and expensive soil	Stabilization of expensive soil with ceramic dust	0 to 30% with an increment of 5%	+ 15.6 ~ 18.1	- 20.4 ~ 17.6	+ 55	+ 150		- 130~24	- 62~35 30~20 32~15	Soil Changes from CH to CL group

Test No.	Conducted By	Material Used	Purpose	Amount of Ceramic Dust used	MDD (kN/m³)	OMC (%)	UCS (kN/m²)	CBR (%)	Compressibility	Swell (kPa)	L.L, P.L, P.I	Results
4	(Cabalar et al., 2017)	Ceramic tiles and low plasticity clay (C.L type soil)	Use of ceramic tiles as a raw material in the design of road pavement for subgrade	0 to 30% with an increment of 5% by dry weight of specimen	+ 17.3~18.4	- 17~13	- 540~260	+ 8~14	-	- 2.69~1.48		Up to 30% of ceramic dust can be alternative material to improve performance of CL-Type soil
5	(James & Pandian, 2018)	Micro ceramic powder and three different lime content (Below ICL, ICL and above ICL)	Use micro ceramic powder as additive to lime in soil stabilization	Increasing proportion to the lime sol mix for 3 wt. %, 5.5 wt. % and 7 wt. %			+ 1398.77~1595.38		+ 12~14%	- 100~50%	- 68~49 27~37 41~12	0.5 wt. % CD dosage is optimal dosage for all three lime to gain 12-14% strength
6	(Agrawal, 2017)	Crushed Ceramic dust	Effect of addition ceramic tiles as a replacement for natural coarse aggregate	0 to 50% with an increment of 10% of substitution					+ 5.43%			Optimal value of ceramic to be used as replacement in mix is about 30%.

Test No.	Conducted By	Material Used	Purpose	Amount of Ceramic Dust used	MDD (kN/m^3)	OMC (%)	UCS (kN/m^2)	CBR (%)	Compressibility	Swell (kPa)	L.L, P.L, P.I	Results
7	(Onakunle et al., 2019)	Lateritic soil stabilized with ceramic dust	Stabilization of lateritic soil from Agbara Nigeria with ceramic dust	0 to 30% with an increment of 5%	+ 17~ 17.5	- 19.3~ 15.6		+ 4.55~ 14.4			- 59~ 35 40~ 23 19~ 12	From standpoint of economy and strength, up to 30% of CD can be used for soil improvement
8	(Tiza et al., 2016)	Ceramic powder was blended with soil	Effect of ceramic powder in construction of subgrade of flexible pavement	5 to 30% with an increment of 5%	+	-	+	+		-	- -	30% ceramic dust considered to be very economical any worthy to improve soil strength parameters
9	(Saxena, 2017)	Dune sand mixed with ceramic tiles	Stabilized dune sand by using ceramic tiles powder	5% to 30% with an increment of 5%	+	-		+				Up to 30% ceramic dust can be used for soil stabilization.

Test No.	**Conducted By**	**Material Used**	**Purpose**	**Amount of Ceramic Dust used**	**MDD (kN/m^3)**	**OMC (%)**	**UCS (kN/m^2)**	**CBR (%)**	**Compressibility**	**Swell (kPa)**	**L.L, P.L, P.I**	**Results**
10	(Prakash, 2017)	Ceramic tiles	Impact of crushed ceramic tiles to replace them for natural coarse aggregate	10 to 50% ceramic tile powder is used with an increment of 10%			+		+			Calculated optimum benefit of ceramic tiles used in the mix is 30%
11	(A. K. Sabat et al., 2011)	Marble Dust, Rice Husk Ash with expensive soil	Stabilization of expensive soil with Marble dust and Rice husk ash	0 to 30% with an increment of 5%	- 15.9~14.9	+ 21.7~24.5	+ 75~200	+ 2.5~8		- 110~0		Optimum proportion of Soil: Rice husk ash: Marble dust was found to be 70: 10: 20.
12	(Beyene et al., 2022)	Natural lime and waste ceramic dust	Use of Natural lime and CD in modifying properties of highly plastic clay		+	-		+				Optimum dosage for natural lime was 6%, and ceramic was 20% for safe road subgrades

2.6 PAVEMENT STRUCTURE

Pavement is one kind of hard surface that can handle foot or vehicle traffic and lasts for a long time. Pavement is made up of long-lasting surface material that is set down. Pavement may also be utilized for a variety of other functions. The primary purpose of this design element is to ensure that the applied vehicle loads are dispersed uniformly over all of the numerous layers that make up the Subgrade. The roadway's asphalt should have adequate traction, be pleasant to drive on, effectively reflect light, and produce a minimal amount of noise pollution. These are the criteria that should be met.

2.6.1 Pavement layers and their function

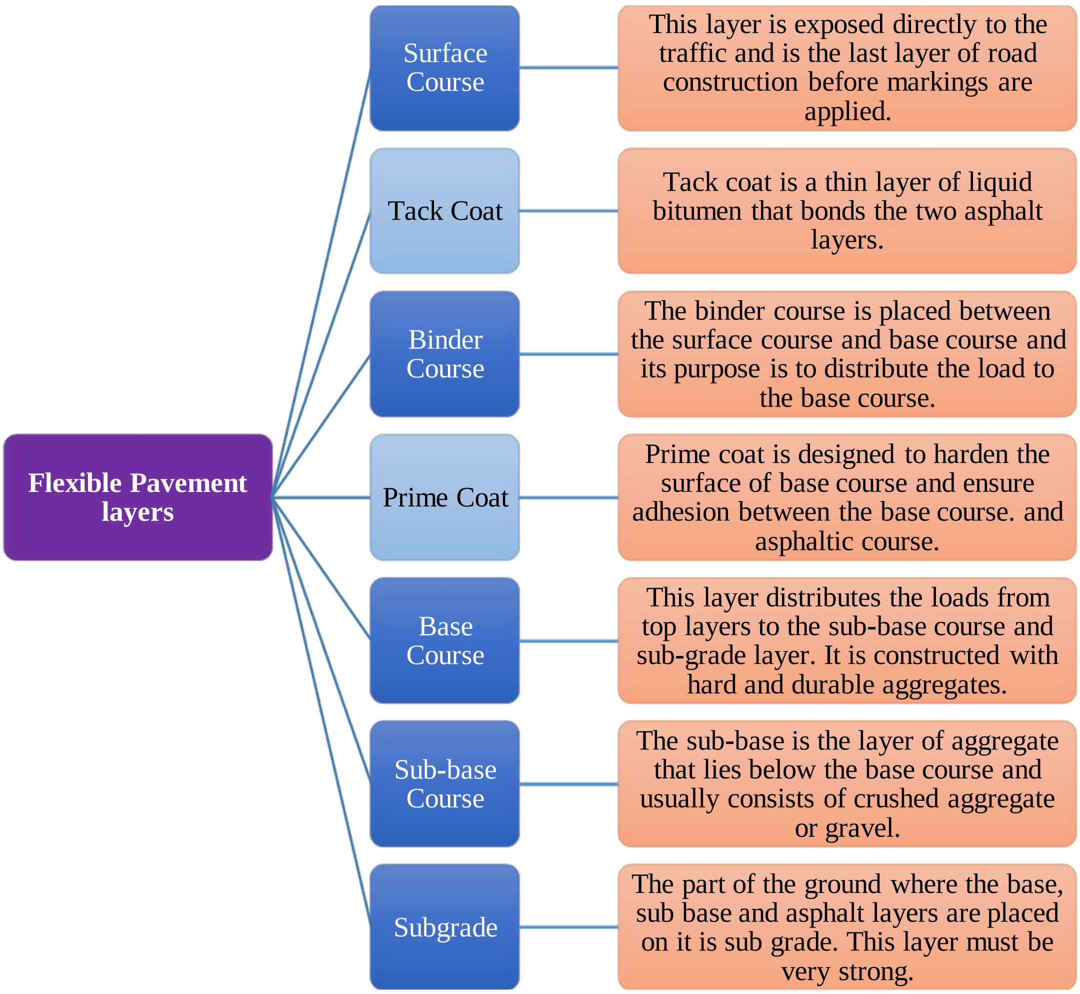

Figure 2.18: Structure of a typical flexible pavement

2.7 SLOPE STABILITY

Slope instability problems are quite common on road embankments and cause failure in the road embankments owing to pavement movement, which results in either substantial settlement or sliding due to insufficient shear strength. Normal fill can be a mixture of several soils, such as silty sand, clayey sand, or silty clay, which are regularly seen. Various areas in Pakistan have embankment material. Swelling or shrinkage-related soil movements in the soils beneath infrastructures such as pavements, embankments, and light to medium-loaded residential and commercial buildings are widespread as a result of climate fluctuations (Khan & Abbas, 2014). Soil movement in pavements causes settlements and surface cracking, resulting in unpleasant driving conditions as well as costly repair and maintenance for roadways across the country.

Geotechnical engineers examine slopes largely using the factor of safety values to estimate how close or far the slopes are to failure. The most frequent analytical approaches are conventional limit-equilibrium techniques. Numerical modeling using finite element analysis methodologies and great commercial softwares such as PLAXIS, GEOSLOPE, GEO5, SLIDE, and others has created a powerful practical alternative to the help of a geotechnical engineer. The goal of this study is to do a slope stability analysis of a man-made slope using the finite element method and the PLAXIS 2D software.

2.7.1 Factors Affecting Slope Stability

Following factors affect the stability of natural and manmade slopes:

- Slope Geometry
- Pore-water pressure
- Weak planes
- Dynamic forces
- Settlement
- Angle of internal friction

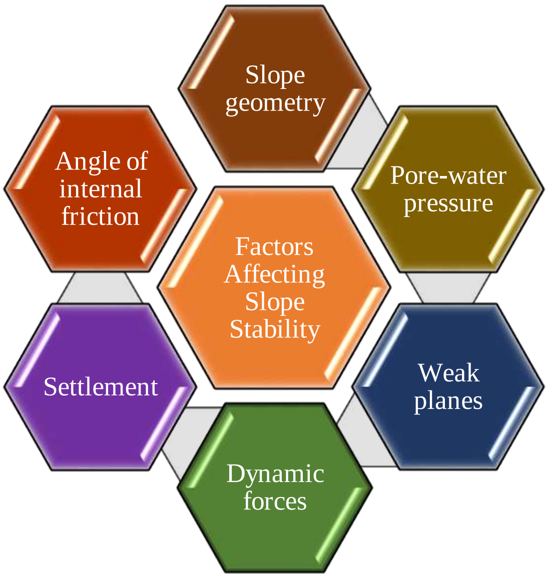

Figure 2.19: Factors effecting stability of slopes

2.7.2 Methods of evaluating safety factor for slopes

Computational methodologies, software design, and high-speed, low-cost technology have all seen fast advancements in recent years. The limit equilibrium and finite element approaches are particularly relevant to slope stability analysis. However, when employing limiting equilibrium methods to assess slopes, many computational challenges and numerical inconsistencies may emerge in determining the critical slip surface and thus creating a factor of safety (depending on the geology). Despite these inherent limitations, limited equilibrium remains the most often utilized strategy due to its simplicity. However, as personal computers became more widely available, the finite element method has become more popular in slope stability analysis. One advantage of finite element over limiting equilibrium is that no assumptions are required about the shape or location of the critical failure surface. In addition, the method can be easily used with others to calculate stresses, movements, pore pressures in embankments and seepage induced failure as well as for monitoring progressive failure (Hammouri et al., 2008).

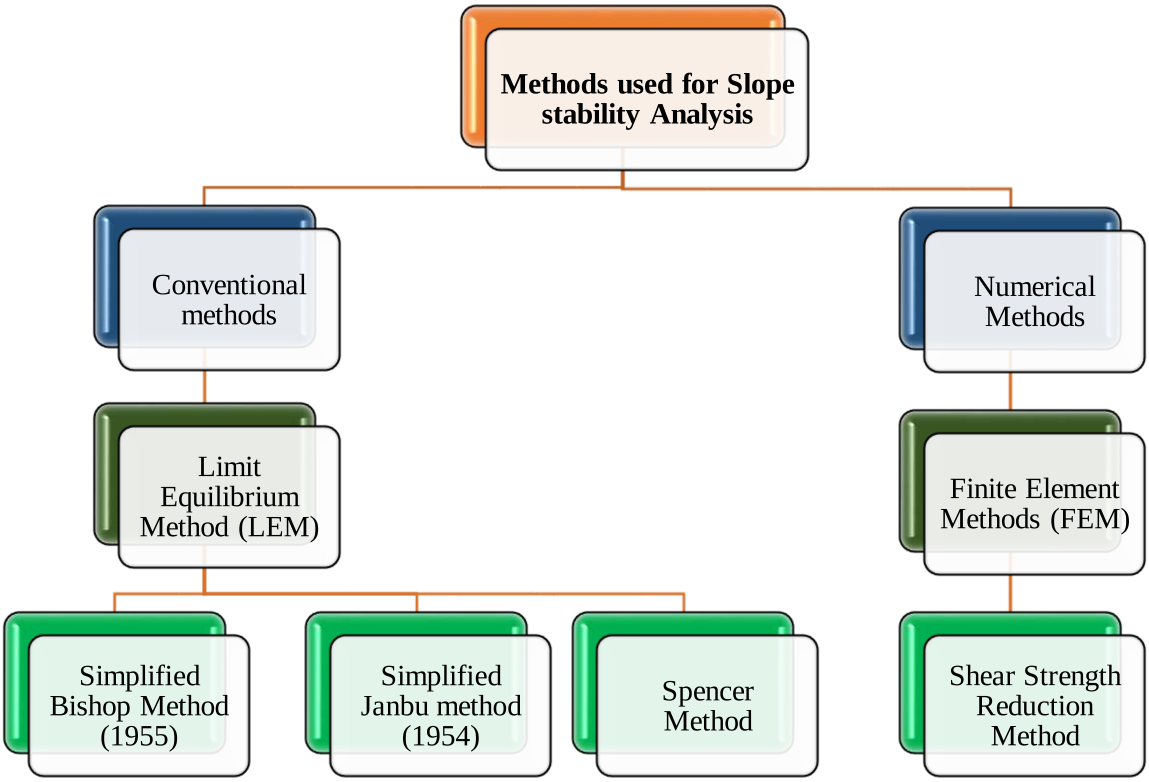

Figure 2.20: Conventional and Numerical Methods used for slope stability analysis

2.7.2.1 Limit equilibrium methods

In limiting equilibrium method for analysis of slope stability, the failure slope's mass is typically discretized into smaller slices for analysis, and each slice is then treated as a separate sliding block. A slide-mass is divided into n smaller slices in all limit equilibrium slope stability analysis methods. A broad system of forces affects each slice. In order to do a slope stability analysis by limiting equilibrium, it is typically necessary to look for the size and location of the more critical failure surfaces. Different methods are used, such as the grid search for failure surfaces with regular shapes and random search methods for failure surfaces with irregular shapes (Boutrup & Lovell, 1980). All kinds of limit equilibrium analysis have the same end result, which can be expressed as a safety factor (Omari & Boddula, 2012). The factor of safety is defined as the ratio of the summation of resisting forces and moments to the summation of driving forces and moments which bring the slope into a state of equilibrium along a given slip surface as given in equation 1. Values of safety factors for different type of constructions are shown in table 2.5.

$$FOS = \frac{\sum \boldsymbol{Resisting\ Forces\ Moments}}{\sum \boldsymbol{Driving\ Forces\ Moments}} \quad (\mathbf{1})$$

Table 2. 2: Value of safety factors for design (Sungkar et al., 2020)

No.	Safety Factor	Description
1	< 1.0	Unsafe
2	1.0 – 1.2	Query safety
3	1.25 – 4.0	Safe for excavation, embankment, query for dam
4	1.5 – 1.75	Safe for dam/reinforcement

The surfaces that provide lower values for the factor of safety are the critical failure surfaces.

2.7.2.2 Finite Element Methods

The slope stability is frequently evaluated using limit equilibrium techniques. On the other hand, the slope stability analysis in a two-dimensional setting has been applied using the finite element method (FEM) with the shear strength reduction (SSR) methodology (SSRFEM) (Zienkiewicz et al., 1977; Smith, I. M., and Griffiths, 1988). The basic concept of finite element method (FEM) is building complicated objects from simple intercommoned, blocks or elements. These interconnected blocks or elements are called finite element mesh as shown in figure 2.24. The mass under examination is represented by an assembly of elements joined at a limited number of nodal points using the finite element approach (Sharma, H., & Lewis, 1994). The finite element method and the limit equilibrium approach vary in that the failure geometry does not need to be estimated for the former. The stress-strain behavior of the material under examination can be used to determine the associated strains when you know the stress conditions. The results of the finite element analysis display a mesh with a stress or deformation vector (Omari & Boddula, 2012).

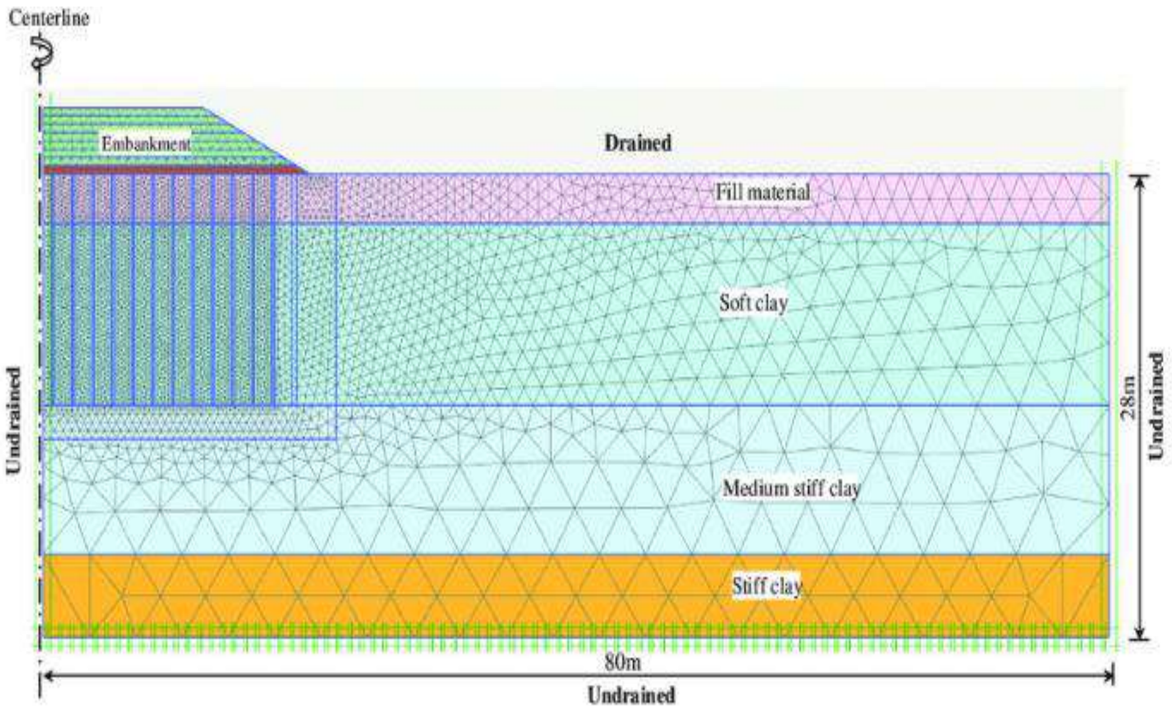

Figure 2.21: 2D Finite element mesh of a road embankment (Dang et al., 2018)

2.7.2.3 Shear Strength Reduction Method

Utilizing a methodical approach, the SSR technique for slope stability analysis uses finite element analysis to identify the stress reduction factor (SRF) or factor of safety value that pushes a slope to the brink of failure. The SRF lowers the shear strengths of all the materials in a slope's FE model. This model is then subjected to a standard FE analysis up until a crucial SRF value that causes instability is reached (Hammah et al., 2005). In the SSR method, a slope is considered unstable when the FE model does not converge to a solution (within a predetermined tolerance). The existing shear strength technique, based on the Mohr–Coulomb criterion, is implemented by reducing the values of friction angle and cohesive strength. For a Mohr–Coulomb material, its shear strength is a linear function of stress level. When the strength parameters of the original Mohr–Coulomb failure envelope have been reduced, the corresponding shear strength of all points in the medium failing in shearing, e.g., in the case of a slope stability problem, can be described with a single shear failure envelope that still satisfy the linear Mohr–Coulomb criterion (Fu & Liao, 2010).

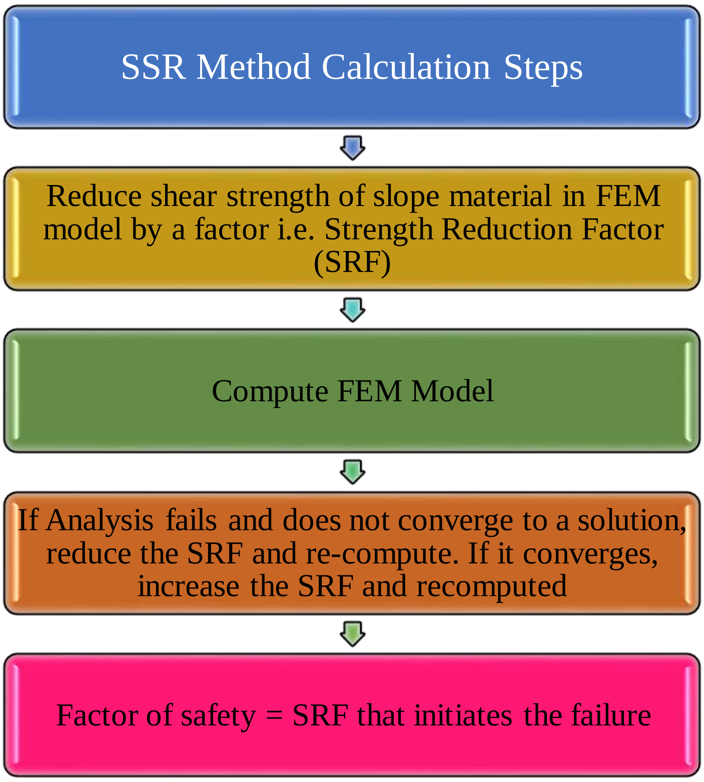

Figure 2.22: Basic steps for Shear strength Reduction approach in Finite Element Method

The Shear Strength Reduction Method (SSRM) is used in geotechnical engineering to analyze the stability of slopes or other geotechnical structures under working load conditions. Initially, the analysis is conducted using characteristic strength and stiffness parameters, resulting in a characteristic strength envelope as shown in figure 2.26 (effective cohesion and angle of internal friction) that represents the potential failure surface. During the working load analysis, Mohr's circles are drawn at various stress points within the structure. Some of these stress points may already touch the yield surface of the characteristic strength envelope, but there can be a significant difference between the actual Mohr's circles and the failure envelope due to the complexity of the constitutive models involved. To obtain the factor of safety using the SSRM, a strength reduction analysis is performed. In this process, the effective cohesion and effective friction angle are incrementally reduced step by step until equilibrium cannot be achieved in the numerical analysis anymore. It's essential to perform these reductions gradually as an abrupt change could lead to convergence issues in the analysis. As the strength parameters are reduced, some stress points will reach the Mohr's circle and will experience failure, causing a redistribution of forces within the structure. This redistribution allows for the system to maintain stability until a critical point is reached, where too many stress points are at their limiting condition (Kazushige Sogawa, 1970). At this stage, the code cannot achieve equilibrium anymore, and the factor of safety is obtained based on the last stable state. The SSRM provides a numerical approach to determine the factor of safety under working load conditions by considering the progressive reduction of shear strength parameters until equilibrium cannot be achieved. It offers valuable insights into the stability of slopes and other geotechnical structures where more complex constitutive models are involved and the failure envelope may not be apparent in the initial working load analysis. Thus factor of safety can be defined as:

$$FOS = \frac{\tan \varphi_{available}}{tan\ \varphi_{failure}} = \frac{c_{available}}{c_{failure}}$$

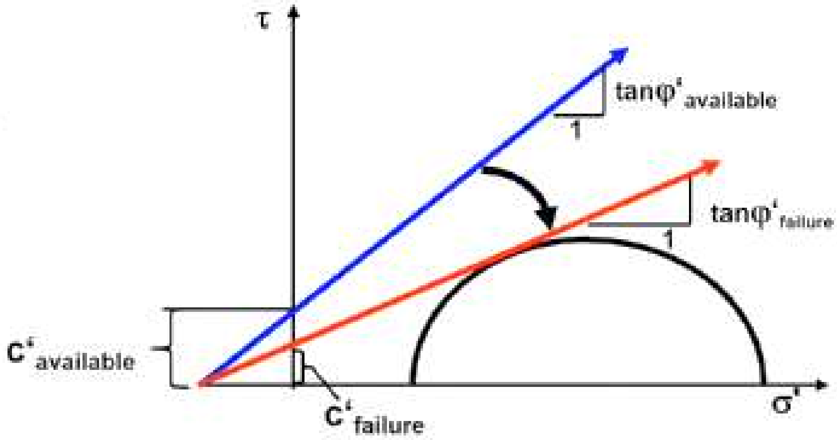

Figure 2.23: Basic concept of Shear Strength Reduction (SSR) Method

2.7.3 Introduction to PLAXIS 2D Software

A robust and user-friendly finite element (FE) software called PLAXIS 2D is used for 2D analyses of stability and deformation in geotechnical engineering and rock mechanics. Leading engineering firms and institutes in the civil and geotechnical engineering fields employ PLAXIS on a global scale. Applications for PLAXIS 2D span from foundations, embankments, and excavations to mining, oil and gas, and reservoir aeromechanics. For performing deformation and safety analysis on soil and rock without taking into account creep, steady state groundwater or thermal flow, consolidation analysis, or other time-dependent effects, PLAXIS 2D has everything you need. When utilizing the finite element method to examine slope stability, there are often two methods. One method is to raise the gravity load, and the other is to lessen the soil mass's strength properties. In this work, the second strategy is used, and a potent finite element software package named PLAXIS is employed.

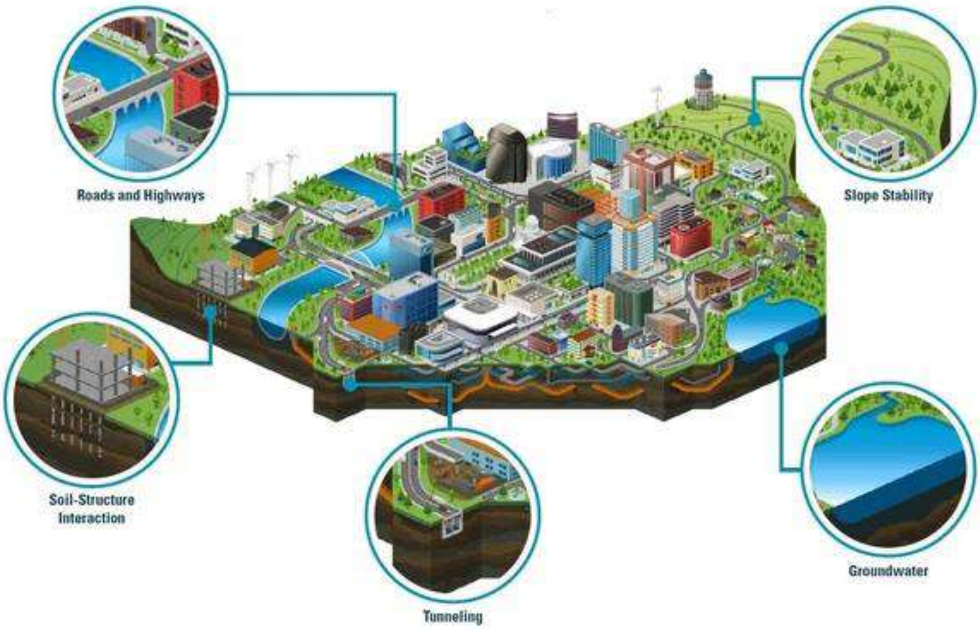

Figure 2.24: Applications of PLAXIS in Geotechnical Engineering (6 Reasons Why You Should Use PLAXIS for Geotechnical Analysis, n.d.)

Drawing the geometry contour first, adding the soil layers, structural objects, construction layers, boundary conditions, and loading are the general order of operations in PLAXIS 2D software. It's crucial to understand that whenever the geometry of an existing model is altered, the finite element mesh must be produced again. The phi/c reduction method is used by PLAXIS 2D to calculate the global safety factor. The load advancement number of stages is used in this procedure. The strength decrease increment during the first calculation step is specified using the incremental multiplier. Automatically, the strength parameters are decreased one at a time until all additional stages have been completed. In a similar manner, interface strength is also decreased. The final stage ought to produce a fully formed failure mechanism. A bigger number of additional steps must be added to the calculation if a failure mechanism has not yet fully established (Omari & Boddula, 2012).

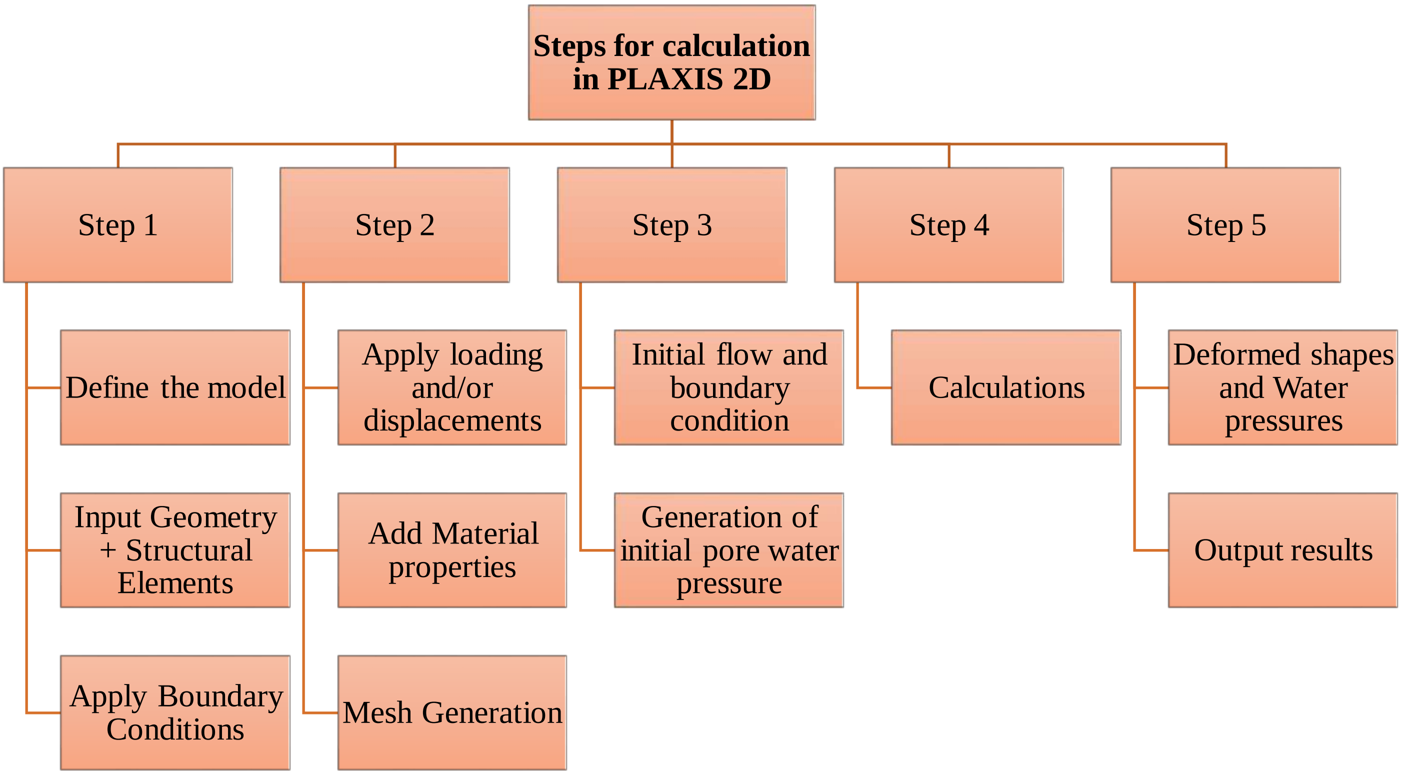

Figure 2.25: General Steps for calculation in PLAXIS 2D software

2.8 RESEARCH REVIEW ON SLOPE STABILITY ANALYSIS THROUGH PLAXIS 2D

The review of prior research on slope stability using the finite element approach is provided in the part that follows, with a focus on the use of PLAXIS 2D software. This introduction seeks to give a thorough overview of the current research and emphasizes the importance of more investigation in this field. This thesis aims to add to the growing body of knowledge and improvements in geotechnical engineering by analyzing the results from earlier investigations.

Ayob et al., 2019 analyzed the efficiency of limit equilibrium (LE) and finite element (FE) approaches after analyzing slope stability evaluations. In order to conduct the study, soil samples were obtained as part of the slope stability tests prior to modeling in the Slope/W and PLAXIS software packages at Maktab Rendah Sains MARA (MARA)

Bentong, a boarding school in Malaysia. According to the study, FE methods are better suited for complicated geometries or those requiring an examination of seepage, consolidation, and other associated hydrological and mechanical characteristics than LE approaches are for simple geometries. The study's findings support the use of FE methods as an additional slope stability analysis tool to supplement LE methods, producing trustworthy results that are consistent with those attained using the LE approach. The outcomes of the two strategies were contrasted, and the FOS values obtained using various techniques were examined. The findings of the research study are shown in the table 2.7.

Table 2. 3: A Comparison of the Resultant FOS Values for the Five LE Methods and One FE Method (Ayob et al., 2019)

Method	Analysis	FOS	% Difference vs Morgenstern and Price's Method
Limit equilibrium method by slope/W	Ordinary method of slices (OM)	1.130	−6.53% (discrepancy ratio of 1.09)
	Bishop's simplified method (BSM)	1.217	0.66% (discrepancy ratio of 0.99)
	Janbu's simplified method (JSM)	1.097	−9.26% (discrepancy ratio of 1.10)
	Morgenstern and price's method (MPM)	1.209	-
	Spencer's method (SM)	1.209	-
Finite element method by PLAXIS	Strength reduction Method (c-Φ)	1.060	−12.32% (discrepancy ratio of 1.14)

With the use of FEM-based software (PLAXIS 2D), *Khan & Abbas, 2014* conducted research on the slope stability study of a highway embankment. Fly ash was used as the fill material, and Geogrids were installed under static conditions to represent lightweight and local embankment fills over a soft subsoil. To assess embankment behavior and suggest materials for future designs, this study used numerical modeling and finite element analysis. The study used physical modeling with a model embankment to evaluate different materials in the lab. In the FEM analysis, the Mohr Coulomb model was employed for the embankment material modeling. When compared to other forms of embankment materials, normal soil reinforced with Geogrid was found to significantly increase the factor of safety of the embankment under static conditions. The study also showed that using fly ash with Geogrid is a cutting-edge ground-improvement strategy for reducing stresses and settlements brought on by earthquakes. It was discovered that using PLAXIS 2D software was a strong, workable substitute for the assistance of the geotechnical expert. According to the study's findings, fly ash and regular soil reinforced with Geogrids can be suggested for usage in future designs of light-weight embankment sections.

Potgieter & Jacobsz, 2019 compared the factors of safety (FOS) computed by limit equilibrium analysis and finite element strength reduction methods in lateral support design for soil-nails and anchors in surface excavations. The study finds that, under certain conditions, the FOS from the finite element strength reduction technique is comparable with limit equilibrium methods. The same failure mechanism and capacity must be specified in both analyses, and caution should be taken to ensure that the yield criterion is not violated when defining in-situ stress states and modelling parameters. Their research emphasized the importance of cross-checking finite element modelling with simpler limit equilibrium methods to ensure that finite element results are correctly interpreted. They concluded that with the finite element strength reduction method, the failure surface is not subject to any prior assumptions, and the failure mechanism is optimized. Stiffness factors, in-situ stresses, or staged construction modeling (which modify the stress state behind the retained excavation face) have no effect on the finite element strength reduction method FOS. Only the yield criteria of the various materials and the initial (unreduced) material qualities have an impact on the FOS.

Potgieter & Jacobsz, 2019 research highlights the significance of numerical modeling, specifically the finite element method (FEM), as an effective approach for evaluating the stability of open pit mine slopes. By utilizing FEM, which is a powerful numerical technique for solving partial differential equations and boundary value problems, they can obtain approximate solutions with high accuracy. To conduct their analysis, they employed the Plaxis software and incorporates the Mohr-Coulomb failure criterion, a widely accepted model in geotechnical engineering, into their element modeling process. This comprehensive approach enables them to simulate the real-world conditions of the open pit mine slope accurately. The research findings indicate that the finite element method successfully identifies instability in the open pit mine slope. Specifically, they discover a safety factor of 0.981, which falls below the desired safety threshold of 1.0, indicating a critical point of instability approximately 7 meters deep from the slope's surface. Based on the outcomes of this study, the researchers assert that numerical methods like FEM offer superior precision in assessing slope stability compared to traditional analytical approaches. Consequently, they advocate for the widespread adoption of numerical techniques in geotechnical evaluations to enhance safety and risk management in mining operations.

Matthews et al., 2014 conducted a research in order to compare the applicability of the LE approach and FE method in slope stability analysis. According to his study, the LE method has been in use since the early 20th century and yields trustworthy and accurate results. The FE method is advised for more complex issues that call for the investigation of coupled hydrological and mechanical behavior since it can show the geometry of failure surfaces. For important slip surfaces that are probably circular, the conventional LE approach is still valid and usable. The non-circular slip surface LE approach, however, may not be adequate for more complex stratigraphy because the critical slip is unlikely to be circular and may overstate the factor of safety. The findings suggested that the approach selection should be based on the difficulty of the problem to be modeled and the data at hand.

METHODOLOGY

3.1 GENERAL

This chapter presents the methodology employed for the numerical modeling of a road embankment stabilized with ceramic dust. The process begins with the collection of soil samples from the embankment site. These samples undergo various laboratory tests, including sieve analysis, Atterberg limit test, Modified Proctor test, direct shear test, and soaked CBR test, to comprehensively characterize the soil's properties. The laboratory findings form the basis for conducting numerical simulations using PLAXIS 2D software. The shear strength reduction method is utilized to calculate the factor of safety, enabling a thorough evaluation of the embankment's stability. This chapter serves as a vital guide to the detailed methodology adopted for the investigation, leading to valuable insights into the effectiveness of ceramic dust in stabilizing the embankment soil.

3.2 COLLECTION OF SOIL SAMPLE (SITE LOCATION)

The road embankment slope failure was found in Renala Khurd (Canal Home Society near Lower Bari Doab canal _ Right Road), Okara, Pakistan at location 30°48'17.51"N 73°35'59.99".

Figure 3.1: Site Location on google map (https://goo.gl/maps/Wd6X4mV72C5mPomM6)

3.3 RESEARCH METHODOLOGY

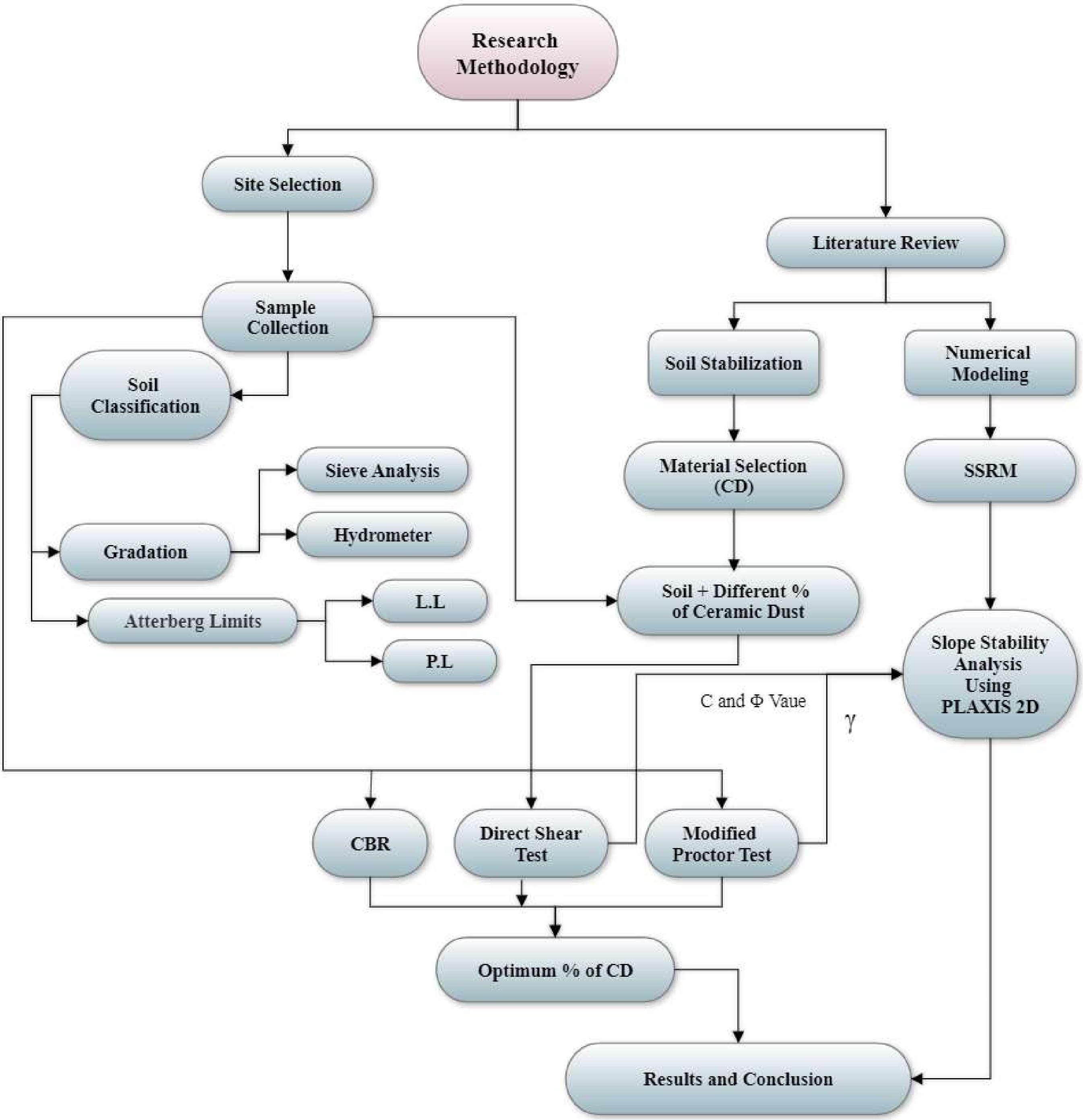

Figure 3.2: Flow Chart of Research Methodology

3.4 EMBANKMENT GEOMETRY

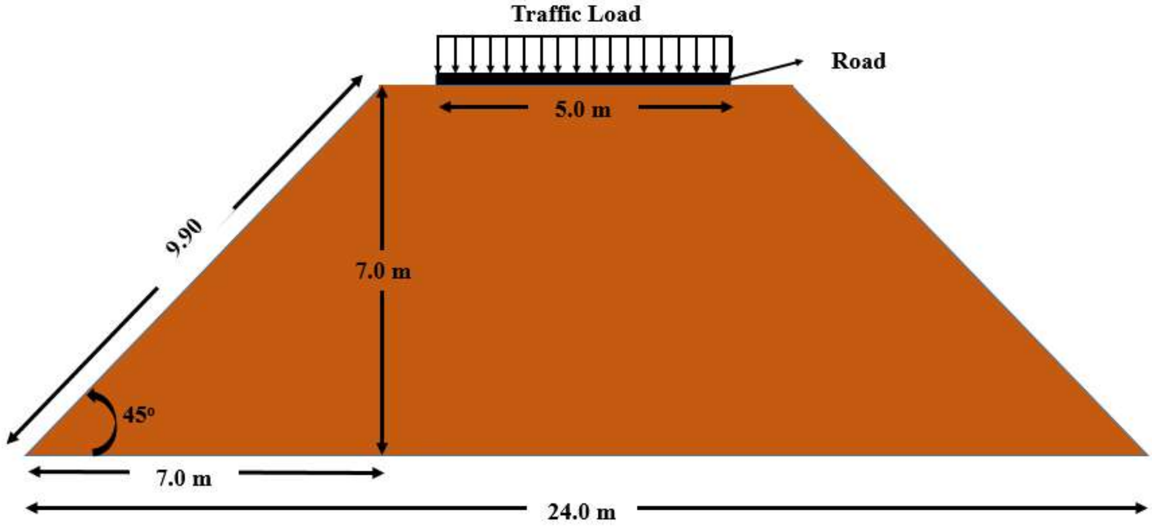

Figure 3.3: Cross-section of Road Embankment

3.5 EXPERIMENTAL PLAN

Laboratory testing was carried out so that the effect of the additive that was discussed earlier can be investigated. The following tests were carried out on both the parent soil and various mix blends with varied proportions of soil and additive.

Table 3.1: Standard References for determining the physical and Mechanical Properties of the soil

Serial No.	Property/ Parameter	Test Name	Reference
Physical Properties			
1	Identification	Color	ASTM D2488-17
Mechanical Properties			
2	Gradation	Classification of Soil	ASTM D6913
		Wetting Sieve Analysis	ASTM D1140-17
		Dry Sieve Analysis	ASTM D6913-04

		Hydrometer Analysis	ASTM D7928
3	P.L, L.L, P.I	Atterberg Limit Test	ASTM D4318-17el
4	Density	Specific Gravity	ASTM D854
5	MDD, OMC	Modified Proctor	ASTM D1557
6	C and Φ	Direct Shear Test	ASTM D3080
7	CBR value	CBR	AASHTO T193

3.6 PREPARATION OF SAMPLE

The sample needs to be dried out and in powder form rather than in lumps. The sample took on the natural appearance of a dry and brittle lump with dimensions ranging from approximately 30 to approximately 70 millimeters. There is a requirement to pulverize the sample in order to transform it into its fundamental grain size form. "Pulverization," also known as "comminution," "crushing," and "grinding," is the act of applying an external force on a solid material of a specified size in order to break it up and make it into smaller pieces than it was before. Other names for this process include "crushing," and "grinding." This technique, rather than breaking up individual particles of the soil sample, isolated the particles from one another.

3.6.1 Soil Pulverization

- The first step is to use a hammer to smash the larger chunks of soil into smaller pieces.
- After that, the residual clumps of soil were pulverized by placing the sample, which weighed between 5 and 7 Kg, into the drum of the pebble mill. As can be seen in Figure 39, the sample was placed into the drum with the assistance of a trowel.
- After that, balls with a total weight of 15 Kg were added to the drum together with the soil sample.
- After that the sample was secured inside its container by firmly screwing down its cover.

- The drum was moved to the rollers of the grinding mill, where the grinding process takes place for a total of 10 minutes per term.
- Then the sample was taken out of the drum using a sieve aperture size of 16.0 mm so that the balls remained on top, and the soil sample was collected further into a container.
- The whole procedure is shown in the figure 3.3.

Figure 3.4: Pulverization of soil using Pebble Mill Apparatus

3.7 DETERMINATION OF PHYSICAL PROPERTIES

3.7.1 Color Determination

A comparison was made between the soil sample and the Munshell color scheme.

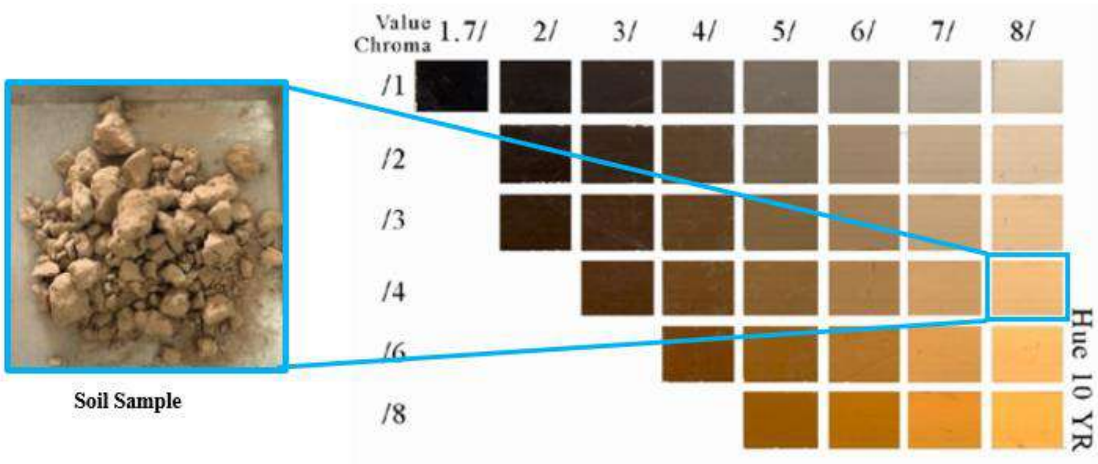

Figure 3.5: Soil Color Determination from Munshell Chart

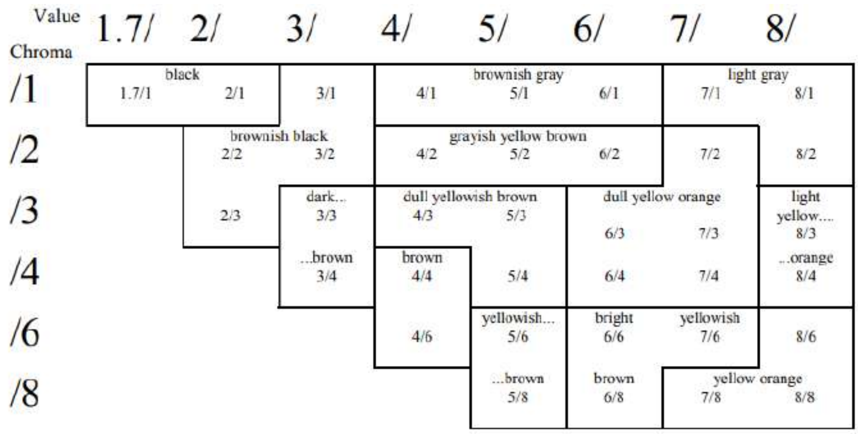

Figure 3.6: Munshell chart with Soil Description

Result from Munshell Color Chart = 8/4 (Light Yellow Orange)

3.8 DETERMINATION OF MECHANICAL PROPERTIES OF SOIL

3.8.1 Wetting Sieve Analysis (ASTM D1140-17)

- An empty washing sieve # 200 was taken and weighed.
- A sample that had been oven-dried for 200 g was put into a weighted empty sieve number 200, and the overall weight was recorded.
- After that, the sample was washed in the right manner until the water that was drained became clean, and soil particles that were finer than 200 were able to pass through the sieve.
- The retained soil material was then kept in the oven for 24 hrs.
- After a period of twenty-four hours, the weight of the soil with the sieve was recorded, and the percentage that passed through #200 was computed as in the table 4.1.

3.8.2 Dry Sieve Analysis (ASTM D6913-04)

- The weight of the oven dried sample was measured and recorded on the datasheet.

- After completing the assembly of all of the necessary sets of sieves, the #4 sieve was placed on top, and the #200 sieve was placed at the bottom.
- After the sample was carefully poured into the top sieve, place a cover over it.
- After inserting the stack of the sieve into the mechanical shaker, it was shaken for a period of ten minutes.
- After that, the stack was taken out of the shaker, and the weight of each sieve, together with the soil that it had held, was recorded after being carefully weighed.
- The weight of the bottom pan after it had been left with the fine soil it had retained was also recorded.

3.8.3 Specific Gravity Test (ASTM D854)

- Take an empty pycnometer and note down its weight in data sheet as A.
- Oven dried soil sample was taken and put this soil sample into the pycnometer, approximately up to half of the pycnometer.
- Weight of the pycnometer and soil was recorded in the data sheet as B.
- The water was then added to the flask until it was two-thirds filled. The mixture was then agitated in the flask by shaking and tuning. The flask was weighted again and noted as C.
- After that, the flask was emptied once more, washed fully, and then filled with distilled water all the way up to the volume-marked point. Note down the weight of the pycnometer filled with water as D. The whole procedure is shown in the figure 3.7 below.

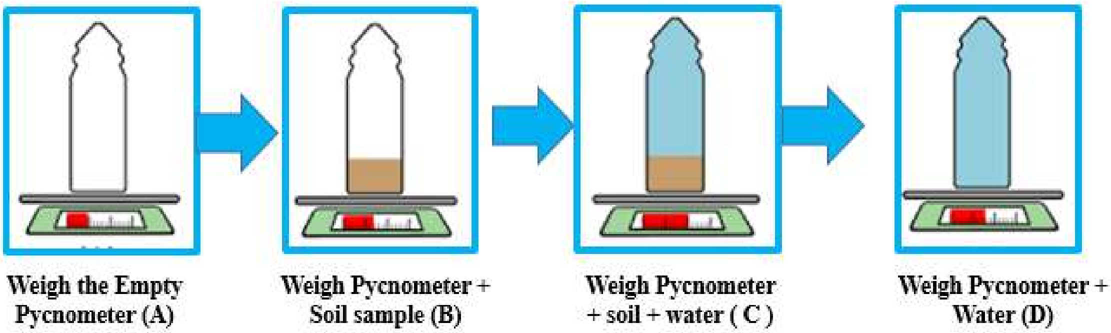

Figure 3.7: Step wise Procedure of Specific Gravity Test

- At the end, the specific gravity was calculated by using the following formula:

Specific Gravity = $G_s = \alpha \times [(B - A) / \{(B - A) - (C - D)\}]$; Where α =1 at 30C°.

3.8.4 Hydrometer Analysis (ASTM D7928)

- A 50 gm of oven-dried, finely pulverized soil sample was taken in the pan, and it was then transferred to the shaker jar.
- After that, a solution of sodium Hexametaphosphate at a concentration of 4% was made in the flask containing 1000 ml of liquid, and 125 ccm of the solution was then transferred to the shaker jar.
- After turning on the shaker, the soil was combined with the solution for a period of five minutes, after which the mixture was left to sit for approximately sixteen hours.
- After this a flask containing 1000 mm of water and designating it as a control flask, the zero correction of the hydrometer was recorded.
- The solution from the jar was transferred to another empty 1000 ml flask, and then water was added to the flask until it reached the correct volume of 1000 ml.
- After that, the hydrometer (152-H) was inserted into the flask at once. A record was kept of the readings taken from the hydrometer, the meniscus, and the temperature. Following the taking of the reading, the hydrometer was then put into the control flask.
- The process of getting a reading from the hydrometer was carried out several times in line with the amount of time that had passed.
- The experiment was terminated as a result of consistent readings that suggested that the soil had attained a homogeneous mixing at that point.

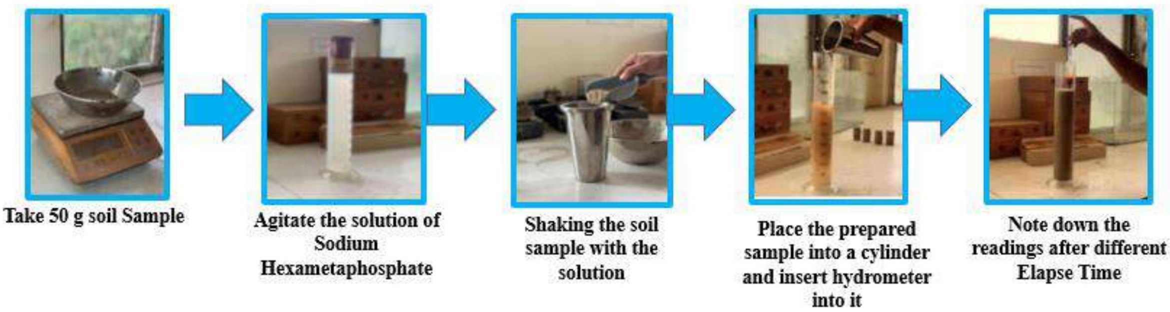

Figure 3.8: Step wise Procedure of Hydrometer Test

3.8.5 Atterberg Limit Test (ASTM D4318-17el)

3.8.5.1 Liquid Limit (L.L) Test

- After being strained through sieve no. 40, the sample is collected in a pan for examination. It has previously been dried by the air and powdered. It was combining the earth with a trace amount of distilled water until the mixture took on the consistency of a smooth, even paste.
- After the mixture has been thoroughly combined, it is covered with a piece of plastic and set aside for two hours.
- The subsequent step was the weighing, numbering, and recording on a data sheet of empty China dishes.
- The Casagrande apparatus was calibrated by measuring the height that the apparatus cup fell from after being dropped. At the point where the cup has risen to its highest point, as determined by spinning the cup, there should be a space of 10mm between the base of the device and the middle of the cup.
- After holding the cup in one hand, the soil sample that had been previously soaked was then added to the cup in an incomplete manner.
- The grooving tool was used to carve a smooth and even groove through the middle of the cup. This grove was straight. Throughout the process of grooving, the tool should be held in a position that is parallel to the surface of the cup.
- Following that, the device was rotated at a rate of around two drips per second after that. The distance along which the numbers were tallied until the two sides of the soil section came into touch at the bottom of the groove was 13 mm (1/2 inch), and the results of this counting were recorded as N in the datasheet.
- The middle of the cup was emptied out, and a sample with a weight of at least 10 gm was obtained from there.
- It is important that the sample contain soil from both sides of the groove's point of contact with the earth.
- The steps involved in doing so are illustrated in the collection of photographs that follows.

- After the sample has been obtained, it is immediately weighed using a precise weighing scale and then placed in an oven set to 110 degrees Celsius for a period of 24 hours.
- After that, the soil sample was mixed again, the apparatus was cleaned, and a tiny quantity was introduced using a water nozzle in order to raise the water content. This was done in order to lower the number of drops that were necessary in order to close the groove.

Figure 3.9: Liquid limit test Procedure

3.8.5.2 Plastic Limit Test

- A soil sample was taken and some distilled water was added to it until it reached the desired consistency, at which point it could be rolled without adhering to the hands.
- Following the creation of three balls weighing 8, 8, and 7 grams each, each ball was rolled between the palm of the hand or a finger and a glass plate.
- It should not take more than two to three minutes for the thread to be bent to the point when its diameter reaches 3.2 millimeters (1/8 inch).
- When the diameter of the thread reaches the appropriate diameter in comparison to the corresponding rod, break the thread into many pieces.
- The procedure was maintained until the thread broke into fragments by alternating rolling, collecting up, kneading, and rolling again.
- Some of the fragments of the disintegrated thread were collected and placed in the containers with weights.
- In addition, once the samples had been weighed, they were put into an oven to assess the amount of moisture in them so that further calculations could be made.
- The whole procedure of plastic limit lest is shown in the figure 3.15.

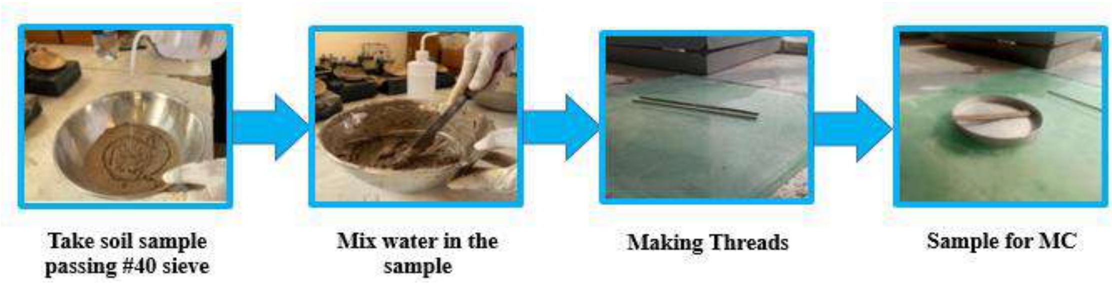

Figure 3.10: Plastic Limit Test Procedure

3.8.6 *Modified Proctor Test (ASTM D1557)*

- After going through sieve no. 04 with the sample, around 4 kilograms of it was collected and then combined with the ideal amount of water (representing approximately 4% of the soil that was obtained).
- We measured and recorded in the datasheet the empty weight of the mold without the collar and with the assembly already connected.
- The mold was readjusted to the base plate and the collar, and then a 4.5 kilogram rammer was used to compact the soil mixture in five layers, with 25 blows delivered to each layer from a height of 45 centimeters.
- To remove the collar without causing any damage, a straight steel edge was used to delicately chip away at the affected portion of the compacted soil.
- After that, the weight of the compressed mold together with the base plate was measured using a weighing scale, and the results were recorded for use in further calculations.
- After removing the little quantity of soil from the sample, it was weighed in a container, the percentage of water in that container was compared to the amount of water that had been supplied at the beginning of the test, and then the container was placed in the oven for twenty-four hours.
- During the test, the bulk density was determined so that the test could be stopped when it reached its maximum point and continued until it began to fall.
- The sample was then removed from the mold, broken up, and placed into sieve no. 04 in the mixing tray. The amount of water that had previously been present in the mixture was then added to the mixture in equal percentages.

- On the same sample, the procedure was carried out many times till the bulk density was reduced.
- The dry density of oven-dried samples was determined after obtaining a reading of the samples after they had been dried in the oven.
- After that, the compaction curve needed to be plotted on a graph with dry density on the ordinate and moisture content on the abscissa in order to determine the optimal moisture content.

3.8.7 Direct Shear Test (ASTM D3080)

- Depending on the criteria for the test, collect a representative soil sample that has not been disturbed or one that has been reshaped (In our case disturbed sample is used).
- With the assistance of the right cutting equipment, the sample should be trimmed to the required size and form (Square shape of 6×6 cm).
- Install the direct shear device in accordance with the instructions provided by the manufacturer. A shear box, which is where the sample is inserted and loaded, a loading mechanism to apply normal load, and a shear mechanism to apply horizontal shear force are the usual components that make up this apparatus.
- Put the soil sample in the shear box and make sure it is centered and level before closing the lid.
- Utilizing the loading mechanism, a confined normal load is going to be applied to the soil sample. The precise testing criteria and the anticipated level of soil strength will both play a role in determining the amount of the normal load that will be applied.
- Throughout the course of the test, take readings of the shear force as well as the displacement at predetermined intervals, and record your findings.
- A large reduction in shear force or an excessive amount of horizontal displacement will be the defining characteristics of the failure.
- Calculate the shear strength parameters, such as cohesion and angle of internal friction, using the collected data. The parameters must be calculated based on the testing criteria.

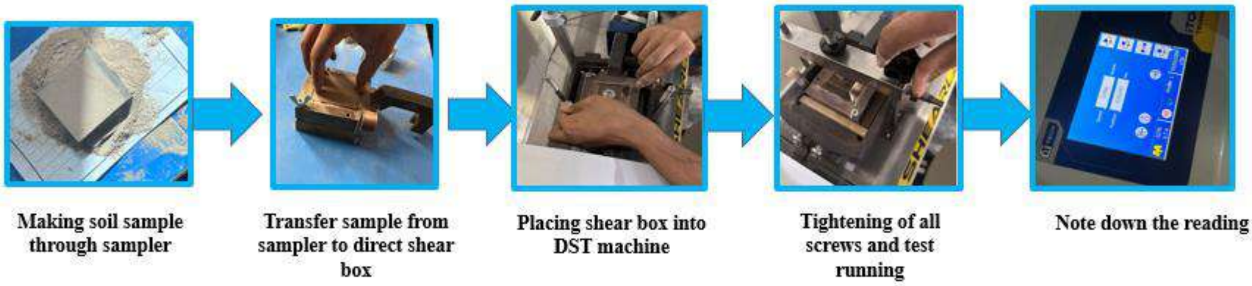

Figure 3. 11: Step-wise procedure for direct shear test

Figure 3. 12: Direct Shear test apparatus used for experiment

3.8.8 California Bearing ratio Test (AASHTO T193)

- In most cases, it is necessary to compact three samples in such a way that the final densities of the samples vary from 95 percent (or less) to 100 percent (or more) of the maximum dry density.
- In general, about 10, 30, and 65 blows are adequate for compacting specimens 1, 2, and 3, respectively. This number of blows should be applied to each layer. In most cases, molding a CBR specimen to 100 percent of the maximum dry density as measured by T 99 (Method D) requires more than 56 blows per layer. This is because the sample for the moisture-density test is reused, but the mixture for the CBR specimen is only combined and compacted once. A single specimen that has been compacted to its maximum dry density at its optimal moisture content, as

measured by either T 99 or T 180, may be the testing method of choice for some laboratories.

- Attach the extension collar, clamp the mold to the base plate, and measure the weight to the closest five grams or one tenth of a pound. After placing the spacer disc within the mold, cover it with a layer of coarse filter paper.
- Combine the three pieces of 6.8 kilograms (15 pounds) that were made in Section 5.1.2 with an appropriate amount of water in order to achieve the desired level of moisture content
- Compact the first of the three portions of the soil-water mixture into the mold using three equal layers and the appropriate rammer if the maximum density was determined by T 99, or using five equal layers if the maximum density was determined by T 180, to give a total compacted depth of approximately 125 mm, compacting each layer with the lowest selected number of blows in order to give a compacted density that is 95 percent or less of the maximum density.
- Take two samples of the material being compacted and analyze them for the amount of moisture it contained at the beginning and the conclusion of the process of compacting it. For fine-grained soils, each moisture sample must have a mass of at least 100 g, and for coarse-grained soils, the sample mass must be at least 500 g. The T 265 standard, Laboratory Determination of Moisture Content of Soils, is the one that needs to be followed in order to get an accurate reading on the soil's moisture level.
- Take off the extension collar, and then use a straightedge to cut the soil so that it is level with the top of the mold. Patching surface imperfections using material of a smaller size is highly recommended. After removing the spacer disc and placing coarse filter paper on the perforated base plate, turning the mold with the compacted soil over and placing it on the filter paper so that the compacted soil is in contact with the filter paper, and finally removing the spacer disc. Attach the collar and secure the perforated base plate, then determine the mass of the mold and the specimen to the closest 5 g (0.01 pound).
- Following the technique outlined in Sections 7.1.4 through 7.1.6, compress the remaining two sections weighing 6.8 kg (15 pounds) by using an intermediate

number of blows per layer to compact the second specimen and the greatest number of blows per layer to compact the third specimen. This is to be done in accordance with the procedure outlined in Sections 7.1.4 through 7.1.6.

- In line with Section 6, prepare specimens for examination.2. Compaction should be place in the CBR molds alone. It is necessary to penetrate each specimen that will be utilized in the development of the compaction curves for the 10-blow, 25-blow, and 56-blow per layer compactive efforts. It will be essential to incorporate a compactive effort that is larger than 56 blows per layer in the event that the specified unit mass is at or near 100 percent of the maximum dry unit mass.

3.9 SLOPE STABILITY ANALYSIS USING PLAXIS 2D V21

PLAXIS 2D is finite element analysis software. Here PLAXIS 2D software to check the stability of slope under different conditions. Following are the steps for calculation in PLAXIS 2D.

3.9.1 General Interface of PLAXIS 2D V21

The general interface of PLAXIS 2D V21 is shown in the figure 3.13.

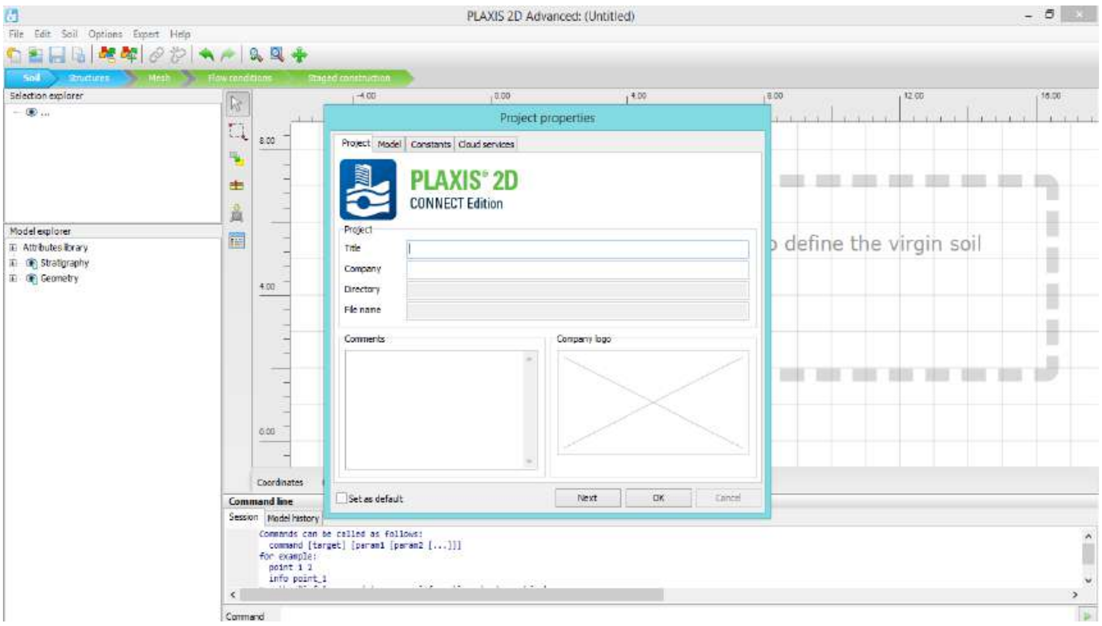

Figure 3.13: General Interface of PLAXIS 2D V21

There are three types of processes in the PLAXIS 2D software. These are

- **Pre-process** includes model creation, defining the problem and definition of the building processes which may include initial situations or construction stages.
- **Calculation**
- **Post-process** includes results and deformations etc.

3.9.2 Creating Geometry of slope in PLAXIS

Soil geometry is shown in figure 3.3 at the very first of this chapter. Now in order to create that soil geometry in PLAXIS, we can either use built in function of PLAXIS with named (Soil polygon) or we can draw geometry by using python scripts at the bottom in the command window. In order to create geometry we first locate coordinates of our geometry. Click on soil polygon option and type the following coordinates in the command window:

- Coordinate 1 (0,0)
- Coordinate 2 (24,0)
- Coordinate 3 (17,7)
- Coordinate 4 (7,7)
- Coordinate 5 (0,0)

Type the above coordinates in the command window without any comma i.e. (0 0) (24 0) (17 7) (7 7) (0 0). This will automatically create the geometry of the soil as shown in figure 3.14.

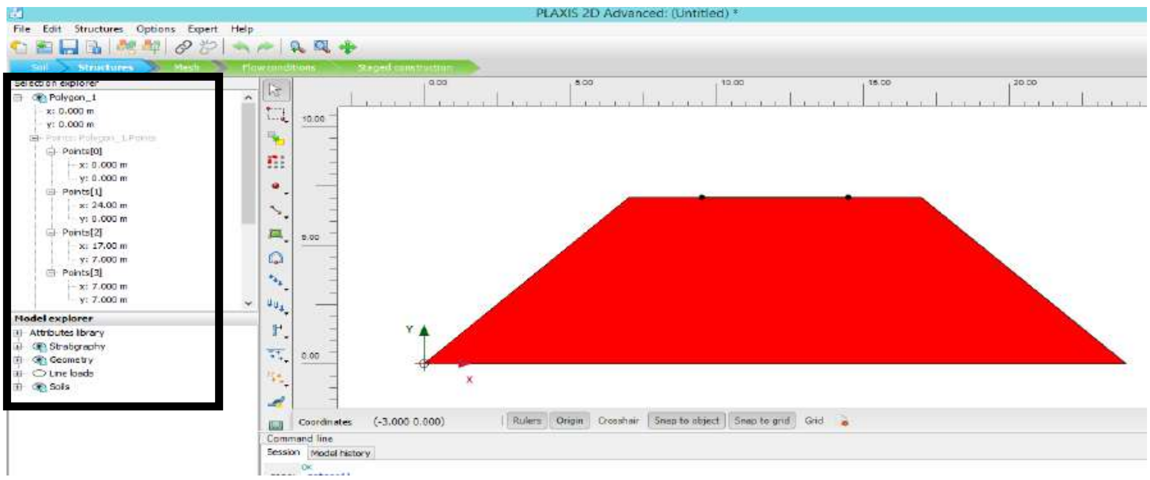

Figure 3.14: Geometry of slope in PLAXIS

3.9.3 Defining Material properties

Now after creating the geometry we had created material properties (such as soil type i.e. in our case different soils with different percentage mix of ceramic dust). Click on the soil tab and then click show material icon, then click on create new material option. A new window will appear in which we can edit soil name, its color, material model (Mohr's coulomb) and drainage type etc. Input the properties of that soil such as unit weight of the soil and its shear strength parameters (c and Ø) values. As we are using strength reduction method, so in this method only soil shear strength is a necessary parameter. After entering all the soil properties click "OK". Similarly create all the soil materials (i.e. soil with zero % addition of ceramic dust say "0% CD" and soil with 5% addition of ceramic dust as "5% CD", with 10%,15%,20%,25%,30%,35% as "10%CD", "15% CD", "20% CD", "25% CD", "30% CD", and "35% CD" respectively. All these selected materials are shown in figure 3.15. After that by simple draw and drop option we can apply any material to any soil layer.

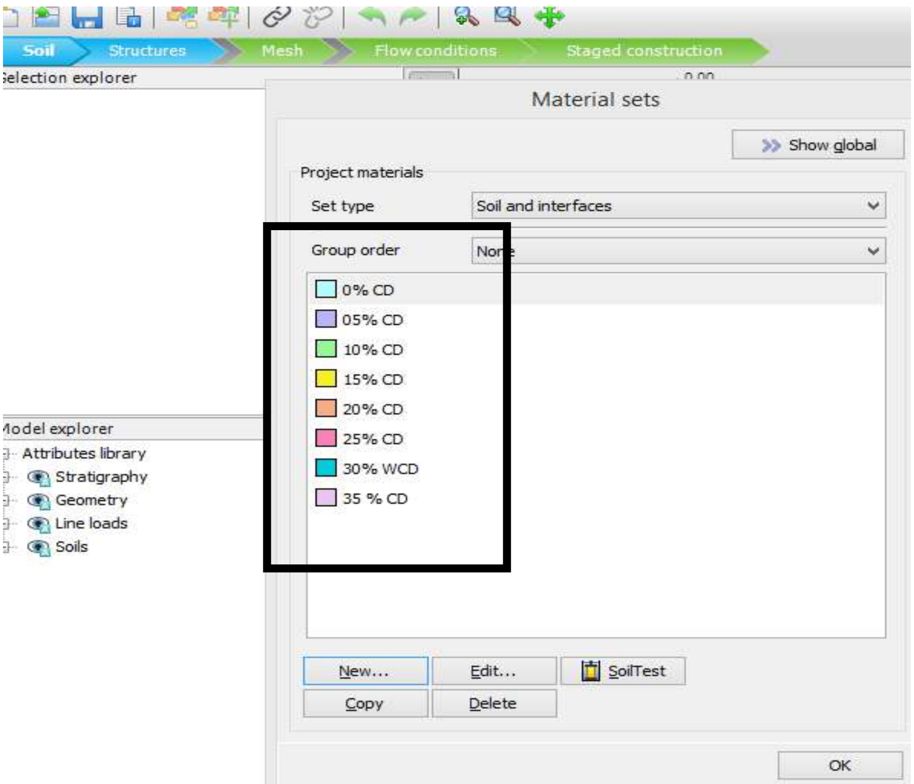

Figure 3.15: Defining materials in the PLAXIS

3.9.4 ***Applying uniform load to the embankment***

After creating soil materials, in the next step we had applied a uniform traffic load of 30kN/m/m (30kN/m^2). In order to apply this load click on structure tab and then click on create load option, then select create line load. Select the location where you want to apply load by using mouse pointer or by using code in command window. Type (9 7) and (14 7) in the command window. It will automatically create the uniform load at the road location as shown in figure 3.31 below.

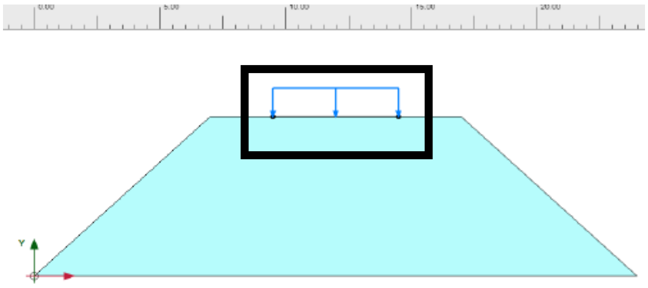

Figure 3.16: Creating uniform traffic load in PLAXIS

3.9.5 Creating FEM Mesh in the PLAXIS

Generate a finite element mesh for the slope geometry. The mesh discretizes the slope into smaller elements, allowing PLAXIS to perform numerical analysis. There are five options for mesh generation (very coarse, coarse, medium, fine and very fine). Finer the mesh more accurate will be the results but for a finer mesh PLAXIS will take more time to perform analysis. So we have selected a medium meshing option. We can see the mesh of the structure by clicking on view mesh option, it will open PLAXIS 2D OUTPUT VIEWER program as shown in the figure 3.17 below.

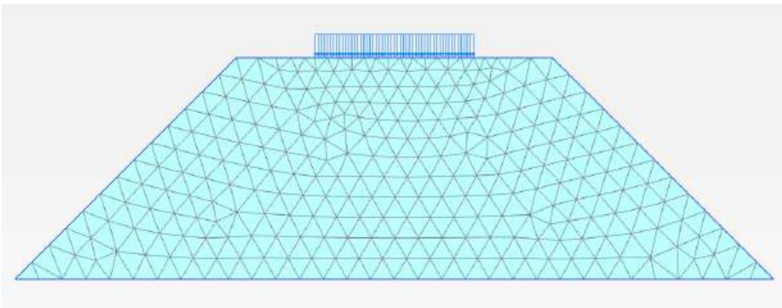

Figure 3.17: FEM mesh of embankment

3.9.6 Selecting points for Curve generation

After creating mesh we will set points for curve generation i.e. the point where we want to analyze the results specifically. It is not mandatory to select the points for curve we can also perform analysis without selecting points for curve. In our case we have selected two point (node 423 and node 3469) at the top of the embankment as sown in figure 3.18 below.

Figure 3.18: Selecting points for curve generation in PLAXIS

3.9.7 Creating Phases for analysis

In In addressing the complexities of slope analysis with considerations for multiple construction stages or time-dependent behaviors, a strategic division into distinct phases becomes pivotal. In this particular context, we have meticulously established two fundamental phases: the deformation phase and the Factor of Safety (FOS) phase. These phases are deliberately devised to facilitate the accurate evaluation of two crucial parameters: firstly, the comprehensive determination of total deformations occurring within the embankment, and secondly, the meticulous assessment of the slope's Factor of Safety under varying percentages of ceramic dust incorporation. The rationale behind crafting these distinct phases lies in our pursuit of a comprehensive understanding. By scrutinizing the embankment's response to the incremental introduction of ceramic dust, we strive to uncover the intricate interplay between material properties and external influences. The embodiment of these phases, as visually represented in Figure 3.19, underpins our analytical approach. The deformation phase, employing gravity loading analysis, delves into the nuanced shifts and settlements, allowing us to quantify cumulative deformations.

Meanwhile, the FOS phase, utilizing safety analysis, serves as a reliable compass for assessing the slope's equilibrium between stability and external forces.

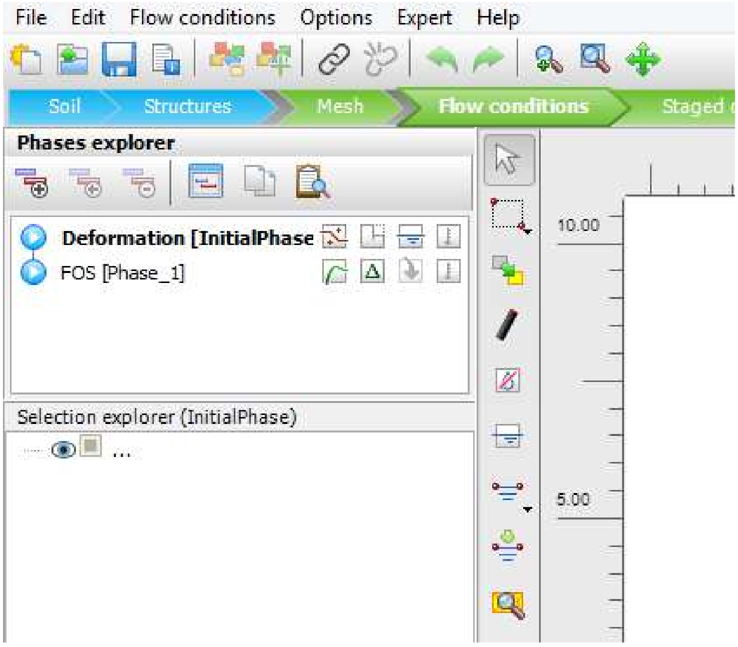

Figure 3.19: Defining different phases of work in PLAXIS

3.9.8 Boundary conditions

In PLAXIS, the simulation of the interactions between the soil-structure system and its surroundings is accomplished through the application of boundary conditions. In order to get findings from your geotechnical study that are reliable and in line with reality, it is very necessary to define acceptable boundary conditions. In the model, the movement of certain nodes or degrees of freedom is constrained by the use of fixities. Fixities can be defined on nodes to indicate the real limitations that are being applied to your project. The most common kinds of fixity are fixed (which prohibits all movement), hinged (which allows rotation but not translation), and partly fixed (which only restricts movement in part). In our case we have defined the closed boundary condition at the bottom of the embankment.

3.9.9 Calculation of Results

Once you have defined all the boundary conditions, run the analysis to obtain results. Click on the calculate option in the staged constructions window, it will start creating resulting results for the given soil embankment for all construction phases as shown in figure 3.35 below.

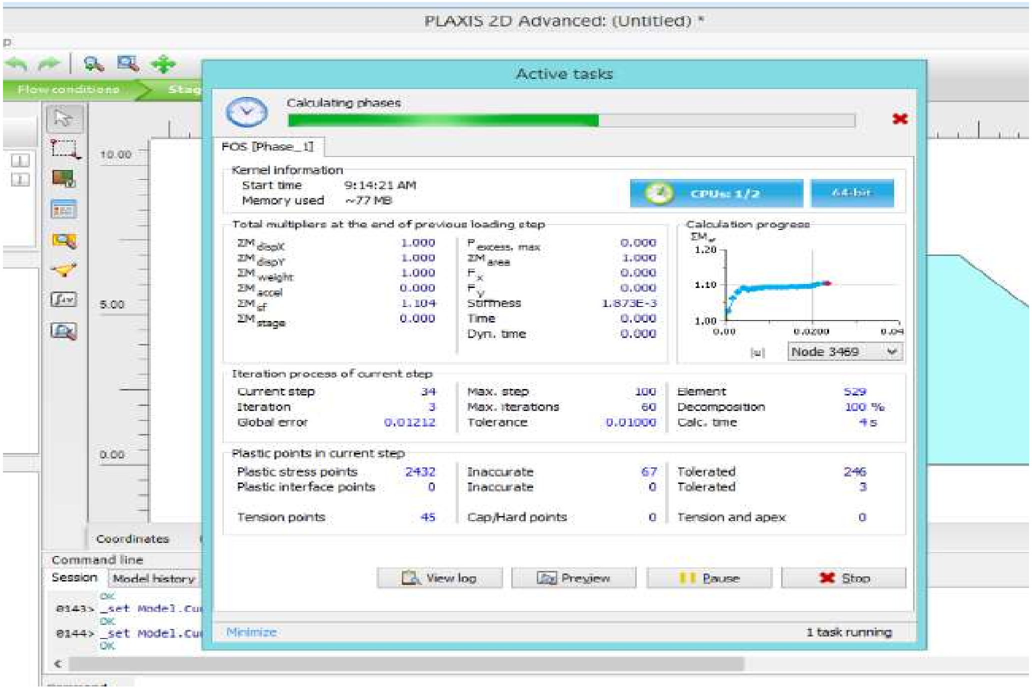

Figure 3.20: Calculations of results in PLAXIS

3.9.10 Analyzing the Results

After the analysis is complete, examine the results to verify that the boundary conditions are producing the expected behavior in the model. We are interested in total deformations and factor of safety of the slope. So we will click on the deformation tab it will show the deformed shape with total deformations produced in the embankment as shown in the figure 3.22. In order to calculate FOS we will go to curve manager and create a new curve between number of steps on x-axis and ΣM_{sf} on y-axis. It will give us the results for the factor of safety as shown in the figure 3.23.

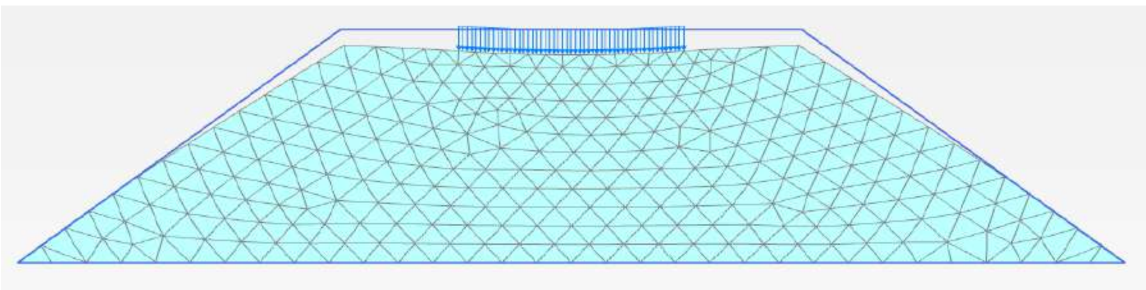

Figure 3.21: Deformed Mesh

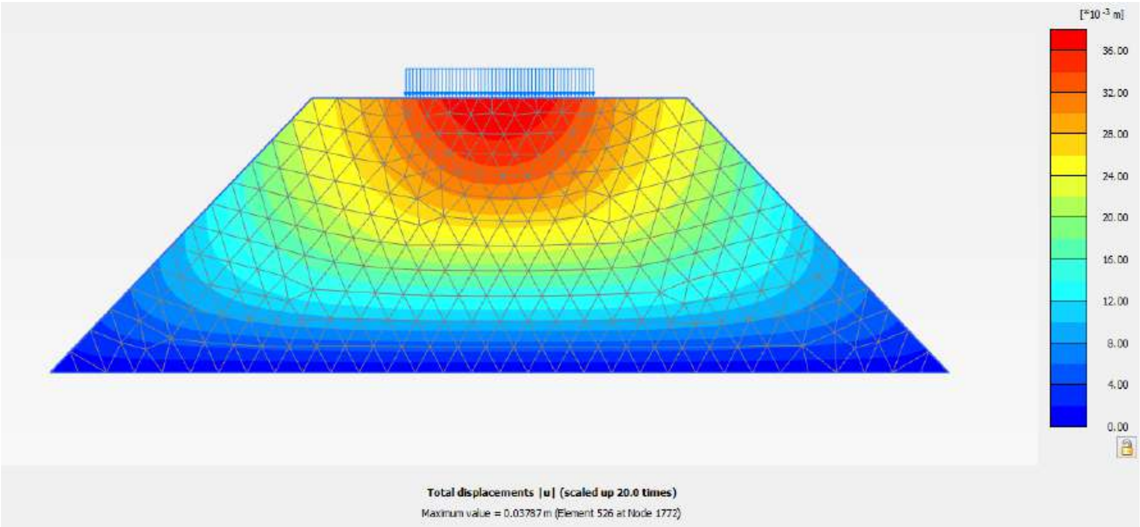

Figure 3. 22: Total Displacements calculation results

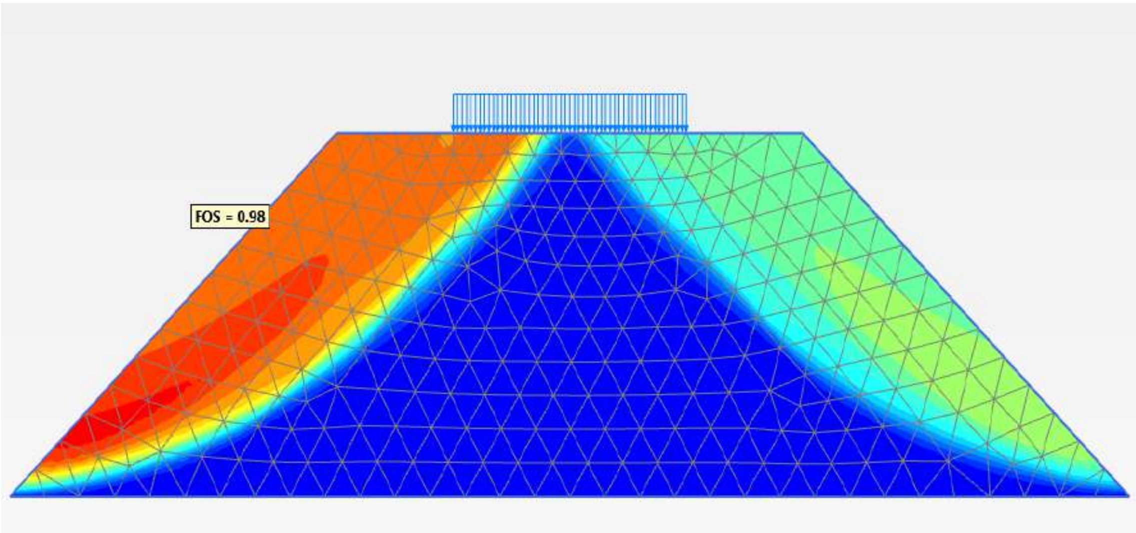

Figure 3.23: Factor of safety value with critical slip surface

After all the results obtained in this chapter, now the attention now moves to Chapter 4, where we will go into a full examination of the results, revealing the efficacy and prospective applications of these results. Now that we have access to a complete array of observations linked to soil stabilization, the focus shifts to Chapter 4.

RESULTS AND DISCUSSION

In this critical chapter, we uncover the climax of our study journey. Here, we offer the convincing results acquired from the thorough examination of an embankment soil slope stabilized with ceramic dust. These findings were gained from the extensive investigation of an embankment soil slope that was stabilized with ceramic dust. This chapter takes a deep dive into the results and discussion of the testing and analysis performed in chapter 3. Moreover the findings of the tests, together with a graphical representation of them, are presented in this chapter. The potential applications of ceramic dust in the future can be determined through study and interpretation. These experimental results and their subsequent discussion will be helpful in understanding the appropriate quantity of additive to use in order to obtain the greatest results, which will also provide a solution that is both environmentally friendly and cost effective.

1.1 SOIL CLASSIFICATION

1.1.1 Wetting sieve analysis of soil

Table 4.1: Observations and calculations for wetting sieve analysis of parent soil

Serial No.	Description		Value
1	Empty weight of sieve # 200	A	277.00 g
2	Weight of soil sample	B	200.00 g
3	Weight retained on Sieve # 200 + empty sieve	C	303.00 g
4	Weight of soil passing through sieve # 200	D	26.00 g

Percentage of soil passing through sieve # 200 = 100 - (D / B) × 100

= 100 - 13

= 87.00 %

1.1.2 Results for Dry sieve Analysis of soil

Table 4.2: Observations and Calculations for dry sieve Analysis of parent soil

Column 1		Column 2	Column 3	Column 4	Column 5
Sieve Size/No.	Opening	Weight Retained	% Retained	Cumulative % Retained	% Finer
#(inch)	mm	(g)	(Col.2/Total)× 100	%	100 – Col.4
#4(0.187")	4.75	11.0	0.55	0.55	99.45
#10(0.0787")	2	12.5	0.625	1.175	98.825
#30(0.0234")	0.6	18.0	0.9	2.075	97.925
#50(0.0117")	0.355	24.5	1.225	3.30	96.70
#60(0.0098")	0.25	38.5	1.925	5.225	94.775
#80(0.0070")	0.18	36.0	1.8	7.025	92.975
#100(0.0059")	0.15	54.0	2.7	9.725	90.275
#200(0.0029")	0.075	127.5	6.375	16.10	83.90
Pan		1678	83.9	100	
Total		2000			

1.1.3 Results for Hydrometer Analysis of Untreated Soil

Table 4.3: Data Required for Hydrometer test Calculations for Soil

Serial No.	Description	Value
1	Hydrometer Number	152H
2	Specific Gravity of soil (G_s)	2.45
4	% finer of #200 sieve for soil, F200	83.90 %
6	Dispersing Agent	Sodium Hexametaphosphate
7	Weight of soil sample (W)	50 g
8	Temperature	26C^o (Same throughout this test)
9	Zero Correction (Z_c)	+ 2
10	Meniscus Correction (M_c)	+ 1

Serial No.	Description	Value
11	Viscosity of Water at 26C° (η)	0.00000864 g.s /cm^2
12	K (From Table for G_s = 2.45)	0.01357
13	Temperature Correction Factor (C_T)	1.65 for 26 C°
14	Correction Factor (a) for G_s = 2.45	1.045 using interpolation

Table 4. 4: Observations and Calculations for Hydrometer Analysis of Parent Soil

Sr. No.	Elapsed Time (T)	Actual Hydrometer Reading (R_a)	Correction for Meniscus	Length (L)	Dia. (D)	Corrected Hydrometer Reading (R_c)	% Finer	% Adjusted Finer
	Min.			cm	mm		%	%
1	0.5	46	47	8.6	0.05628	45.65	95.41	80.048
2	1	44	45	9.6	0.04205	43.65	91.23	76.541
3	2	36	37	11.1	0.03197	35.65	74.51	62.513
4	4	25	26	12	0.0235	24.65	51.52	43.224
5	8	21	22	12.7	0.0171	20.65	43.16	36.210
6	16	10	11	14.5	0.01292	9.65	20.17	16.921
7	32	5	6	15.3	0.00938	4.65	9.72	8.154
8	64	2	3	15.8	0.00674	1.65	3.45	2.893

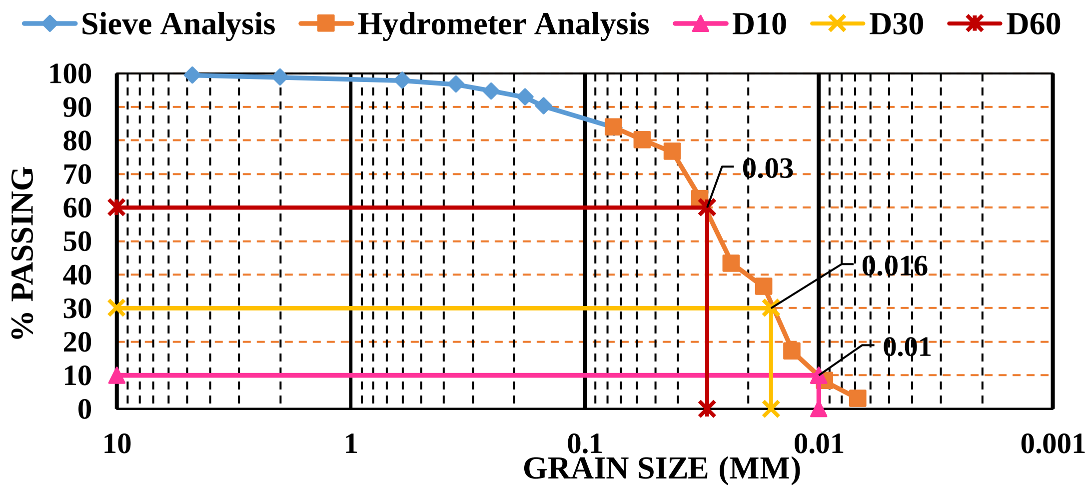

Figure 4.1: Gradation Curve for Soil

1.1.4 Liquid Limit Test Results

Table 4.5: Calculations for Liquid limit test of Parent soil

Sample No.	1			2			3			4		
Can Name	A	B	C	A	B	C	A	B	C	A	B	C
No. of Blows	16	22	31	18	21	31	14	23	29	13	20	28
Empty can weight (g)	20.5	28.2	30.3	22.3	25.4	23.8	30.2	33.1	22.9	24.6	30.5	31.7
Can + Wet Sample (g)	40.5	48.2	50.3	42.3	45.4	43.8	50.2	53.1	42.9	44.6	50.5	51.7
Wet Sample Weight (g)	20.0	20.0	20.0	20.0	20.0	20.0	20.0	20.0	20.0	20.0	20.0	20.0
Can + Dry Sample (g)	33.5	42.2	45.3	34.1	37.4	39.6	42.7	48.1	45	27.5	45.5	47.6
Dry weight of sample (g)	13	14	15	11.8	12	15.8	12.5	15	16	14.5	15	15.9
Moisture Content (%)	35	30	25	34.4	29.4	21.0	37.5	25.0	20.0	27.5	25.0	20.5

Result: From Graph shown in figure 4.2 , L.L of the soil came out to be 25.2 %

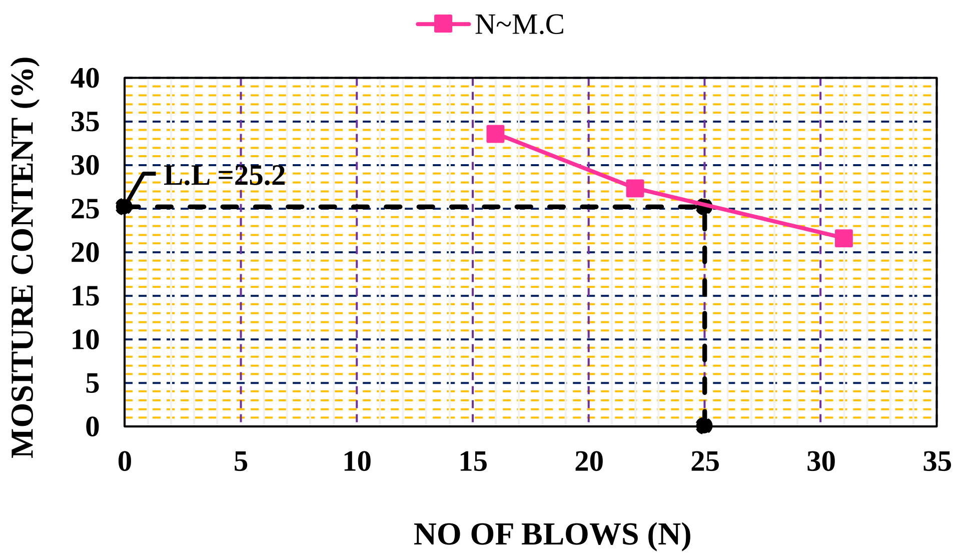

Figure 4.2: Liquid Limit Test Graph of the Parent Soil

1.1.5 Plastic Limit Test Results

Table 4.6: Results for Plastic limit Test of parent soil

Sr. No.	Description	Sample 1	Sample 2	Sample 3
1	Weight of empty can (g)	20.50	28.20	25.40
2	Weight of wet sample + can (g)	28.50	34.70	33.40
3	Wet Sample Weight (g)	8.00	6.50	8.00
4	Can + Dry Sample (g)	27.00	33.50	31.83
5	Dry weight of sample (g)	6.50	5.30	6.43
6	Moisture Content (%)	18.75	18.46	19.63
Result: Average Plastic Limit (P.L) = 18.95 %				

Table 4.7: Properties of soil for Classification

Description	Values
Percentage of Fines (< #200 Sieve)	83.9 % (From table 4.2)
Percentage of gravels (100 - # 4 Sieve passing)	0.55 % (From table 4.2)
Percentage of sand (#4 passing - #200 passing)	15.55 % (From table 4.2)
Liquid limit of the soil	25.2 (From figure 4.2)
Plastic limit of the soil	18.95 (From Table 4.6)
Plasticity Index (P.I) = L.L – P.L	6.25
D_{10}	0.01 mm (From figure 4.1)
D_{30}	0.016 mm (From figure 4.1)
D_{60}	0.03 mm (From figure 4.1)
$C_u = D_{60} / D_{10}$	3
$C_c = (D_{30})^2 / [D_{60} \times D_{10}]$	0.853
Group Index (G.I)	4
USCS Classification	**CL-ML (Sandy Silty Clay)**
AASHTO Classification	**A-4(4), Silty soil**

1.2 CERAMIC DUST CLASSIFICATION

1.2.1 Gradation curve for Ceramic Dust

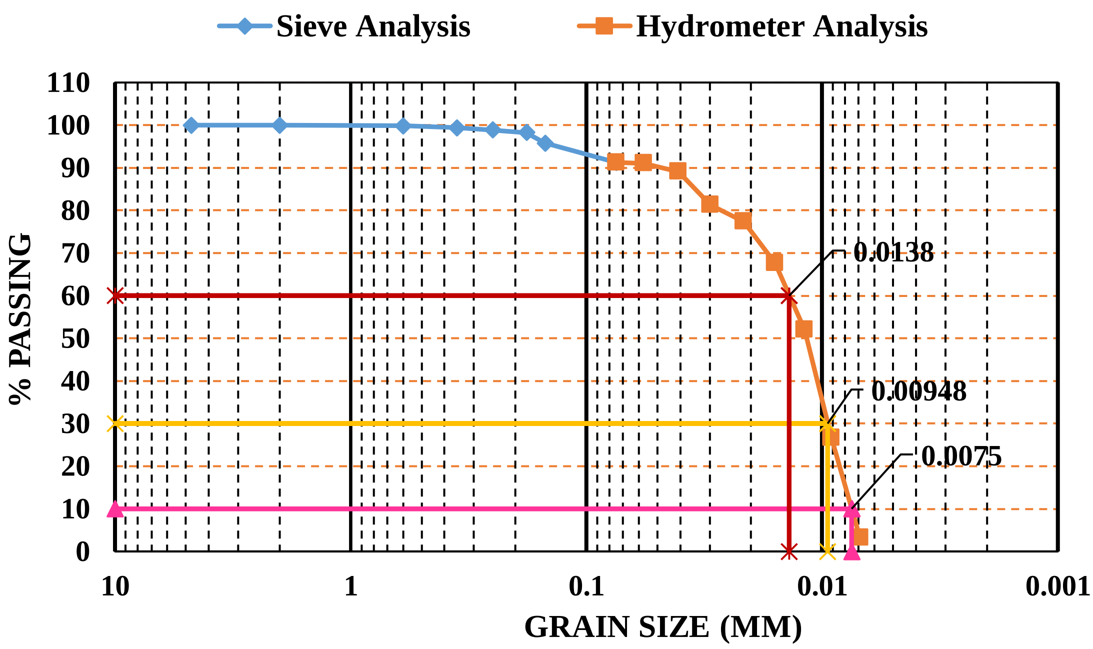

Figure 4.3: Grain size distribution curve for Ceramic Dust

1.2.2 Liquid limit test Results for Ceramic Dust

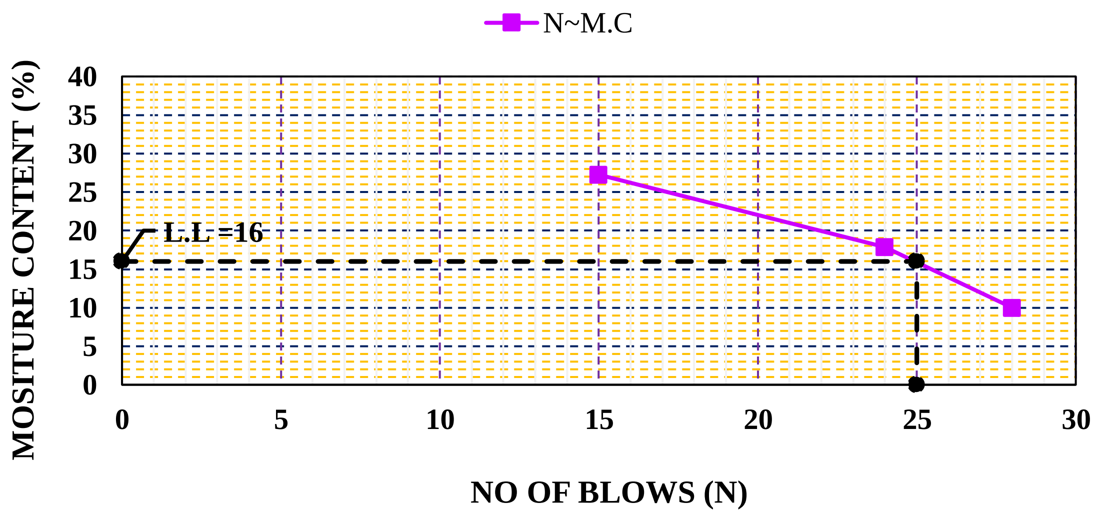

Figure 4.4: Liquid Limit Test Graph for the Ceramic Dust

1.2.3 Plastic Limit Test Results for Ceramic Dust

Table 4.8: Plastic limit test results for Ceramic dust

Sr. No.	Description	Sample 1	Sample 2	Sample 3
1	Weight of empty can (g)	28.20	25.40	30.30
2	Weight of wet sample + can (g)	36.20	33.40	38.30
3	Wet Sample Weight (g)	8.00	8.00	8.00
4	Can + Dry Sample (g)	35.40	32.70	37.50
5	Dry weight of sample (g)	7.20	7.30	7.20
6	Moisture Content (%)	10.00	8.75	10.00
Result: Average Plastic Limit (P.L) = 9.58 %				

Table 4.9: Properties of ceramic dust for Classification

Description	Values
Percentage of Fines (< #200 Sieve)	91.27% (From figure 4.3)
Percentage of gravels (100 - # 4 Sieve passing)	100 % (From figure 4.3)
Percentage of sand (#4 passing - #200 passing)	15.55 % (From figure 4.3)
Liquid limit of the ceramic dust	16 (From figure 4.4)
Plastic limit of the ceramic dust	9.58 (From table 4.8)
Plasticity Index (P.I) = L.L – P.L	6.42
D_{10}	0.0075 mm (From figure 4.3)
D_{30}	0.00948 mm (From figure 4.3)
D_{60}	0.0138 mm (From figure 4.3)
$C_u = D_{60} / D_{10}$	1.84
$C_c = (D_{30})^2 / [D_{60} \times D_{10}]$	0.868
Group Index (G.I)	2
USCS Classification	**CL-ML (Falls into Sandy Silty Clay)**
AASHTO Classification	**A-4(2), Fall into silty soil category**

1.2.4 Atterberg Limits Test Results with 30% Addition of Ceramic Dust

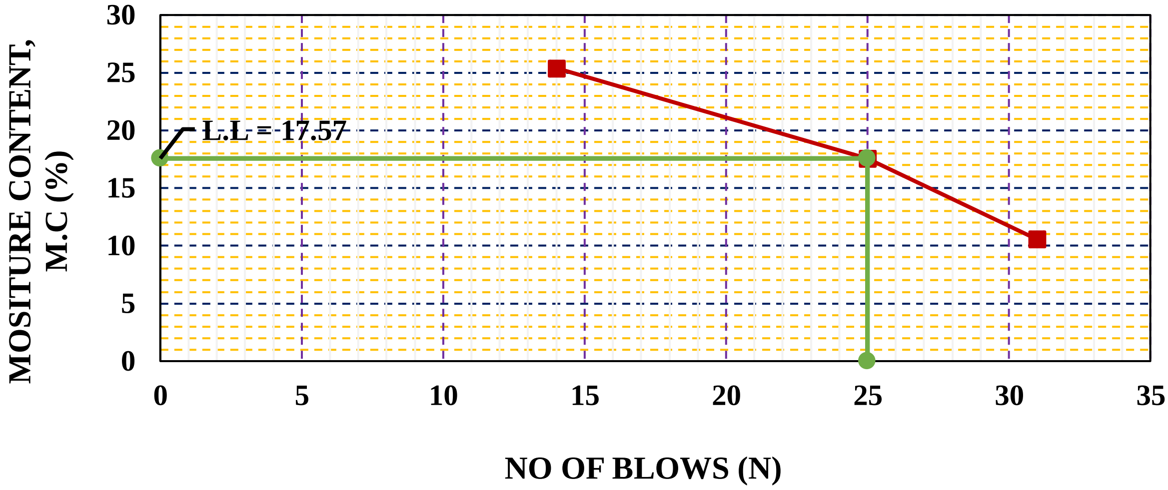

Figure 4. 5: Liquid Limit test Graph (With 30% Addition of CD)

Table 4. 10: Plastic Limit Test Results (30% Addition of CD)

Sr. No.	Description	Sample 1	Sample 2	Sample 3
1	Weight of empty can (g)	25.40	30.70	33.10
2	Weight of wet sample + can (g)	33.40	38.80	41.10
3	Wet Sample Weight (g)	8.00	8.00	8.00
4	Can + Dry Sample (g)	33.50	37.80	40.30
5	Dry weight of sample (g)	7.1	7.1	7.2
6	Moisture Content (%)	11.25	11.25	10.00
Result: Average Plastic Limit (P.L) = 10.83%				

1.3 RESULTS OF SPECIFIC GRAVITY TEST

Table 4.11: Specific Gravity Test Results (Parent soil)

Sr. No.	Observations	Symbol	Sample 1	Sample 2
1	Weight of Pycnometer	A (g)	467	467
2	Weight of Pycnometer +Soil	B (g)	705	724.5
3	Weight of Pycnometer +Soil +Water	C (g)	990.5	1002
4	Weight of Pycnometer + Water	D (g)	849.5	849.5

5	Specific Gravity	G_s	2.454	2.452
Average Specific Gravity of Soil = G_s = 2.453				

Table 4. 12: Specific Gravity Test Results (Ceramic Dust)

Sr. No.	Observations	Symbol	Sample 1	Sample 2
1	Weight of Pycnometer	A (g)	467	467
2	Weight of Pycnometer +Soil	B (g)	650	680
3	Weight of Pycnometer +Soil +Water	C (g)	956	975
4	Weight of Pycnometer + Water	D (g)	852	852
5	Specific Gravity	G_s	2.316	2.367
Average Specific Gravity of Ceramic Dust = G_s = 2.342				

1.4 RESULTS OF MODIFIED PROCTOR TEST

Modified proctor test is performed as per ASTM D1557 and complete calculations are discussed in section 3.8.6.Results of the Modified proctor test are shown below:

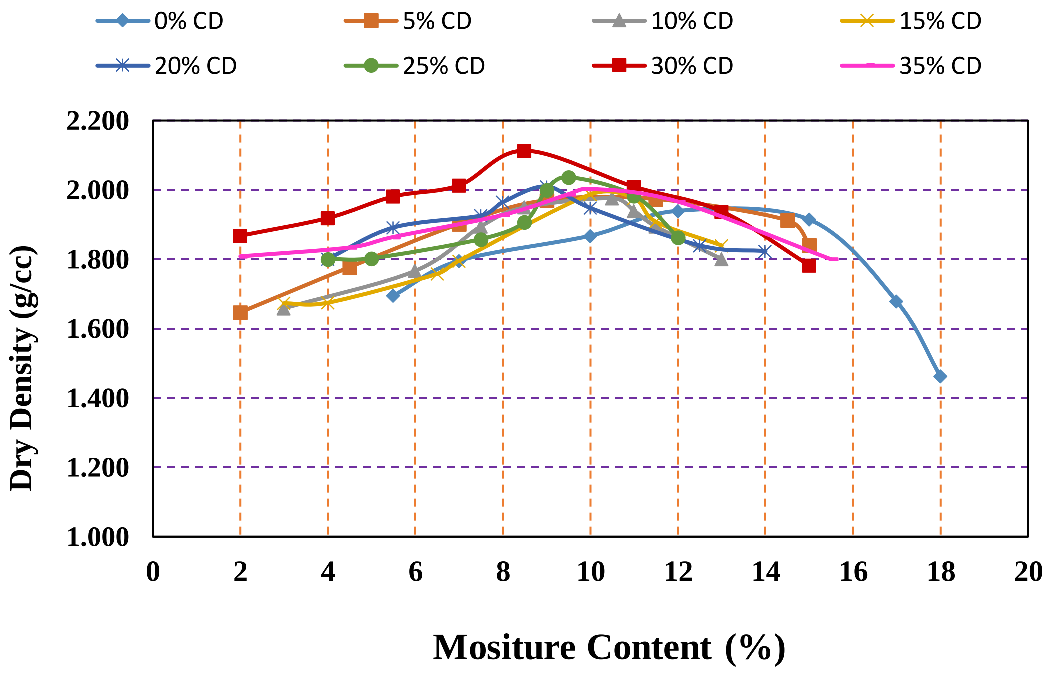

Figure 4.6: Modified Test Results (At Different % of CD)

Following table shows the summary of results obtained from modified proctor test.

Table 4. 13: Summary of the modified proctor test results

Percentage of CD	MDD (g/cc)	OMC (%)
0 % CD (Parent soil)	1.940	12.0
5 % CD addition	1.974	11.5
10 % CD addition	1.976	10.5
15 % CD addition	1.987	10.0
20 % CD addition	2.010	9.0
25 % CD addition	2.037	9.5
30 % CD addition	2.113	8.5
35 % CD addition	2.003	10.0

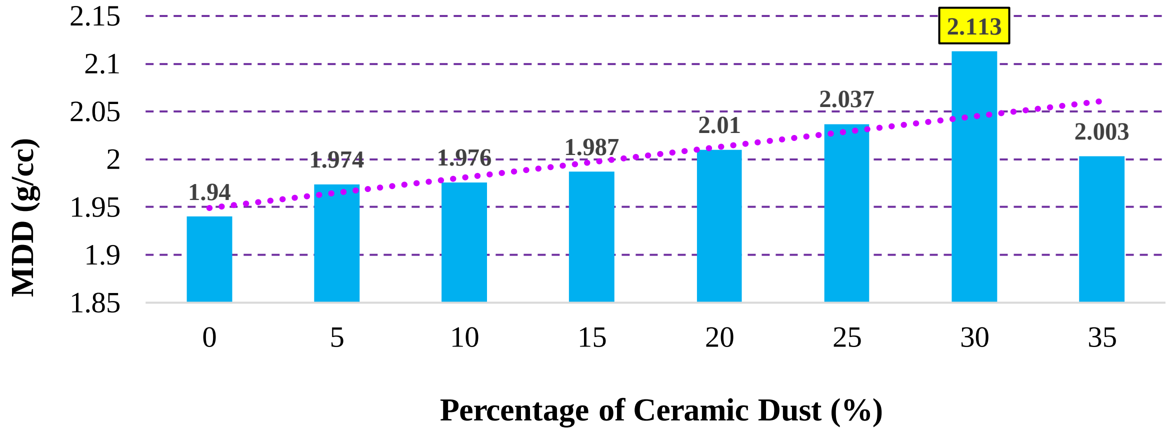

Figure 4.7: Variation of MDD with Addition of CD

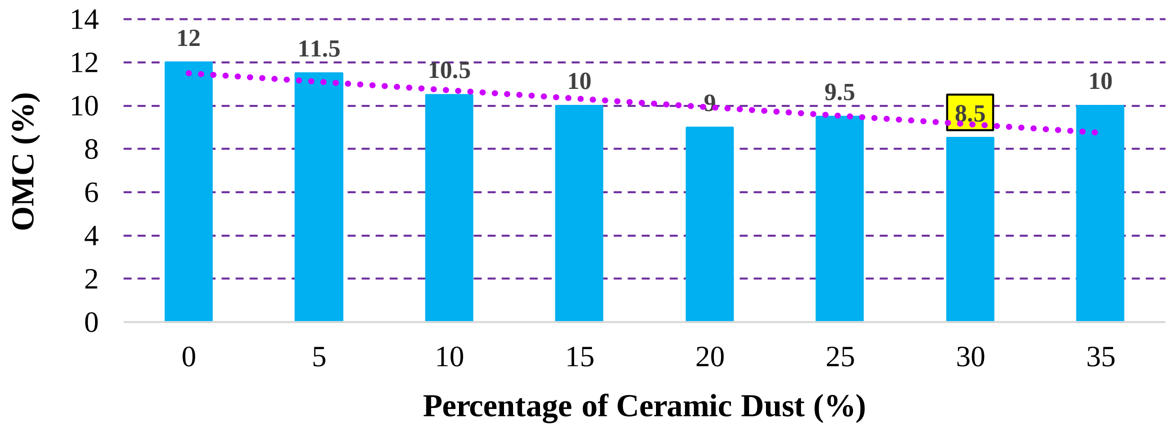

Figure 4.8: Variation in OMC with addition of OMC

The findings of the Modified Proctor test point to an obvious pattern that is associated with the incorporation of ceramic dust into the soil. The Maximum Dry Density (MDD) of the soil experiences an increase that is proportional to the increase in the percentage of ceramic dust present in the soil. According to this trend, it appears that the incorporation of ceramic dust into stabilized soil increases both its ability to be compacted and its density. On the other hand, the optimal moisture content (OMC) displays a continuous decline as the percentage of ceramic dust rises. This pattern suggests that the presence of ceramic dust lowers the required percentage of water in the soil in order to achieve the highest possible level of soil compaction. As a consequence of this, the soil that has been stabilized becomes less vulnerable to problems that are caused by moisture and offers a higher level of stability. In conclusion, the findings of the Modified Proctor test demonstrate beyond a reasonable doubt that the incorporation of ceramic dust into the ground causes a rise in the MDD while simultaneously causing a fall in the OMC.

1.5 RESULTS OF DIRECT SHEAR TEST

Direct shear test is performed as per ASTM D3080 and complete observations and calculations are discussed in section 3.8.7. Results of the direct shear test are shown below:

Observations and Calculations for Direct Shear Test

Height of sampler	=	2.3 cm
Area of sampler	=	$6\times6 = 36\ cm^2$
Volume of sampler	=	$82.8\ cm^3$
Vertical stress calculations		
For 2kg normal load		
Vertical stress	=	$[2\times10]/\ 36 = 0.556\ kg/cm^2$
	=	$0.556 \times 98.07 = 54.48$ kPa
For 4kg normal load		
Vertical stress	=	$[4\times10]/\ 36 = 1.111\ kg/cm^2$
	=	$1.111 \times 98.07 = 108.97$ kPa
For 8kg normal load		
Vertical stress	=	$[8\times10]/\ 36 = 2.222\ kg/cm^2$
	=	$2.222 \times 98.07 = 217.94$ kPa

Table 4.14 shows the summary of the end observations obtained from direct shear test machine.

Table 4. 14: Results of Direct Shear Test

% of CD	Normal Load (Kg)	Peak Vertical Stress (kPa)	Peak Horizontal Stress (kPa)
0%	2	54.480	32.447
	4	108.970	62.327
	8	217.940	110.449
5%	2	54.480	39.876
	4	108.970	53.432
	8	217.940	114.921
10%	2	54.480	40.786
	4	108.970	70.432
	8	217.940	125.023
15%	2	54.480	46.906
	4	108.970	70.321
	8	217.940	130.786
20%	2	54.480	59.654
	4	108.970	69.765
	8	217.940	145.034
25%	2	54.480	60.564
	4	108.970	70.987
	8	217.940	146.897
30%	2	54.480	63.032
	4	108.970	80.141
	8	217.940	155.98
35%	2	54.480	35.010
	4	108.970	60.654
	8	217.940	102.321

Following table shows the summary of results obtained from direct shear test.

Table 4. 15: Summary of the Direct Shear test results

Percentage of CD	Cohesion (kPa)	Friction Angle (°)
0 % CD (Parent soil)	8.39	25.272
5 % CD addition	9.13	25.367
10 % CD addition	13.49	27.271
15 % CD addition	16.68	27.434
20 % CD addition	22.02	28.651
25 % CD addition	22.61	28.908
30 % CD addition	25.12	30.405
35 % CD addition	14.18	22.175

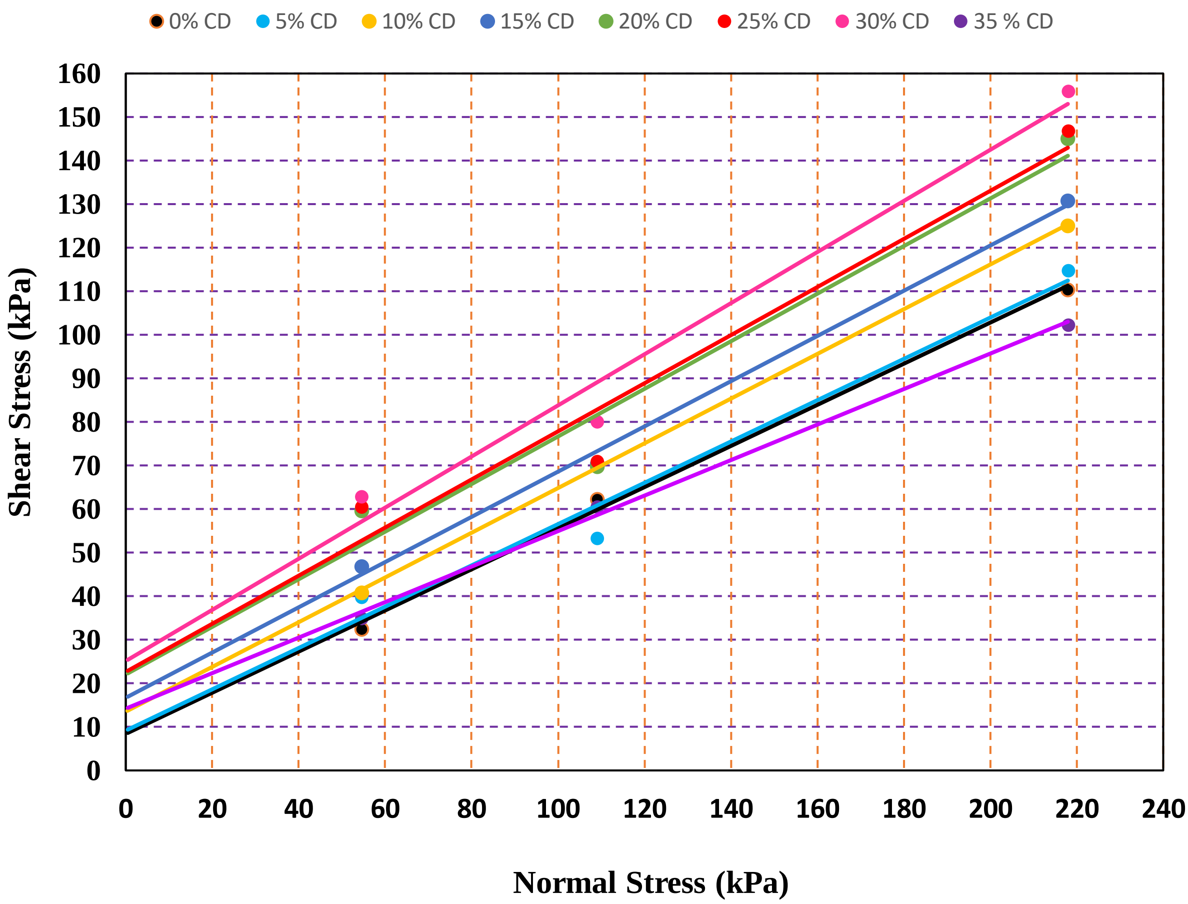

Figure 4.9: Results for shear strength parameters of soil at different % of ceramic dust

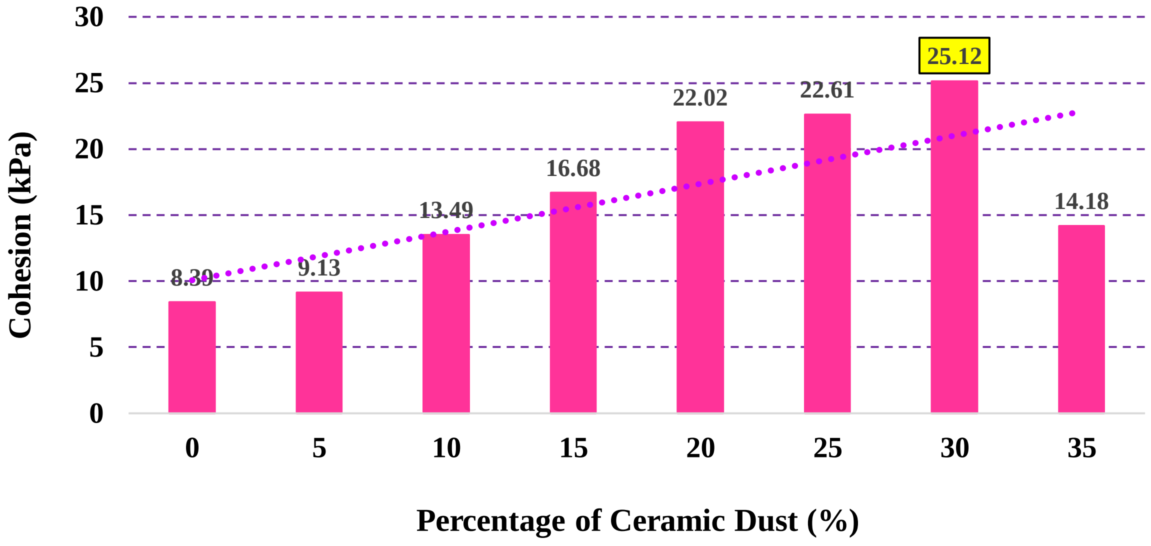

Figure 4.10: Effect of addition of Ceramic dust on Cohesion (c)

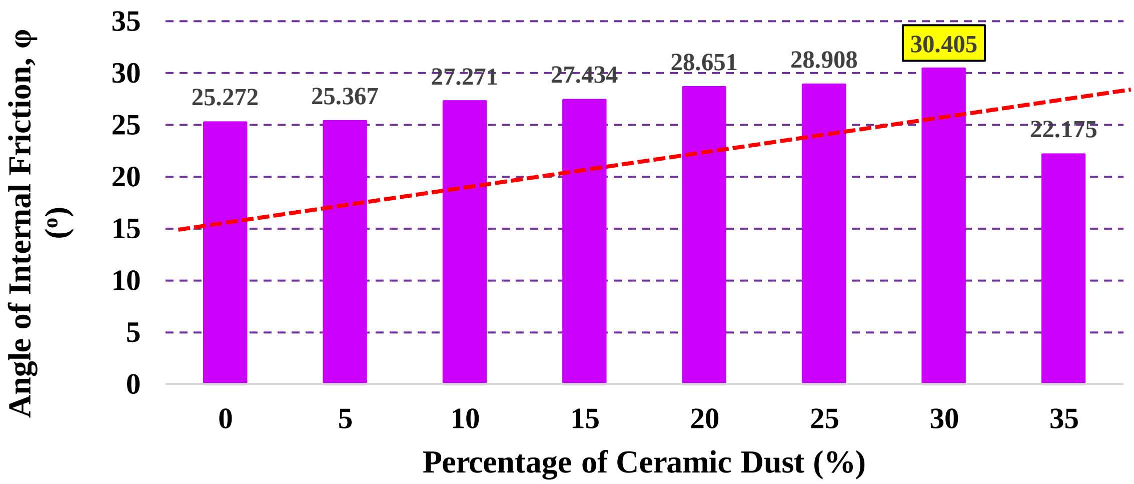

Figure 4.11: Effect of addition of Ceramic dust on internal friction angle (Φ)

The findings of the direct shear test make it abundantly evident that the incorporation of ceramic dust has a discernible influence on the cohesiveness as well as the internal friction angle of the soil. Both the angle of internal friction and the cohesiveness of the material progressively rise up to a particular percentage of ceramic dust in this case it is 30%. This suggests that the presence of ceramic dust increases the shear strength of the soil as well as its ability to withstand deformation. However, it is crucial to take into account that once the addition level reaches 30%, the cohesiveness and internal friction angle values begin to fall. This indicates that adding an excessive amount of ceramic dust may not be helpful for the stabilization of the soil.

1.6 RESULTS FOR CALIFORNIA BEARING RATIO TEST

California bearing ratio test was performed at parent soil and optimum percentage of ceramic dust as per AASHTO T193 and complete observations are discussed in section 3.8.7. Following table shows the summary of results obtained from CBR test.

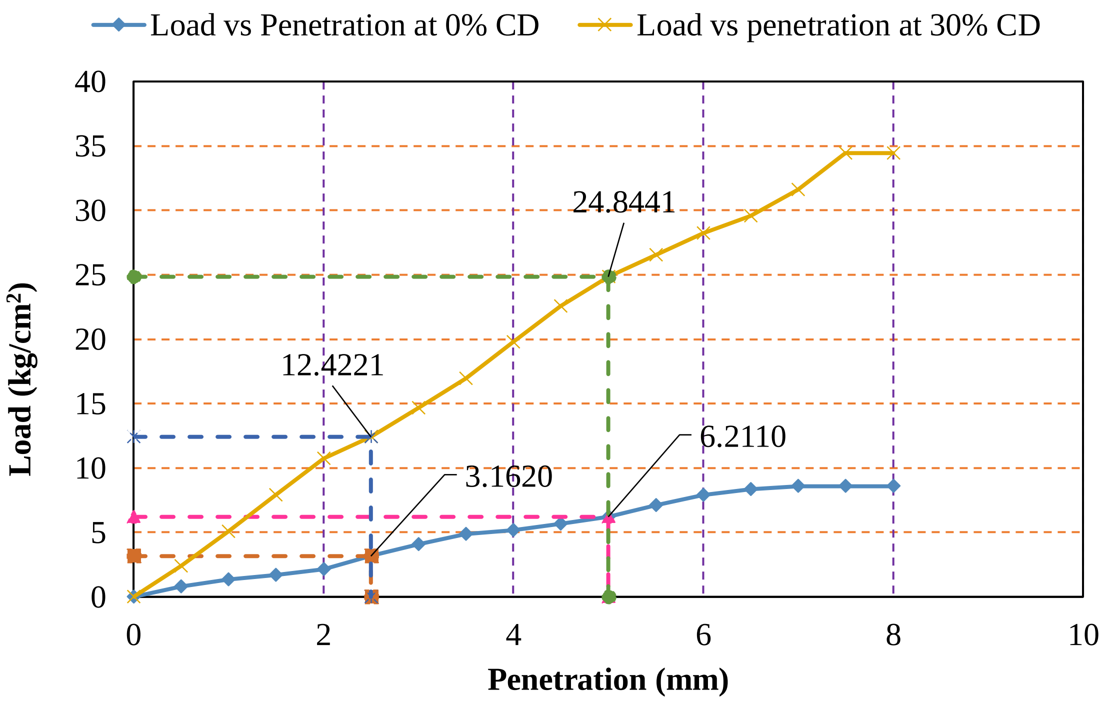

Figure 4.12: Load vs Penetration curve for CBR test

Table 4. 16: Results of the CBR Value 0% addition of CD and at optimum % of CD

% of CD	Description	Value
0 % CD (Parent Soil)	Axial load at 2.5mm penetration	3.162 kg/cm^2
	Standard Load at 2.5mm penetration	70.0 kg/cm^2
	CBR value at 2.5mm penetration	4.52 %
	Axial load at 5.0 mm penetration	6.211 kg/cm^2
	Standard Load at 5.0 mm penetration	150.0 kg/cm^2
	CBR value at 5.0 mm penetration	4.14 %
	Final CBR value	**4.52 %**

30 % CD (Optimum %)	Axial load at 2.5mm penetration	12.422 kg/cm^2
	Standard Load at 2.5mm penetration	70.0 kg/cm^2
	CBR value at 2.5mm penetration	17.75 %
	Axial load at 5.0 mm penetration	24.85 kg/cm^2
	Standard Load at 5.0 mm penetration	150.0 kg/cm^2
	CBR value at 5.0 mm penetration	16.56 %
	Final CBR value	**17.75**

$$\%\ Increase\ in\ the\ CBR\ value\ =\ 293\ \%$$

1.6.1 Design of Flexible Pavement using CBR method

In this section, we will analyze the economic aspects of our project. We'll design the flexible pavement using the CBR method, considering a normal traffic load of 15,000 pounds. To ensure the pavement's serviceability, we'll calculate the total required thickness based on the CBR value of the original soil and also at the optimum percentage of ceramic dust addition.

CBR value of parent soil = 4.52%

CBR value at optimum percentage of CD = 17.75%

1.6.1.1 Design of pavement at CBR of 4.52%

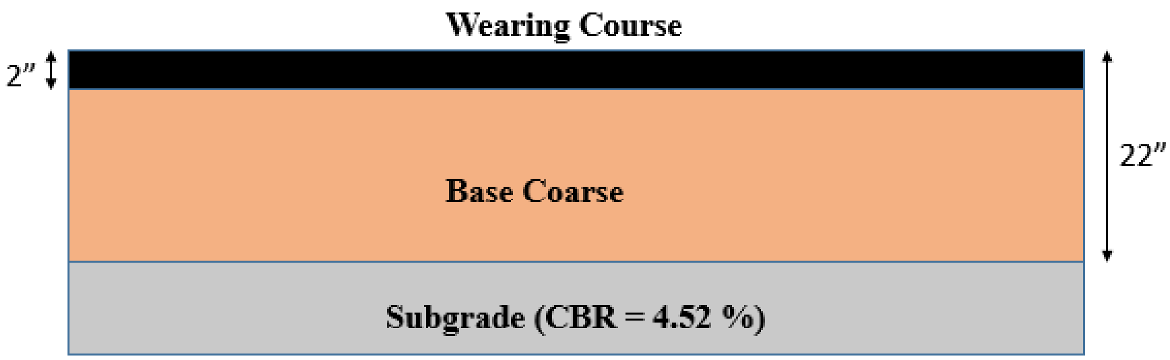

Figure 4.13: Design of the pavement using Parent soil CBR value

1.6.1.2 Design of pavement at CBR of 17.75%

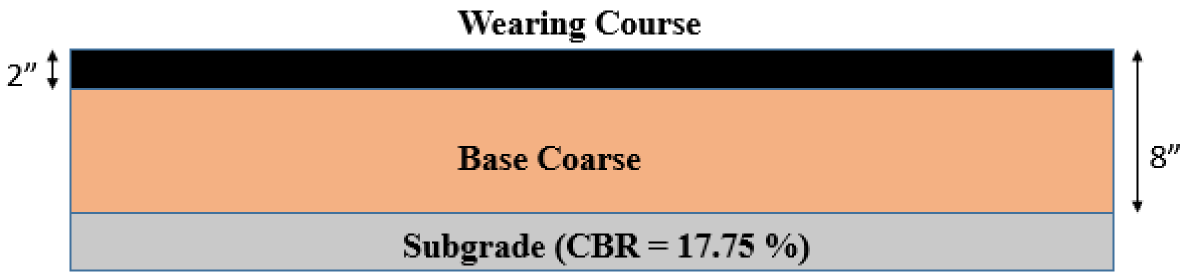

Figure 4.14: Design of the pavement considering optimum percentage of CD, CBR value

The addition of thirty percent ceramic dust to the soil resulted in a significant increase in the soil's strength and its capacity to support loads, as shown by the results of the CBR tests and the pavement design. The CBR value of the parent soil was 4.52%, which shows that it performs pretty poorly. However, after adding 30% ceramic dust, the CBR value increased to 17.75%, showing a significant improvement. Ceramic dust was added to the soil, which resulted in a considerable rise in the soil's capacity to handle traffic loads and resist deformation. This significant increase indicates that the soil's ability to withstand traffic loads and resist deformation has been significantly strengthened.

1.7 RESULTS OF THE SLOPE STABILITY ANALYSIS

Slope stability analysis was perform using strength reduction method using PLAXIS 2D software by considering parent soil properties and different percentages of ceramic dust addition. The complete procedure was discussed in chapter 3, section 3.8.9. Following table shows the summary of results obtained from shear strength reduction method using FEM.

Table 4. 17: Results for FOS and total Displacement at different % of CD

Percentage of CD	FOS	Total Displacement
0 % CD (Parent soil)	0.980	3.787 cm
5 % CD addition	1.118	3.833 cm
10 % CD addition	1.403	3.466 cm

15 % CD addition	1.652	3.480 cm
20 % CD addition	1.665	3.511 cm
25 % CD addition	1.745	3.547 cm
30 % CD addition	1.752	3.651 cm
35 % CD addition	1.322	3.633 cm

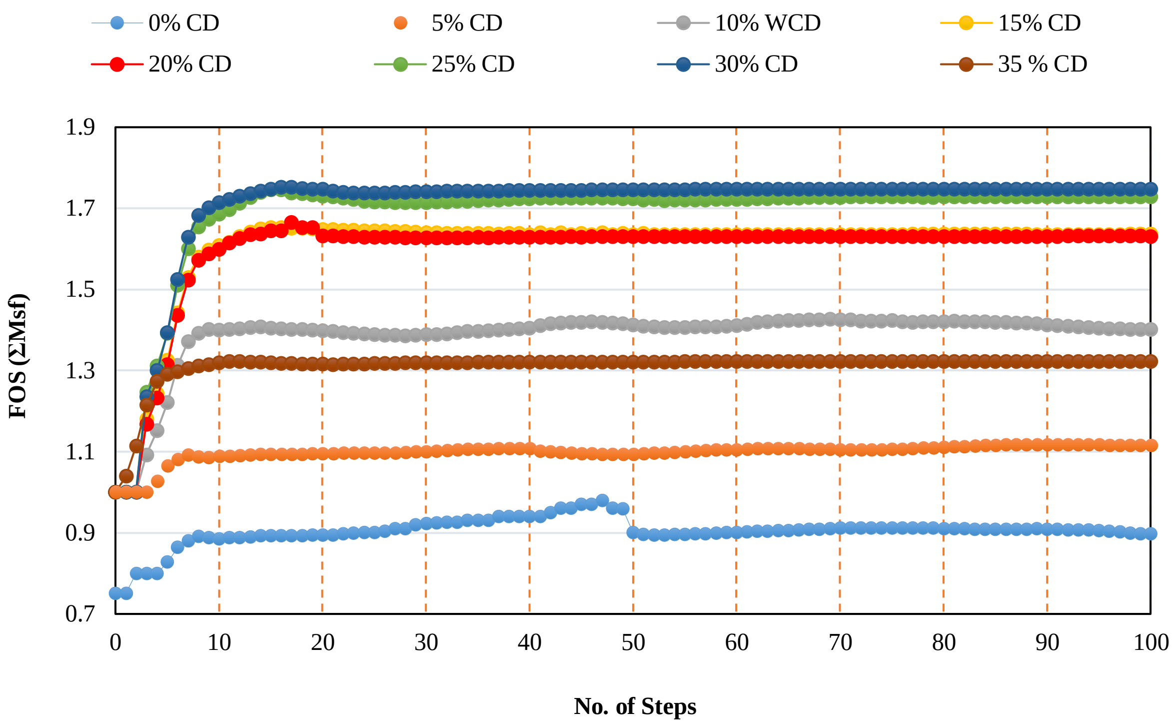

Figure 4.15: FOS using strength reduction, method at different percentages of CD.

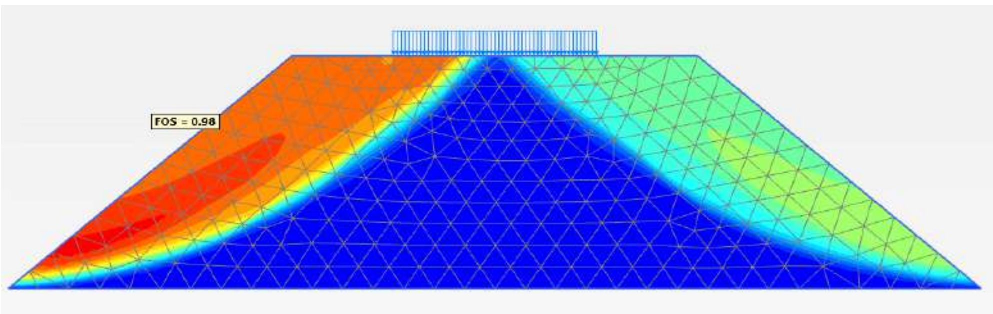

Figure 4.16: Critical Slip surface at 0% addition of CD

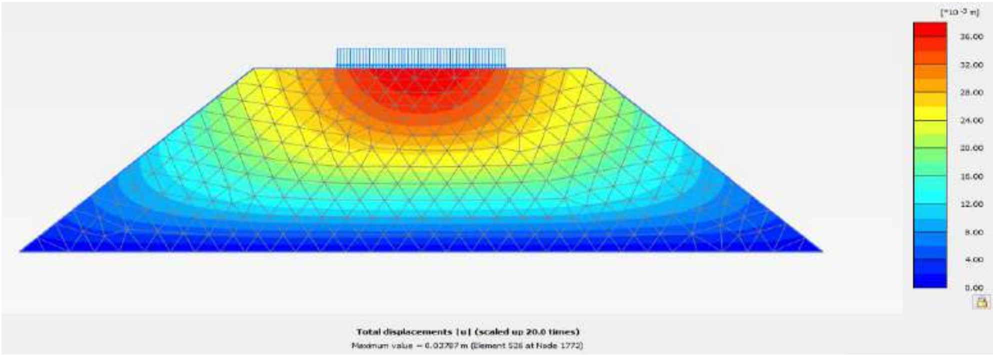

Figure 4.17: Total deformations at 0% CD addition

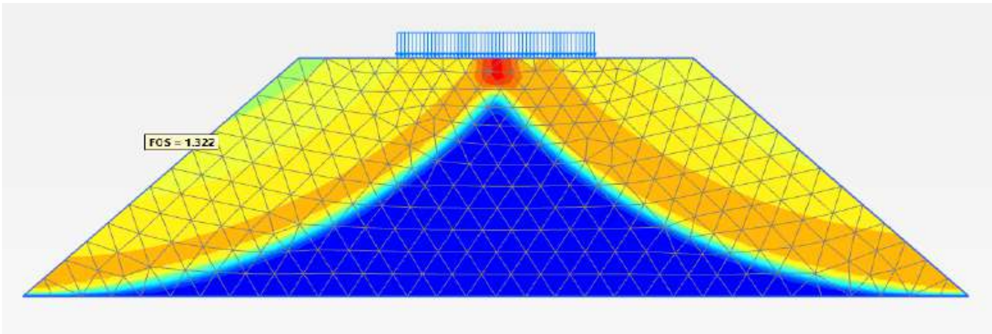

Figure 4.18: Critical Slip surface at 30% addition of CD

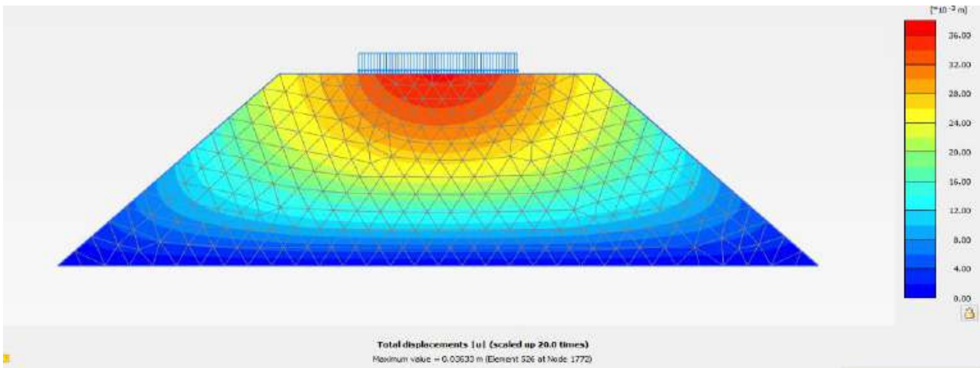

Figure 4.19: Total deformations at 30% CD addition

With the increase in percentage of ceramic dust the value of factor of safety for slope goes on increasing such that at 30% addition of ceramic dust we get maximum value of FOS which is 1.756. Similarly at 30% addition of ceramic dust the total displacement produced in the embankment is also less than that of displacement produced at 0% addition of ceramic dust. This means that addition of ceramic dust up to 30% is suitable for slope stability.

CONCLUSIONS AND RECOMMENDATIONS

The primary purpose of this research was to identify the optimal proportion of ceramic dust to incorporate into the soil at which point the physical characteristics of the ground attain their full potential. The findings that were obtained have been extremely helpful, as they have shown that the Maximum Dry Density (MDD), the cohesiveness (c), and the Factor of Safety (FOS) of the slope all increase in proportion to the amount of ceramic dust that is present in the slope. On the other hand, the Optimum Moisture Content (OMC) and the Internal Friction Angle (Φ) both decrease as the percentage of ceramic dust in the mixture increases. In addition to the aforementioned outcomes, several other important conclusions have been drawn from this study as mentioned below.

5.1 CONCLUSIONS

- Results shows positive influence of ceramic dust on the compaction characteristics of the soil. The results indicate that with an increase in the percentage of ceramic dust, the MDD of the soil increases, while the OMC decreases. The MDD of the untreated soil is 1.940 g/cc, and with 30% addition of ceramic dust, it increases to 2.113 g/cc. Similarly, the OMC of the untreated soil is 12%, which decreases as the percentage of ceramic dust increases, reaching 8.5% at 30% addition of ceramic dust.
- The DST results reveal a significant increase in the cohesion (c) of the soil with the addition of ceramic dust. The cohesion of the untreated soil is approximately 8.39 kPa, and with 30% ceramic dust addition, it experiences a remarkable 199.4% increase, reaching 25.12 kPa.

- The internal friction angle steadily increases with the addition of ceramic dust. For the untreated soil, the internal friction angle is 25.272 degrees, and at the optimum percentage of ceramic dust (30% addition), it increases to 30.405 degrees.
- The CBR test demonstrates a substantial increase in the California Bearing Ratio (CBR) value with the addition of ceramic dust. At the optimum 30% addition of ceramic dust, there is an impressive 293% increase in CBR compared to untreated soil.
- The pavement design using the CBR method shows that at 30% ceramic dust addition, only 8 inches of pavement thickness is required, while untreated soil demands a 22-inch thickness. This highlights the cost-effectiveness of using ceramic dust, as thinner pavement layers lead to potential construction cost savings.
- The Liquid Limit and Plastic Limit tests illustrate that the plasticity of the soil decreases with the increase in ceramic dust content. The Liquid Limit decreases from 25.2 to 17.57, and the Plastic Limit decreases from 18.95 to 10.83 at 30% ceramic dust addition.
- The slope stability analysis using PLAXIS 2D software, employing the strength reduction method, confirms that the Factor of Safety (FOS) of the embankment slope increases with the addition of ceramic dust. At the optimum 30% addition, the FOS increases by approximately 78%, indicating enhanced slope stability and safety.

Overall, these conclusive results demonstrate the efficacy of ceramic dust as a soil stabilizing agent. The significant improvements in soil properties, strength, and slope stability provide promising opportunities for sustainable and cost-effective road embankment construction. These findings contribute to the advancement of geotechnical engineering practices, promoting the utilization of ceramic dust to enhance infrastructure development and minimize environmental impact.

5.2 RECOMMENDATIONS

- Based on considerations of both strength and economics it is recommended that up to 30% of ceramic dust can be used to enhance the subgrade of flexible pavement.
- It is important to investigate the impact that ceramic dust has on other problematic soils.
- According to the findings of the evaluation, it is proposed that in future research activities, a cost analysis or economic consideration as well as a possible comparison between unstabilized and stabilized roads should be carried out with more precision.
- Conduct more detailed shear strength tests, such as Triaxial shear tests, to study the stress-strain behavior and undrained strength characteristics of the ceramic dust-stabilized soil. This will provide a more comprehensive understanding of its shear strength properties under different loading conditions.
- To better understand stress redistributions and soil layer interactions, consider 3D numerical modelling of the embankment slope.

REFERENCES

Abderrazak, S. (2018). Model Study of Slope Stability in Open Pit by Numerical Modeling Using the Finite Element Method. *Aspects in Mining & Mineral Science*, *1*(3), 5–7. https://doi.org/10.31031/amms.2018.01.000514

Afrin, H. (2017). A Review on Different Types Soil Stabilization Techniques. *International Journal of Transportation Engineering and Technology*, *3*(2), 19. https://doi.org/10.11648/j.ijtet.20170302.12

Agrawal, A. (2017). *UTILIZATION OF CERAMIC WASTE AS A REPLACEMENT OF AGGREGATES AND ITS EFFECT ON VARIATION OF EXPENDITURE Some of the authors of this publication are also working on these related projects: waste management View project Safety Management View project*. *August*.

Archibong, G. A., Sunday, E. U., Akudike, J. C., Okeke, O. C., & Amadi, C. (2020). *A REVIEW OF THE PRINCIPLES AND METHODS OF SOIL*. *March*.

Arora, K. R. (2011). *Soil Mechanics & Foundation Engineering* (Seventh). Standard Publisher Distributors.

Ayob, M., Kasa, A., Sulaiman, M. S., & Devi, N. (2019). *Slope Stability Evaluations Using Limit Equilibrium and Finite Element Methods Slope Stability Evaluations Using Limit Equilibrium and Finite Element Methods Faculty of Ocean Engineering Technology and Informatics , University Malaysia Faculty of Bioengin*. *December*.

Beyene, A., Tesfaye, Y., Tsige, D., Sorsa, A., Wedajo, T., Tesema, N., & Mekuria, G. (2022). Experimental study on potential suitability of natural lime and waste ceramic dust in modifying properties of highly plastic clay. *Heliyon*, *8*(10), e10993. https://doi.org/10.1016/j.heliyon.2022.e10993

Binici, H. (2007). Effect of crushed ceramic and basaltic pumice as fine aggregates on concrete mortars properties. *Construction and Building Materials*, *21*(6), 1191–1197. https://doi.org/10.1016/j.conbuildmat.2006.06.002

Boutrup, E., & Lovell, C. W. (1980). Searching techniques in slope stability analysis. *Engineering Geology*, *16*(1–2), 51–61. https://doi.org/10.1016/0013-7952(80)90006-X

Cabalar, A. F., Hassan, D. I., & Abdulnafaa, M. D. (2017). Use of waste ceramic tiles for road pavement subgrade. *Road Materials and Pavement Design*, *18*(4), 882–896. https://doi.org/10.1080/14680629.2016.1194884

Chen, James, A., Idusuyi, & Felix, O. (2015). Effect of Waste Ceramic Dust (WCD) on Index and Engineering Properties of Shrink-Swell Soils. *International Journal of Engineering and Modern Technology*, *1*(8), 2504–8848.

D7928 Standard Test Method for Particle-Size Distribution (Gradation) of Fine-Grained Soils Using the Sedimentation (Hydrometer) Analysis. (n.d.). Retrieved August 5, 2023, from https://www.astm.org/d7928-21e01.html

Dang, L. C., Dang, C. C., & Khabbaz, H. (2018). Numerical Analysis on the Performance of Fibre Reinforced Load Transfer Platform and Deep Mixing Columns Supported Embankments. *Sustainable Civil Infrastructures*, *1*, 157–169. https://doi.org/10.1007/978-3-319-63889-8_13

Direct Shear Test - Civil Engineering Portal - Biggest Civil Engineering Information Sharing Website. (n.d.). Retrieved August 5, 2023, from https://www.engineeringcivil.com/direct-shear-test.html

El-Dieb, A. S., Taha, M. R., & Abu-Eishah, S. I. (2019). *Ceramic Materials: Synthesis, Characterization, Applications and Recycling,*. https://books.google.com/books?hl=en&lr=&id=KBT8DwAAQBAJ&oi=fnd&pg=PA7&dq=El-Dieb+AS,+Taha+MR,+Abu-Eishah+SI+2018+The+Use+of+Ceramic+Waste+Powder+(CWP)+in+Making+Eco-Friendly+Concretes,+In+Ceramic+Materials-Synthesis,+Characterization,+Applications+and+Re

Ene, E., & Okagbue, C. (2009). Some basic geotechnical properties of expansive soil modified using pyroclastic dust. *Engineering Geology*, *107*(1–2), 61–65. https://doi.org/10.1016/j.enggeo.2009.03.007

Firoozi, A. A., Guney Olgun, C., Firoozi, A. A., & Baghini, M. S. (2017). Fundamentals of soil stabilization. *International Journal of Geo-Engineering*, *8*(1). https://doi.org/10.1186/s40703-017-0064-9

Flexible Pavement Definition and Explanation - Highway Traffic Engineering. (n.d.). Retrieved July 23, 2023, from https://www.aboutcivil.org/flexible-pavement-road.html

Fu, W., & Liao, Y. (2010). Non-linear shear strength reduction technique in slope stability calculation. *Computers and Geotechnics*, *37*(3), 288–298. https://doi.org/10.1016/j.compgeo.2009.11.002

Hammah, R. E., Yacoub, T. E., Corkum, B. C., & Curran, J. H. (2005). The shear strength reduction method for the generalized Hoek-Brown criterion. *American Rock Mechanics Association - 40th US Rock Mechanics Symposium, ALASKA ROCKS 2005: Rock Mechanics for Energy, Mineral and Infrastructure Development in the Northern Regions*, *i*.

Hammouri, N. A., Husein Malkawi, A. I., & Yamin, M. M. A. (2008). Stability analysis of slopes using the finite element method and limiting equilibrium approach. *Bulletin of Engineering Geology and the Environment*, *67*(4), 471–478. https://doi.org/10.1007/s10064-008-0156-z

Hejazi, S. M., Sheikhzadeh, M., Abtahi, S. M., & Zadhoush, A. (2012). A simple review of soil reinforcement by using natural and synthetic fibers. *Construction and Building Materials*, *30*, 100–116. https://doi.org/10.1016/j.conbuildmat.2011.11.045

How To Conduct Wet Sieving - Precision Eforming. (n.d.). Retrieved August 5, 2023, from https://precisioneforming.com/sieve-products/conduct-wet-sieving/

James, J., & Pandian, P. K. (2018). Strength and microstructure of micro ceramic dust admixed lime stabilized soil. *Revista de La Construccion*, *17*(1), 5–22. https://doi.org/10.7764/RDLC.17.1.5

Kazushige Sogawa, and M. D. P. (1970). NII-Electronic Library Service. *Chemical Pharmaceutical Bulletin*, *43*, 2091. http://www.mendeley.com/research/geology-volcanic-history-eruptive-style-yakedake-volcano-group-central-japan/

Khan, S. A., & Abbas, S. M. (2014). Numerical Modelling of Highway Embankment By Different Ground Improvement Techniques. *I Nternational Journal of I Nnovative Resear Ch in Advanced Engineering (I JI RAE*, *1*(10), 2349–2163. www.ijirae.com

Langfelder, L. J., & Nivargikar, V. R. (1967). Some Factors Influencing Shear Strength and Compressibility of Compacted Soils. *Highway Research Board*, *177*, 4–21. http://onlinepubs.trb.org/Onlinepubs/hrr/1967/177/177-002.pdf

Ma, B., Su, C., Ren, X., Gao, Z., Qian, F., Yang, W., Liu, G., Li, H., Yu, J., & Zhu, Q. (2019). Preparation and properties of porous mullite ceramics with high-closed porosity and high strength from fly ash via reaction synthesis process. *Journal of Alloys and Compounds*, *803*, 981–991. https://doi.org/10.1016/j.jallcom.2019.06.272

Mamat, R. C., Samad, A. M., Kasa, A., Razali, S. F. M., Ramli, A., & Omar, M. B. H. C. (2020). Slope stability prediction of road embankment on soft ground treated with prefabricated vertical drains using artificial neural network. *IAES International Journal of Artificial Intelligence*, *9*(2), 236–243. https://doi.org/10.11591/ijai.v9.i2.pp236-243

Matthews, C., Farook, Z., & Helm, P. (2014). Slope stability analysis – limit equilibrium or the finite element method ? *Ground Engineering*, *May*, 22–28.

MD Sahadat Hossain, P. D. . P. E., Islam, M. A., Badhon, F. F., & Imtiaz, T. (2021). *Sieve Analysis*. Mavs Open Press.

Number, T. P. (2008). *Guideline for Pulverization of Stabilized Bases*. *79968*(0).

Obianigwe, N., & Ngene, B. U. (2018). Soil Stabilization for Road Construction: Comparative Analysis of a Three-Prong Approach. *IOP Conference Series: Materials Science and Engineering*, *413*(1). https://doi.org/10.1088/1757-899X/413/1/012023

Omari, A., & Boddula, R. kumar. (2012). *Slope Stability Analysis of Industrial Solid Waste Landfills, Department of Civil, Environmental and Natural Resources Engineering, Lulea University of Technology*. 1–93.

Onakunle, O., Omole, D. O., & Ogbiye, A. S. (2019). Stabilization of lateritic soil from Agbara Nigeria with ceramic waste dust. *Cogent Engineering*, *6*(1). https://doi.org/10.1080/23311916.2019.1710087

Park, J., & Santamarina, J. C. (2017). Revised Soil Classification System for Coarse-Fine Mixtures. *Journal of Geotechnical and Geoenvironmental Engineering*, *143*(8), 1–13. https://doi.org/10.1061/(asce)gt.1943-5606.0001705

Potgieter, J. T., & Jacobsz, S. W. (2019). Comparing the Factors of Safety From Finite Element and Limit Equilibrium Analyses in Lateral Support Design. *Journal of the South African Institution of Civil Engineering*, *61*(4), 29–41.

https://doi.org/10.17159/2309-8775/2019/v61n4a3

Prakash, R. (2017). Experimental Studies on Concrete Made With Ceramic Waste, Copper Slag and Lathe Waste. *International Journal for Research in Applied Science and Engineering Technology*, *V*(IX), 503–508. https://doi.org/10.22214/ijraset.2017.9073

Program flow chart of PLAXIS analysis. | Download Scientific Diagram. (n.d.). Retrieved July 26, 2023, from https://www.researchgate.net/figure/Program-flow-chart-of-PLAXIS-analysis_fig1_328821986

Queensland. (2016). How soils form. *Queensland Government*. https://www.qld.gov.au/environment/land/management/soil/soil-explained/forms

Rabie, M. (2014). Comparison study between traditional and finite element methods for slopes under heavy rainfall. *HBRC Journal*, *10*(2), 160–168. https://doi.org/10.1016/j.hbrcj.2013.10.002

Rajapakse, R. (2017). Material Quality Control. *Construction Engineering Design Calculations and Rules of Thumb*, 355–370. https://doi.org/10.1016/B978-0-12-809244-6.00020-2

Ramaji, A. E. (2012). A review on the soil stabilization using low-cost methods. *Journal of Applied Sciences Research*, *8*(4), 2193–2196.

Rani, Tg., Shivanarayana, C., Prasad, D., & Prasada Raju, D. (2014). Strength Behaviour of Expansive Soil Treated with Tile Waste. *International Journal of Engineering Research*, *10*(12), 52–57. www.ijerd.com

Reasons Why You Should Use PLAXIS for Geotechnical Analysis. (n.d.). Retrieved July 26, 2023, from https://blog.virtuosity.com/6-reasons-why-you-should-use-plaxis-and-soilvision-for-geotechnical-analysis-project

Sabat, A. (2012). A study on some geotechnical properties of lime stabilised expansive soil-quarry dust mixes. *International Journal of Emerging Trends in Engineering and Development*, *1*(2), 42–49. http://rspublication.com/ijeted/jan 12 pdf/5.pdf

Sabat, A. K. (2012). Stabilization of expansive soil using waste ceramic dust. *Electronic Journal of Geotechnical Engineering*, *17 Z*(January 2012), 3915–3926. https://doi.org/10.1149/10701.19011ecst

Sabat, A. K., Nanda, R. P., Engineering, C., & Durgapur, N. I. T. (2011). *Effect of marble dust on strength and durability of Rice husk ash*. *1*(4), 939–948.

Saber, S. A., & Iravanian, A. (2021). *International Journal of Sustainable Construction Engineering and Technology Using Waste Ceramic Dust in Stabilization of Clay Soils*. *1*, 68–79. http://penerbit.uthm.edu.my/ojs/index.php/ijscet

Santosh, K. G. (1987). *Soil Mechanics*. Khanna Publishers.

Saxena, D. (2017). Stabilization of Dune Sand with Porcelain Waste as Admixture. *International Journal of Engineering Trends and Technology*, *52*(1), 7–11. https://doi.org/10.14445/22315381/ijett-v52p202

Sharma, H., & Lewis, S. (1994). *Waste Containment Systems,Waste Stabilization and Landfills.* John Wiley and Sons Inc.

Smith, I. M., and Griffiths, D. V. (1988). *Programming the finite element method* (Second). https://books.google.com.pk/books?hl=en&lr=&id=ZbtiAAAAQBAJ&oi=fnd&pg=PR15&dq=Smith,+I.+M.,+and+Griffiths,+D.+V.+~1988!.+Programming+the+finite+element+method,+2nd+Ed.,+Wiley,+Chichester,+U.K.&ots=4_oq4naVAR&sig=_CyiqbCOCbBmRQ5LQiurh9cq29E&redir_esc=y#v=o

Soil - Composition and Factors Affecting Soil Formation - Study Wrap. (n.d.). Retrieved July 20, 2023, from https://studywrap.com/soil-composition-and-factors-affecting-soil-formation/

Soil - Formation, Composition, & Structure | Britannica. (n.d.). Retrieved July 19, 2023, from https://www.britannica.com/science/soil/Time

Soil Types – RainMachine. (n.d.). Retrieved July 20, 2023, from https://support.rainmachine.com/hc/en-us/articles/228001248-Soil-Types

Specific Gravity of Soil By Pycnometer Method-Procedure and Calculations - The Constructor. (n.d.). Retrieved August 5, 2023, from https://theconstructor.org/geotechnical/specific-gravity-soil-pycnometer-procedure-calculations/2677/

Sungkar, M., Munirwansyah, M., Munirwan, R. P., & Safrina, D. (2020). Slope stability analysis using Bishop and Finite Element Methods. *IOP Conference Series: Materials Science and Engineering*, *933*(1). https://doi.org/10.1088/1757-899X/933/1/012035

Tiza, M. T., Singh, S., Kumar, A., Michael, T., & Singh, S. K. (2016). *Expansive Soil Stabilization Using in Dustrial Solid Wastes a Review(Conference Paper) Expansive Soil Stabilization Using Industrial Solid Wastes a Review*. *October*. https://www.researchgate.net/publication/308916053

Upadhyay, A., & Kaur, S. (2016). Review on Soil Stabilization Using Ceramic Waste. *International Research Journal of Engineering and Technology*, *3*(7), 1748–1750.

Velbel, M. A. (n.d.). *6 . Weathering and Soil-Forming Processes*.

What is the Atterberg Limits Test? - Definition from Trenchlesspedia. (n.d.). Retrieved August 5, 2023, from https://www.trenchlesspedia.com/definition/4544/atterberg-limits-test

Zienkiewicz, O. C., Humpheson, C., & Lewis, R. W. (1977). Associated and non-associated visco-plasticity and plasticity in soil mechanics. *Geotechnique*, *27*(1), 101–102. https://doi.org/10.1680/geot.1977.27.1.101

Zimbili, O., Salim, W., & Ndambuki, M. (2014). A Review on the Usage of Ceramic Wastes in Concrete Production. In *International Scholarly and Scientific Research & Innovation* (Vol. 8, Issue 1).

APPENDIX A

Table A- 1: Results for DST at different % of CD

Serial No.	For 2kg normal load (54.480 kPa)			For 4kg normal load (108.970 kPa)			For 8kg normal load (217.940 kPa)		
	Horizontal Deformation	Vertical Deformation	Shear Stress	Horizontal Deformation	Vertical Deformation	Shear Stress	Horizontal Deformation	Vertical Deformation	Shear Stress
	mm	mm	kPa	mm	mm	kPa	mm	mm	kPa
With 0% CD addition (Parent Soil)									
1	0	0.472	15.857	0	0.729	23.039	0	0.014	2.701
2	0	0.472	20.103	0	0.751	31.715	0	0.97	29.828
3	0	0.472	21.282	0	0.751	35.594	0	1.106	54.544
4	0	0.472	22.331	0	0.751	36.747	0	1.106	64.372
5	0	0.472	23.405	0	0.751	38.765	0	1.106	67.832
6	0.301	0.472	23.851	0.313	0.804	51.267	0.317	1.106	96.505
7	0.598	0.472	25.685	0.614	0.832	54.124	0.615	1.11	106.491
8	0.915	0.473	27.101	0.921	0.85	54.805	0.923	1.111	106.465
9	1.203	0.473	27.074	1.209	0.851	55.932	1.215	1.119	105.783
10	1.507	0.48	27.861	1.507	0.852	55.854	1.511	1.12	104.787
11	2.73	0.502	27.599	2.723	0.881	57.898	2.717	1.144	104.604
12	3.955	0.526	29.433	3.954	0.927	56.719	3.945	1.172	101.38
13	5.164	0.552	28.699	5.166	0.942	55.277	5.169	1.209	95.64
14	6.372	0.593	32.447	6.379	0.955	62.327	6.381	1.239	110.449
With 5% CD addition									
1	0	0.196	0.026	0	0.021	22.409	0	0.253	24.456
2	0	0.196	0.026	0	0.028	29.774	0	0.355	32.654
3	0	0.196	0.026	0	0.028	33.26	0	0.525	40.092
4	0	0.196	0.971	0	0.028	35.619	0	0.703	44.453
5	0	0.196	11.197	0	0.028	36.248	0	0.715	56.011
6	0.315	0.211	24.406	0.338	0.028	47.308	0.282	0.736	70.505
7	0.617	0.221	29.517	0.64	0.028	51.423	0.579	0.747	77.346

Serial No.	For 2kg normal load (54.480 kPa)			For 4kg normal load (108.970 kPa)			For 8kg normal load (217.940 kPa)		
	Horizontal Deformation	Vertical Deformation	Shear Stress	Horizontal Deformation	Vertical Deformation	Shear Stress	Horizontal Deformation	Vertical Deformation	Shear Stress
	mm	mm	kPa	mm	mm	kPa	mm	mm	kPa
8	0.923	0.226	32.033	0.94	0.028	50.873	0.878	0.785	82.614
9	1.208	0.237	34.864	1.237	0.028	49.667	1.175	0.817	87.017
10	1.505	0.24	36.437	1.533	0.028	49.3	1.477	0.845	90.975
11	2.705	0.25	38.297	2.721	0.029	50.48	2.674	0.917	99.912
12	3.919	0.258	38.926	3.941	0.026	52.786	3.9	0.974	103.608
13	5.148	0.272	38.429	5.162	0.024	53.432	5.121	1.026	113.489
14	6.371	0.287	39.876	6.378	0.022	47.518	6.324	1.069	114.921
With 10% CD addition									
1	0.02	0.015	1.154	0	0.168	0.367	0.086	1.399	4.88
2	0.038	0.031	0.656	0.099	0.199	1.837	0.062	2.547	34.867
3	0.027	0.033	8.237	0.15	0.015	11.457	0.012	2.569	52.086
4	0.028	0.033	14.423	0.197	0.02	28.493	0.05	2.602	60.342
5	0.09	0.033	17.175	0.254	0.021	34.678	0.107	2.626	66.082
6	0.389	0.034	25.273	0.556	0.176	45.634	0.396	2.751	84.481
7	0.688	0.048	30.174	0.845	0.208	49.434	0.685	2.824	95.725
8	0.986	0.087	34.237	1.148	0.313	52.134	0.983	2.866	104.165
9	1.274	0.114	37.356	1.442	0.313	54.86	1.28	2.917	110.979
10	1.574	0.135	38.543	1.736	0.313	55.777	1.582	2.95	117.453
11	2.766	0.199	38.651	2.938	0.338	61.543	2.782	3.046	118.324
12	4	0.241	39.764	4.155	0.338	65.71	3.988	3.114	120.983
13	5.212	0.33	40.786	5.361	0.338	69.091	5.189	3.149	124.065
14	6.416	0.293	37.321	6.566	0.338	70.432	6.391	3.177	125.023
With 15% CD addition									
1	0	0	0.341	0.087	0.047	1.259	0.001	0.111	0.84
2	0.003	0.008	1.548	0.152	1.227	17.014	0.014	0.66	3.49
3	0.003	0.015	1.286	0.201	1.41	30.066	0.033	0.673	2.283
4	0.035	0.015	16.098	0.258	1.419	36.12	0.072	0.673	31.431
5	0.088	0.015	21.995	0.314	1.419	38.872	0.122	0.688	47.707
6	0.379	0.015	30.592	0.611	1.445	48.885	0.405	0.746	81.57
7	0.678	0.015	34.235	0.915	1.473	54.153	0.697	0.797	95.461

Serial No.	For 2kg normal load (54.480 kPa)			For 4kg normal load (108.970 kPa)			For 8kg normal load (217.940 kPa)		
	Horizontal Deformation	Vertical Deformation	Shear Stress	Horizontal Deformation	Vertical Deformation	Shear Stress	Horizontal Deformation	Vertical Deformation	Shear Stress
	mm	mm	kPa	mm	mm	kPa	mm	mm	kPa
8	0.978	0.015	36.148	1.203	1.498	58.005	0.995	0.837	104.556
9	1.278	0.015	38.323	1.497	1.515	60.679	1.285	0.874	111.422
10	1.575	0.015	39.162	1.792	1.528	63.274	1.58	0.901	115.38
11	2.783	0.015	42.753	3.001	1.589	67.493	2.783	0.969	123.898
12	3.989	0.015	44.221	4.223	1.623	67.624	4.011	1.019	125.995
13	5.199	0.015	44.902	5.419	1.662	69.143	5.224	1.063	129.166
14	6.403	0.013	46.906	6.637	1.705	70.321	6.428	1.102	130.786
With 20% CD addition									
1	0.003	0.002	1.758	0	0.213	0.236	0.05	0.875	31.216
2	0.005	0.057	1.863	0	0.226	17.522	0.096	0.899	45.736
3	0.005	0.059	1.837	0	0.226	27.348	0.155	0.939	52.838
4	0.005	0.059	1.837	0	0.226	31.98	0.209	0.939	57.792
5	0.005	0.059	1.837	0	0.226	35.789	0.276	0.955	60.57
6	0.256	0.082	35.471	0	0.245	45.987	0.558	1.029	75.274
7	0.553	0.096	38.118	0.145	0.286	50.234	0.854	1.081	85.181
8	0.843	0.107	40.555	0.446	0.328	55.765	1.147	1.136	91.786
9	1.138	0.128	40.949	0.753	0.359	59.897	1.442	1.178	97.395
10	1.438	0.165	42.521	1.056	0.398	60.234	1.739	1.211	125.765
11	2.633	0.218	46.033	2.453	0.501	64.532	2.935	1.336	132.654
12	3.86	0.255	50.764	3.568	0.555	65.786	4.145	1.429	137.076
13	5.083	0.368	55.897	5.662	0.592	68.125	5.344	1.507	139.954
14	6.287	0.418	59.654	6.244	0.638	69.765	6.558	1.573	145.034
With 25% CD addition									
1	0	0.468	4.38	0	0.219	0.708	0	0.079	0.262
2	0	0.665	17.196	0	0.228	0.761	0.035	0.41	1.312
3	0	0.676	20.001	0	0.228	0.761	0.169	1.355	2.939
4	0	0.676	22.386	0	0.228	0.682	0.154	1.457	3.542
5	0	0.68	23.801	0	0.228	0.525	0.164	1.457	0.446
6	0.25	0.738	28.755	0.147	0.247	47.628	0.401	1.457	68.935
7	0.554	0.79	32.477	0.448	0.288	52.608	0.691	1.485	86.836

Serial No.	For 2kg normal load (54.480 kPa)			For 4kg normal load (108.970 kPa)			For 8kg normal load (217.940 kPa)		
	Horizontal Deformation	Vertical Deformation	Shear Stress	Horizontal Deformation	Vertical Deformation	Shear Stress	Horizontal Deformation	Vertical Deformation	Shear Stress
	mm	mm	kPa	mm	mm	kPa	mm	mm	kPa
8	0.855	0.821	40.445	0.755	0.33	56.015	0.984	1.525	96.796
9	1.154	0.838	41.231	1.058	0.361	58.427	1.275	1.563	103.217
10	1.455	0.85	41.152	1.355	0.4	61.152	1.565	1.593	108.512
11	2.649	0.9	42.384	2.556	0.503	68.203	2.742	1.693	125.286
12	3.863	0.935	45.874	3.764	0.557	75.541	3.947	1.756	138.862
13	5.069	0.977	49.741	4.974	0.594	78.818	5.164	1.817	140.278
14	6.272	1.017	50.497	6.18	0.634	76.957	6.36	1.845	139.544
With 30% CD addition									
1	0	0.021	0.079	0	0.635	0.236	0	0.042	0.63
2	0	0.021	0.079	0	0.664	17.512	0	0.071	0.315
3	0	0.021	0.079	0	0.67	26.345	0	0.596	4.093
4	0	0.021	0.079	0	0.683	30.958	0	0.605	17.041
5	0	0.021	0.079	0	0.696	34.26	0	0.616	37.092
6	0	0.021	30.04	0	0.728	44.98	0.288	0.616	71.217
7	0	0.021	35.02	0.146	0.757	51.663	0.606	0.591	85.212
8	0.176	0.021	37.117	0.458	0.782	56.067	0.911	0.591	90.067
9	0.494	0.021	39.03	0.755	0.819	58.609	1.196	0.591	109.675
10	0.796	0.021	45.034	1.058	0.839	60.182	1.498	0.591	125.386
11	1.998	0.021	52.543	2.253	0.893	64.532	2.698	0.622	130.987
12	3.2	0.021	58.345	3.466	0.939	70.01	3.904	0.696	135.645
13	4.41	0.021	60.986	4.662	0.99	75.674	5.101	0.741	150.123
14	5.618	0.021	63.032	5.867	1.035	80.141	6.31	0.783	155.98
With 35% CD addition									
1	0	0.304	6.162	0	0.693	23.222	0	1.126	19.107
2	0	0.424	17.117	0	0.703	29.853	0	1.584	53.651
3	0	0.424	21.39	0	0.709	32.762	0	1.499	65.655
4	0	0.424	23.539	0	0.725	34.099	0	1.45	69.901
5	0.083	0.424	24.089	0	0.739	34.597	0	1.45	71.5
6	0.385	0.424	28.571	0.371	0.836	34.282	0.315	1.45	81.303
7	0.691	0.46	31.611	0.673	0.935	32.238	0.619	1.45	82.43

Serial No.	For 2kg normal load (54.480 kPa)			For 4kg normal load (108.970 kPa)			For 8kg normal load (217.940 kPa)		
	Horizontal Deformation	Vertical Deformation	Shear Stress	Horizontal Deformation	Vertical Deformation	Shear Stress	Horizontal Deformation	Vertical Deformation	Shear Stress
	mm	mm	kPa	mm	mm	kPa	mm	mm	kPa
8	0.986	0.48	32.371	0.974	1.016	34.308	0.923	1.451	84.893
9	1.286	0.505	33.000	1.26	1.091	36.379	1.211	1.458	85.601
10	1.579	0.52	33.996	1.56	1.155	39.236	1.509	1.462	85.129
11	2.777	0.547	34.704	2.74	1.324	48.383	2.724	1.526	86.492
12	4.004	0.566	34.363	3.952	1.435	53.651	3.944	1.526	80.988
13	5.23	0.595	35.01	5.171	1.501	57.804	5.163	1.54	95.674
14	6.459	0.618	33.603	6.393	1.546	60.654	6.391	1.565	102.321

Table A- 2: Results for FOS at different % of CD

No. of Steps	FOS at different % of Ceramic Dust							
	0%	5%	10%	15%	20%	25%	30%	35%
1	0.750	1.000	1.000	1.000	1.000	1.000	1.000	1.000
2	0.750	1.000	1.000	1.000	1.000	1.000	1.000	1.039
3	0.800	1.000	1.000	1.000	1.000	1.000	1.000	1.114
4	0.800	1.000	1.092	1.180	1.167	1.246	1.236	1.214
5	0.800	1.027	1.152	1.243	1.232	1.311	1.299	1.273
6	0.827	1.065	1.220	1.325	1.315	1.391	1.393	1.290
7	0.863	1.082	1.312	1.442	1.435	1.510	1.524	1.296
8	0.880	1.093	1.372	1.529	1.522	1.599	1.628	1.304
9	0.891	1.088	1.392	1.580	1.571	1.654	1.683	1.310
10	0.887	1.086	1.401	1.596	1.587	1.672	1.701	1.315
11	0.885	1.088	1.399	1.608	1.599	1.686	1.713	1.318
12	0.887	1.089	1.402	1.615	1.614	1.696	1.722	1.322
13	0.888	1.091	1.403	1.630	1.626	1.712	1.730	1.322
14	0.890	1.093	1.405	1.642	1.634	1.727	1.736	1.321
15	0.892	1.094	1.408	1.649	1.636	1.739	1.742	1.320

No. of Steps	FOS at different % of Ceramic Dust							
	0%	**5%**	**10%**	**15%**	**20%**	**25%**	**30%**	**35%**
16	0.893	1.094	1.405	1.652	1.645	1.745	1.747	1.319
17	0.892	1.094	1.402	1.652	1.644	1.745	1.751	1.317
18	0.893	1.094	1.401	1.651	1.665	1.737	1.752	1.317
19	0.893	1.094	1.401	1.650	1.652	1.736	1.749	1.316
20	0.893	1.095	1.399	1.649	1.652	1.733	1.747	1.315
21	0.894	1.096	1.398	1.647	1.631	1.730	1.746	1.315
22	0.894	1.096	1.396	1.647	1.631	1.728	1.743	1.315
23	0.898	1.096	1.393	1.645	1.630	1.724	1.738	1.315
24	0.899	1.096	1.391	1.645	1.630	1.721	1.738	1.316
25	0.900	1.096	1.389	1.645	1.629	1.717	1.737	1.316
26	0.901	1.097	1.388	1.644	1.629	1.716	1.738	1.317
27	0.903	1.097	1.387	1.644	1.628	1.715	1.738	1.317
28	0.910	1.098	1.386	1.643	1.628	1.714	1.739	1.318
29	0.910	1.098	1.386	1.642	1.627	1.714	1.739	1.318
30	0.920	1.099	1.386	1.641	1.627	1.714	1.740	1.318
31	0.923	1.101	1.388	1.640	1.627	1.714	1.741	1.318
32	0.924	1.102	1.388	1.639	1.627	1.715	1.741	1.319
33	0.925	1.104	1.390	1.638	1.627	1.716	1.741	1.319
34	0.926	1.105	1.394	1.638	1.627	1.716	1.742	1.319
35	0.930	1.106	1.396	1.638	1.627	1.718	1.742	1.320
36	0.930	1.107	1.397	1.638	1.628	1.719	1.742	1.320
37	0.930	1.107	1.397	1.638	1.628	1.720	1.742	1.320
38	0.940	1.108	1.399	1.636	1.628	1.720	1.743	1.320
39	0.940	1.108	1.401	1.638	1.628	1.721	1.743	1.320
40	0.940	1.108	1.403	1.638	1.628	1.722	1.743	1.320
41	0.940	1.108	1.405	1.635	1.628	1.723	1.743	1.320
42	0.940	1.102	1.410	1.639	1.628	1.724	1.744	1.320
43	0.950	1.100	1.415	1.634	1.629	1.725	1.744	1.320
44	0.960	1.099	1.416	1.639	1.629	1.724	1.744	1.320
45	0.960	1.097	1.418	1.635	1.629	1.725	1.744	1.320
46	0.970	1.096	1.418	1.638	1.629	1.725	1.744	1.321
47	0.970	1.095	1.419	1.635	1.630	1.725	1.744	1.320

No. of Steps	FOS at different % of Ceramic Dust							
	0%	5%	10%	15%	20%	25%	30%	35%
48	0.980	1.095	1.419	1.639	1.629	1.725	1.745	1.321
49	0.960	1.094	1.417	1.635	1.630	1.724	1.745	1.321
50	0.958	1.094	1.415	1.638	1.629	1.724	1.745	1.321
51	0.900	1.095	1.412	1.635	1.630	1.723	1.745	1.321
52	0.895	1.095	1.408	1.638	1.630	1.720	1.745	1.321
53	0.894	1.096	1.407	1.634	1.630	1.721	1.745	1.321
54	0.894	1.097	1.406	1.634	1.630	1.718	1.746	1.321
55	0.895	1.098	1.406	1.634	1.630	1.720	1.746	1.321
56	0.896	1.100	1.406	1.634	1.630	1.720	1.746	1.321
57	0.897	1.102	1.407	1.634	1.630	1.720	1.746	1.321
58	0.898	1.104	1.407	1.634	1.630	1.720	1.746	1.321
59	0.899	1.105	1.407	1.634	1.630	1.721	1.746	1.322
60	0.900	1.105	1.409	1.634	1.630	1.721	1.746	1.322
61	0.901	1.106	1.411	1.635	1.630	1.722	1.747	1.322
62	0.902	1.106	1.414	1.634	1.630	1.722	1.747	1.321
63	0.903	1.107	1.418	1.635	1.630	1.723	1.747	1.321
64	0.904	1.108	1.420	1.634	1.630	1.724	1.747	1.321
65	0.905	1.108	1.422	1.635	1.630	1.724	1.747	1.321
66	0.906	1.108	1.423	1.635	1.630	1.725	1.746	1.321
67	0.907	1.108	1.424	1.635	1.630	1.725	1.746	1.322
68	0.908	1.107	1.425	1.635	1.630	1.726	1.746	1.322
69	0.909	1.107	1.425	1.635	1.630	1.726	1.746	1.322
70	0.910	1.106	1.425	1.635	1.630	1.727	1.746	1.322
71	0.911	1.105	1.425	1.635	1.630	1.727	1.747	1.322
72	0.911	1.105	1.424	1.635	1.630	1.727	1.747	1.322
73	0.911	1.105	1.421	1.635	1.630	1.727	1.746	1.322
74	0.911	1.105	1.421	1.635	1.630	1.727	1.747	1.322
75	0.911	1.105	1.422	1.635	1.630	1.727	1.747	1.322
76	0.911	1.106	1.423	1.635	1.630	1.727	1.747	1.322
77	0.911	1.107	1.419	1.635	1.630	1.727	1.747	1.322
78	0.912	1.108	1.419	1.635	1.630	1.727	1.747	1.322
79	0.911	1.109	1.419	1.636	1.630	1.727	1.747	1.322
80	0.911	1.110	1.420	1.636	1.630	1.727	1.747	1.322
81	0.910	1.111	1.421	1.636	1.630	1.727	1.747	1.322

No. of Steps	FOS at different % of Ceramic Dust							
	0%	**5%**	**10%**	**15%**	**20%**	**25%**	**30%**	**35%**
82	0.910	1.112	1.421	1.636	1.630	1.727	1.747	1.322
83	0.909	1.113	1.420	1.636	1.630	1.728	1.747	1.322
84	0.909	1.114	1.420	1.636	1.630	1.728	1.747	1.322
85	0.909	1.115	1.419	1.636	1.630	1.728	1.747	1.322
86	0.908	1.116	1.419	1.636	1.630	1.728	1.747	1.322
87	0.909	1.117	1.419	1.636	1.630	1.727	1.747	1.322
88	0.909	1.117	1.418	1.636	1.630	1.728	1.747	1.322
89	0.909	1.118	1.416	1.636	1.630	1.729	1.747	1.322
90	0.909	1.118	1.415	1.635	1.630	1.728	1.747	1.322
91	0.909	1.118	1.412	1.635	1.630	1.728	1.747	1.322
92	0.908	1.118	1.411	1.635	1.631	1.728	1.747	1.322
93	0.907	1.118	1.410	1.635	1.631	1.728	1.746	1.322
94	0.907	1.117	1.408	1.635	1.631	1.728	1.746	1.322
95	0.906	1.117	1.406	1.635	1.631	1.728	1.746	1.322
96	0.905	1.117	1.404	1.635	1.631	1.728	1.746	1.322
97	0.904	1.117	1.403	1.635	1.631	1.728	1.746	1.322
98	0.902	1.116	1.402	1.635	1.631	1.728	1.746	1.322
99	0.899	1.116	1.401	1.635	1.631	1.728	1.747	1.322
100	0.898	1.116	1.401	1.636	1.631	1.728	1.747	1.322